PERFUSION SOLUTION OPTIMIZATION BY SUBSTRATE ALTERATION AND NANOPARTICLE DELIVERY FOR CARDIAC HYPOTHERMIC MACHINE PERFUSION

APPROVED BY SUPERVISORY COMMITTEE

_____
Matthias Peltz, M.D., Advisor

_____
Michael Jessen, M.D., Chair

_____
Kytai Nguyen, Ph.D.

_____
Robert Eberhart, Ph.D.

_____
Eunsook Jin, Ph.D.

Acknowledgements

First and foremost, I would like to thank my parents. Their support and encouragement has continuously helped me achieve my goals. Their spirit of perseverance has taught me to view obstacles as speed bumps instead of road blocks and to always believe in myself in the face of adversity. Thank you for the sacrifices you made so I could explore my interests and follow my passions wherever they may have led. I could not have done this without you and words will never be enough to adequately describe my gratitude and love for you both. I thank my siblings, Cyerra and Christian, for being my sounding boards since birth. Despite physically being on different coasts, you both have always been only a phone call away and have given me a fun-filled respite from science when needed. Your work ethic has always inspired me to be better and I could not have done this without your unwavering confidence in me. Thank you to my grandparents for bravely paving the way so that I could have opportunities that they dreamed of.

I would like to thank the Peltz Lab. I thank Dr. Peltz and Dr. Jessen for giving me the tools and freedom to explore answers to my scientific questions and come up with new ideas in the process. I chose UT Southwestern for my graduate studies because my summer experience in your lab gave me an exciting glimpse into cardiovascular research and showed me how I could contribute. Your continuous support has been much appreciated over the past five years. Working with you both has developed me into a scientist with the ability to ask probing questions and focus on the process just as much as the results. Dr. Peltz, thank you for encouraging me to develop my presentation and written skills by allowing me to present at conferences and write

manuscripts early on. That exposure and your mentorship have been instrumental in developing me into a well-rounded scientist, engineer, and critical thinker. Thank you for the opportunity to work in your lab. I would also like to thank the lead research scientist in the Peltz lab, LaShondra Powell. Your expertise in a variety of lab techniques and willingness to learn have been crucial throughout my graduate studies. You helped me to troubleshoot experiments, drive them to completion and are always there to bounce ideas around. I have learned a lot from you and I thank you for your patience.

I would also like to thank my dissertation committee. Your guidance helped me to dig deeper and uncover new ways to answer my questions. Your expertise, advice, insights, and questions have elevated the level of my work.

Finally, I would like to thank Dr. Nancy Street. I chose to return to UT Southwestern because of the Peltz/Jessen Lab and because of you. You have been my mentor outside of the lab since my first summer as a SURF student. You've been a calming presence and your unwavering support has meant the world to me. I hope to one day affect a student as positively as you have affected me. Thank you for your guidance.

PERFUSION SOLUTION OPTIMIZATION BY SUBSTRATE ALTERATION AND NANOPARTICLE DELIVERY FOR CARDIAC HYPOTHERMIC MACHINE PERFUSION

by

CYONNA THERESA HOLMES

DISSERTATION

Presented to the Faculty of the Graduate School of Biomedical Sciences

The University of Texas Southwestern Medical Center at Dallas

In Partial Fulfillment of the Requirements

For the Degree of

DOCTOR OF PHILOSOPHY
The University of Texas Southwestern Medical Center at Dallas
Dallas, Texas
May, 2018

PERFUSION SOLUTION OPTIMIZATION BY SUBSTRATE ALTERATION AND NANOPARTICLE DELIVERY FOR CARDIAC HYPOTHERMIC MACHINE PERFUSION

Cyonna Theresa Holmes, Ph.D.

The University of Texas Southwestern Medical Center at Dallas, 2018

Supervising Professor: Matthias Peltz, M.D.

Current heart donor procurement involves a period of cold storage during transport and rarely exceeds 6 hours. While this method reduces myocardial metabolism, it still results in ATP depletion, lactate accumulation, and myocyte damage. Hypothermic machine perfusion (HMP) has emerged as an alternative technique. Previous studies from our laboratory showed HMP maintains myocardial oxygen consumption, preserves ATP, reduces myocardial injury, minimizes lactate accumulation, and improves cardiac function after transplantation for storage intervals of over fourteen hours. Though HMP is more advantageous, myocardial metabolism

and adjunctive protective strategies under these conditions are poorly understood. The purpose of this study was to 1) Determine myocardial substrate preferences during HMP 2) Evaluate the effect of metformin and insulin on substrate oxidation in the perfused heart 3) Demonstrate delivery of nanoparticles to the heart during HMP. In Aim 1, I investigated myocardial substrate selection by perfusing isolated rat hearts octanoate, ketones, or acetate with and without an anaplerotic substrate. ^{13}C magnetic resonance spectroscopy (MRS) was performed on myocardial extracts and substrate contributions to oxidative metabolism were assessed by isotopomer analysis. Additional samples were analyzed by gas chromatography/mass spectroscopy to determine substrate effects on tricarboxylic acid (TCA) cycle intermediates and isotopomer distributions. Aim 2 assessed the ability of metformin and insulin to alter myocardial substrate oxidation during normokalemic, hyperkalemic, and post-ischemic reperfusion using a rat normothermic Langendorff model. Substrate selection and oxidation rates were determined by ^{13}C MRS and isotopomer analysis as in Aim 1. Cardiac function and efficiency were measured. For Aim 3, a nanoparticle delivery system was constructed, and a nanoparticle perfusion model was validated for future addition of nanoparticles to the perfusate to modify cardiac injury. Nanoparticles were characterized and then tested in three and six-hour perfusion models for their ability to localize in cells.

Data from Aim 1 demonstrated that octanoate and acetate were preferentially oxidized during HMP. Ketone oxidation remained a minor contributing substrate. TCA cycle intermediates were increased in all substrate containing groups compared to hearts immediately recovered or perfused without oxidizable substrate. An anaplerotic

substrate was not required to achieve these results. In Aim 2, during normokalemia, insulin reduced ketone oxidation while the combination of insulin and metformin restored the control profile. Metformin reduced fatty acid oxidation in the cardioplegia model while neither drug influenced substrate selection during post-ischemic reperfusion. Cardiac function and efficiency were not altered in treatment groups. Lastly, Aim 3 results indicated that nanoparticles (diameter=376±98nm; polydispersity index=0.16±0.06; encapsulation efficiency=65±12%) showed successful uptake, reduced lactate, and increased high energy phosphate ratios in the 3-hour model. Outcomes from these experiments demonstrate that myocardial substrate preferences are different during HMP compared to normothermia. Nanoparticle delivery to myocardium during HMP is possible and has the potential to modify myocardial injury by delivering therapeutic agents, miRNA (miRNA-499), or other gene products. This data is critical in designing preservation solutions for the machine perfused heart.

TABLE OF CONTENTS

PRIOR PUBLICATIONS

Holmes C, et al. Influence of Metformin and Insulin on Myocardial Substrate Oxidation under Conditions encountered during Cardiac Surgery. *Surgery* 2018 Feb; 163(2): 436-443.

Brant SM, **Holmes C,** et al. Successful Transplantation in Canines After Long-Term Coronary Sinus Machine Perfusion after Preservation of Donor Hearts. *J Heart Lung Transplant* 2016 Aug 17;35(8):1031-6.

PUBLISHED ABSTRACTS

Holmes C, Powell L, Peltz M, Jessen M. Oxidative Substrate Increases Oxygen Consumption, Increases TCA Cycle Intermediates and Reduces Lactate Production in the Machine Perfused Heart. American Heart Association 2017 Scientific Sessions, New Orleans, LA, November 13-16, 2016 (Circulation. 2016;134:A20879)

Holmes, C, Clarke N, Powell LM, Jessen ME, Peltz M. Influence of Fatty Acids, Acetate, and Ketones on Myocardial Substrate Selection and TCA Cycle Intermediates During Hypothermic Machine Perfusion of Donor Hearts. *J Heart Lung Transplant,* vol. 35, iss. 4, 2016, S178-S179.

Brant SM, **Holmes C**, West L, Cobert M, Jessen ME, Peltz M. Influence of Oxidative and Anaplerotic Substrates on Myocardial Metabolism During Hypothermic Machine Perfusion. International Society for Heart and Lung Transplantation 34th Annual Meeting, San Diego, CA, April 10-13, 2014 (J Heart Lung Transplant 2014; 33(4):S259).

Brant SM, Cobert ML, West LM, **Holmes C**, Jessen ME, Peltz M. Metformin Reduces Fatty Acid Oxidation in the Isolated Perfused Rat Heart. 9th Annual Academic Surgical Congress, San Diego, CA, February 4-6, 2014 (J Surg Res 2014;186:494).

LIST OF FIGURES

APPENDIX

LIST OF TABLES

ABBREVIATIONS

ADP…Adenosine diphosphate

AMP…Adenosine monophosphate

ATP...Adenosine triphosphate

BP…Bypass

CP…Cardioplegia

DCD…Donation after Circulatory Death

FC…Freeze-Clamped

HMP…Hypothermic Machine Perfusion

KHB…Krebs Heinslet Buffer

miRNA…MicroRNA

MRS…Magnetic Resonance Spectroscopy

NK…Normokalemia

NP…Nanoparticle

NRC…Non-Recirculating

NS…No Substrate

P407…Polaxomer 407

PEG…Polyethylene glycol

PCr…Phosphocreatine

Pi…Inorganic phosphate

PLGA…Poly (lactic-co-glycolic acid)

RC…Recirculating

TCA Cycle…Tricarboxylic Acid Cycle

Chapter One

Introduction

1.1 Heart Transplantation

Heart failure affects over 5.7 million people of the US population (Mozaffarian et al. 2015; Friedrich and Böhm 2007; Chen-Scarabelli et al. 2015) and is most commonly caused by coronary artery disease, cardiomyopathy, heart valve disease or congenital defects. Diabetes and high blood pressure can increase one's risk of some of these pathologies and disease progression can lead to end-stage heart failure. Goal directed medical therapy and conventional surgery, such as coronary artery bypass or valve operations can be used to treat many patients but are ineffective or too high risk for patients with the most advanced heart failure. For these patients, inotropic therapy of surgical implantation of life-prolonging device such as left ventricular assist devices are options. However, heart transplantation remains the most effective treatment. Cardiac transplantation most commonly involves the procurement of a heart from a donor having experienced brain death or rarely circulatory death. This heart is then implanted into a recipient in need of a new heart in order to extend life. The first human heart transplantation was performed in South Africa in December of 1967 by Dr. Christian Barnard. After it was confirmed that the only means of treatment for the patient was a transplant, a donor heart was sought. The donor heart was excised, placed in hypothermic solution, perfused ex-vivo and subsequently implanted into the recipient (Barnard 1967). This first patient survived for 18 days, ultimately dying of sepsis. While this was revolutionary, the feat was simplified by having both the donor and recipient in adjacent operating rooms—no prolonged period of transport was required. From 1967-

1968, over 50 heart transplants were performed with the first transplant in the US performed by Dr. Norman Shumway at Stanford Medical Center(Haller Jd Fau - Cerruti and Cerruti 1968; Kantrowitz A Fau - Haller et al. 1968; Kantrowitz 1998). Early outcomes were poor with most recipients dying in the first year after transplantation (Brink and Hassoulas 2009; Thomson 1969; Barnard Cn Fau - Barnard et al. 1981). Since then, various advances in the field have been made. The one year survival rate has increased to 90% and median survival approaches 12 years according to the International Society of Heart and Lung Transplantation registry (Lund et al. 2016).

In 2014, 4,764 heart transplants were performed globally with the majority of those being adult heart transplants for recipients aged 40-69 (Lund et al. 2016). Though the number of performed transplants has increased, issues such as graft failure, infection, and organ failure still plague the procedure. Differing from early heart transplants, current transplants are not often performed with the donor and recipient in adjoining operation rooms. Often, the heart has to travel some distance in order to reach the recipient. This is referred to as the transport interval. During this time, the heart is stored in a cooler immersed in preservation solution to make it easy to transport between the donor and recipient. Prior to transport, the heart is arrested by flushing it with a cold, potassium cardioplegia solution, excised from the donor and stored in a cooler at hypothermic temperatures for *ex vivo* transport. The heart can withstand up to 6 hours of ischemic time though recipient mortality begins to significantly increase as the ischemic time exceeds 3 hours (Lund et al. 2016). This is known as static preservation—the heart sits on ice, temporarily stunned, while in transit to the recipient. Upon arrival at the recipient's operating room, the heart is removed from the cooler,

implanted into the recipient, and the patient is removed from bypass. If successful, the heart reanimates in the recipient's thoracic cavity. The number of transplants performed is greatly limited by the number of available donors and of these, only 30% are deemed suitable for transplantation using the current cold storage preservation technique. Improvements in preservation technique could substantially increase the number of available heart donors

1.2 Static Preservation and its Limits

Static Preservation is the current standard of care used clinically to store and transport hearts during transplantation. Its adoption is largely based on the facts that it is simple, cost-effective, and not mechanically cumbersome. Additionally, cold storage decreases metabolic processes and reduces the activity of degradative enzymes thus putting a lesser demand on the donor organ while in transit (Guibert et al. 2011). Cold storage also alters gene expression in the donor organ. In a murine transplant study by Amberger and group, comparing gene expression in hearts that underwent cold storage for ten hours versus those that did not, higher transcriptional activity was seen in hearts without a cold storage interval. This finding is expected as cold storage is known to reduce cellular processes. However, the study highlights that the genes related to glycolysis, oxygen transport, and cell structure (adenylate kinase-4, enolase-3, myoglobin, and Z-band PDZ motif protein) were upregulated during reperfusion in the group that did not undergo cold storage (Amberger et al. 2002). Genes related to metabolism and cell structure were down-regulated in the cold-storage groups (malate dehydrogenase, epoxide hydrolase-2, and myosin heavy chain-3) (Amberger et al.

2002). Some genes found in the cold, storage heart were not found in control hearts which might imply that specific genes are only evident during prolonged ischemic storage. These gene profiles illustrate reduced activity of cellular function and metabolic processes during cold storage. Myocardial oxygen demand is reduced in response to reduced heart rate, contractility, and inhibited aerobic metabolism. Though myocardial energy demand is reduced, energy in the form of adenosine triphosphate (ATP) is still needed to maintain vital cell functions. Furthermore, static preservation leads to metabolic changes induced by ischemia. This includes ATP and energy store depletion, lactate and waste accumulation, endothelial dysfunction, reduced oxygen profile, and an increase in apoptosis and necrosis all occur during cold preservation (Rosenbaum et al. 2008; Rosenbaum et al. 2007). Lactate accumulation and waste build-up leads to decreases in pH within the heart which results in intramyocardial acidosis. ATP begins to break down to serve as a driving energy force in the heart. Anaerobic glycolysis can generate some ATP but is insufficient to meet the energy demands of the heart long-term even when metabolism is reduced during cold storage. In the absence of oxygen as the final electron acceptor from the reducing equivalents generated by the citric acid or tricarboxylic (TCA) cycle, ATP is gradually degraded to adenosine diphosphate (ADP) and then adenosine monophosphate (AMP). Dephosphorylated purine products that result from ATP catabolism (inosine, xanthine, adenosine, and hypoxanthine) escape through the cell membrane, further depleting precursors for ATP generation. This results in necrosis due to inhibition of the electron transport chain and inadequate flux through the citric acid cycle (Rivard et al. 2009).

ATP depletion also results in the dysfunction of the Na+/K+ and Ca2+/ATPase pumps. Dysfunction of these pumps causes Na+ accumulation which leads to water influx in an attempt by myocytes to restore the osmolar balance. This swelling then causes cell

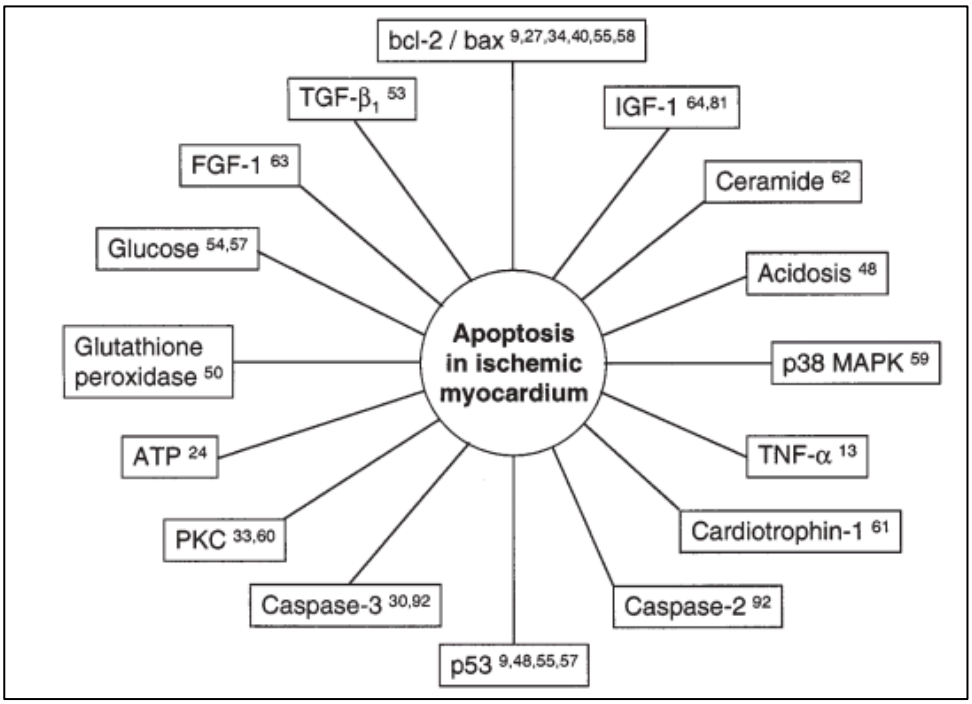

Figure 1.1: Downstream targets and effects of Myocardial Ischemia (Maulik, Yoshida T Fau - Das, and Das 1998).

rupture. Dysfunction of the Ca2+ pump results in the escape of calcium ion stores which inactivates lipases (Beatrice Mc Fau - Stiers, Stiers Dl Fau - Pfeiffer, and Pfeiffer 1984; McAnulty Jf Fau - Southard, Southard Jh Fau - Belzer, and Belzer 1987; McAnulty, Southard, and Belzer 1988). Cell death in cardiomyocytes *in vitro* has been reported to be induced by hypoxia. ATP depletion of less than 70% typically leads to an apoptotic profile while greater than 70% ATP loss results in myocyte necrosis (Elsässer, Suzuki, and Schaper 2000; Tanaka et al. 1994; Leist et al. 1997). Others have suggested a mix of acidosis, caspase activity and reperfusion injury causes oxidative stress which leads to apoptosis (Figure 1.1)) (Maulik, Yoshida T Fau - Das, and Das 1998).

The cause of apoptosis in the static preserved heart cannot be attributed to one factor, but the process is made evident by Terminal deoxynucleotidyl transferase dUTP nick end labeling (TUNEL) in various models (Kanoh et al. 1999; Rivard et al. 2009).

Endothelial dysfunction in cold storage is another common limitation to static storage. Nitrite and nitrate production cause cellular damage resulting in this dysfunction. The endothelium already sustains damage prior to static preservation. Brain damage causes inflammation of organs prior to explantation of the donor and the static storage interval, warm ischemic during heart implantation, and reperfusion with oxygenated blood exacerbates this inflammatory damage to the endothelium (Takada et al. 1998; Land 2002; van der Hoeven et al. 1999). Edema prior to cardiac implantation could be a result of this cellular damage increasing membrane permeability to allow extracellular fluid influx (Rivard et al. 2009). Edema formation is an issue as there is no lag-time or recovery interval once the heart is implanted. While extracellular edema due to hydrostatic forces seems to be well tolerated and resolves early after reperfusion, intracellular edema from ischemic damage is not readily reversible (Poston et al. 2004). The heart must function almost immediately, but cellular edema impairs its contractile function, limiting the storage time before the heart sustains permanent damage. Clinically, an increasing number of patients are receiving ventricular assist device support as a bridge to transplantation. Transplantation following the surgical removal of these is more laborious (Birks et al. 2004; Jacobs, Rega F Fau - Meyns, and Meyns 2010). This results in a longer ischemic or storage interval exacerbating the issues brought on by cold storage.

Ischemia reperfusion injury is another negative effect of cold, static storage. Ischemia-reperfusion refers to the period of cold-storage followed by implantation of the donor organ into the recipient where the organ is then reanimated or perfused again with the patient's circulating blood. Transition from cooling to warming induces changes on a cellular level. The deleterious side effects of ischemia are not immediately corrected by perfusion. Inflammation, endothelial dysfunction, and enhanced membrane permeability persist despite the influx of oxygen and energy generating substrates. Oxygen itself can lead to free radical generation, exacerbating cellular injury. The rapid change in pH from ischemia to reperfusion has also been implicated in cell death. The

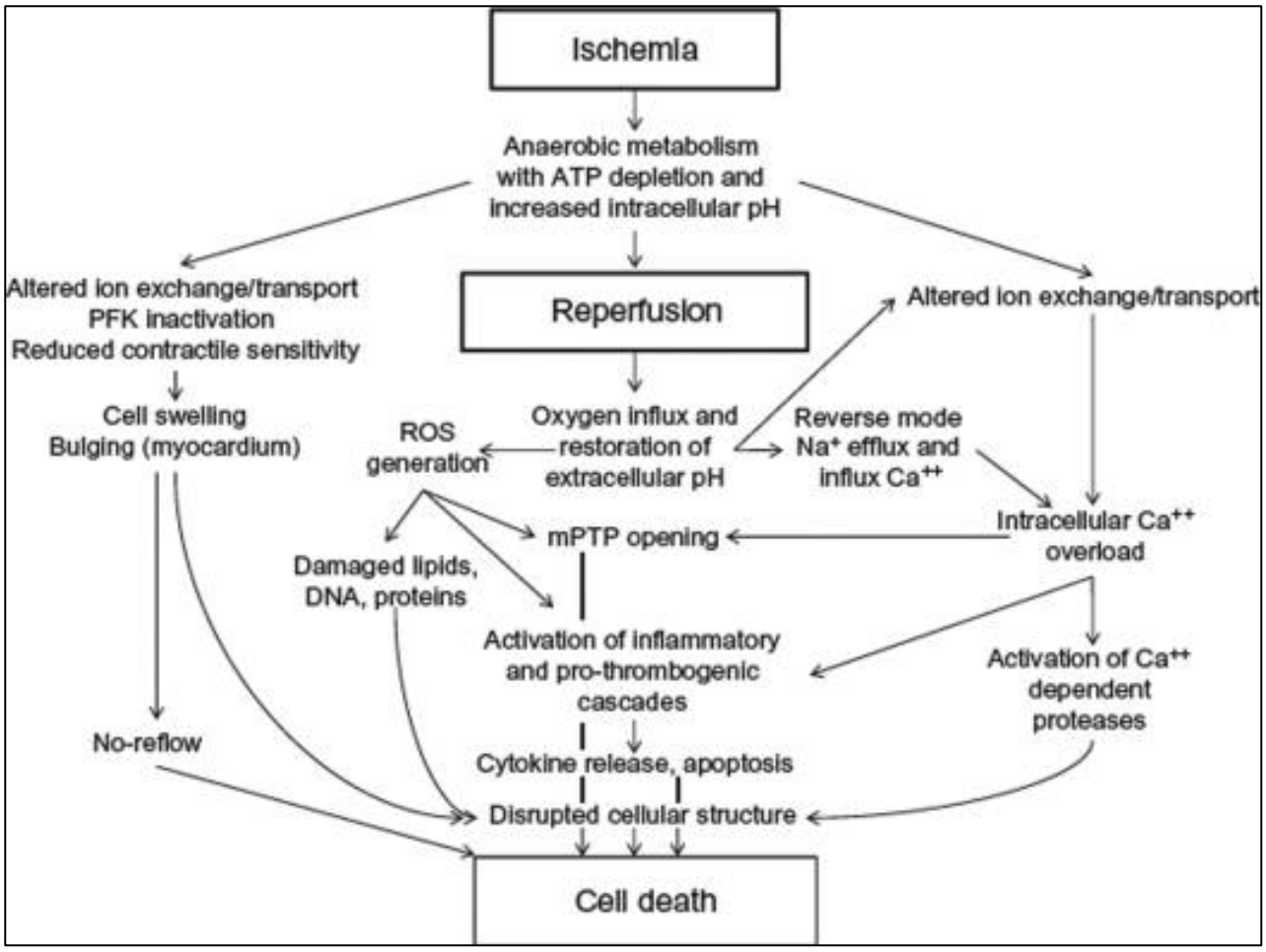

Figure 1.2: Ischemia Reperfusion Cascade and the pathways that lead to cell death (Kalogeris et al. 2012).

cascade of effects from ischemia-reperfusion are depicted in Figure 1.2 from Kalogeris et al (Kalogeris et al. 2012).

The four to six-hour storage interval restricts the distance from which donor hearts can be procured. Effectively, there may be more hearts available, but the limitations of static preservation cause geographical constraints on heart procurement. Additionally, many hearts from donors that are at higher risk for ischemic injury due to reduced ejection fraction, older age, left ventricular hypertrophy, presence of coronary artery disease or prolonged arrest, for example, are not considered for similar reasons. This creates a donor shortage with more people on the waitlist than there are available hearts. Groups have made attempts to improve cold-static storage by offering more protection to the heart through changing the solution hearts are flushed with prior to storage. For example, instead of merely maintaining the high potassium concentration solution used to arrest the heart, the addition of adenosine and lidocaine to the solution may allow for storage at cold or warm temperatures. After 8 hours, Rudd et al showed that this solution used in static preservation resulted in partial recovery of ventricular pressures, reduced lactate accumulation compared to Celsior solution (Genzyme, Cambridge, MA) and reduced troponin release after an hour of reperfusion (Rudd and Dobson 2011). Overall, while some minor differences can be demonstrated between different preservation solutions, none of these are sufficient to substantially change clinical practice. Machine perfusion preservation seeks to address these issues and provide an improved alternative to the current standard of care.

1.3 Machine Perfusion

Machine perfusion for cardiac preservation involves the continuous delivery of oxygenated solution during the storage and transport interval. In contrast to static preservation, the heart is provided with recirculating fluid over this interval to mitigate the negative effects associated with static storage. Delivery of continuous perfusate flow permits ongoing oxidative metabolism, replenishment of ATP stores, and washout of lactate and waste metabolites. Oxidative metabolism allows for the maintenance of cellular processes and membrane integrity which reduces cell death. Perfusate can be introduced starting at either the aorta or the coronary sinus. Another advantage of machine perfusion is better control over environmental aspects like temperature and flow rate. Currently, there are two major machine perfusion preservation strategies for heart preservation: normothermic and hypothermic perfusion. The TransMedics Organ Care System (OCS) designed and manufactured by TransMedics, Inc. (Andover, MA) and the LifeCradle® (Frisco, TX) (Figure 1.3) are representative devices for these different techniques.

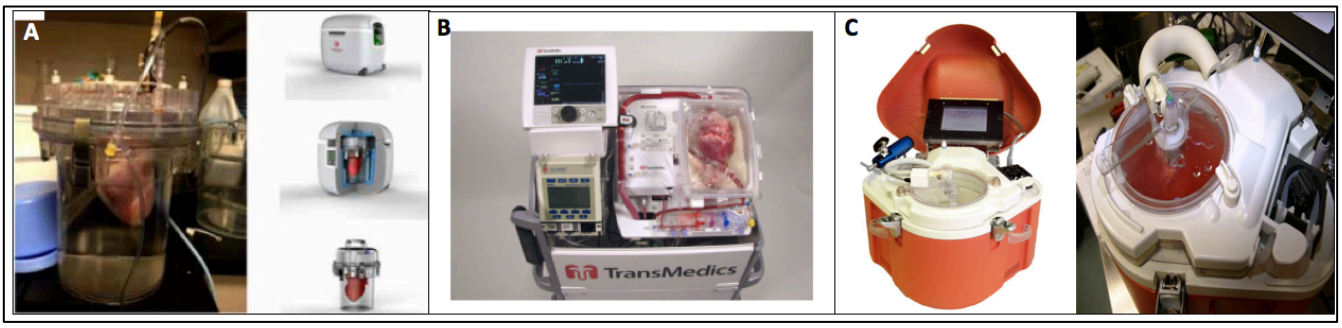

Figure 1.3: Cardiac Preservation Devices. A: Paragonix Hypothermic Storage B: Normothermic Device by TransMedics C: LifeCradle by Organ Transport Systems.

Both devices largely maintain the portability associated with storing a heart in a cooler for transport, but they differ in perfusion method. OCS is a normothermic perfusate device while the LifeCradle is a hypothermic machine device. During normothermic perfusion, the heart is perfused with a warm (approximately 37°C) fluid resulting in a beating heart model. During hypothermic perfusion, the heart is perfused with a cold, high potassium solution resulting in a non-beating heart model that begins beating again after reperfusion post implantation.

1.3.1 Normothermic Perfusion

OCS utilizes warm, donor blood with additives as a perfusion solution. Normothermic perfusion significantly reduces ischemic time, elongates the storage interval, and can provide real-time measurements such as oxygen saturation and coronary flow. The device has undergone clinical trials showing success in both ideal and marginal donors with a preservation of at least ten hours (Garcia Saez et al. 2014; Stamp et al. 2015; Garcia Saez et al. ; Ardehali et al. 2015). Normothermic perfusion allows for viability assessments of the heart in real time. Because the heart is beating and not arrested, any issues can be readily discovered. For example, in a normothermic model, a heart with a slow rate might indicate contractility issues. Warm perfusion might also provide a better environment for repair processes for damaged myocardial tissue. Physiological healing factors and processes that require physiological temperatures can occur in this setting. However, normothermic perfusion does have its limitations. Continuously providing donor blood caused the accidental delivery of vasoconstrictors to the heart (Messer, Ardehali, and Tsui 2015). The device requires one liter of blood just to begin

the flow in the circuit. This does not include the amount needed for perfusion. Procuring this could prove to be a limitation to the device and normothermic perfusion. Because normothermic perfusion is a beating heart model, the oxygen and energy demand of the heart in this state are like those in the body—the work demand on the heart is high in this model for a prolonged period of time requiring greater replenishment. Most importantly, maintaining the heart in a beating state *ex vivo* for long periods of time would require a robust device with great monitoring capabilities. Any perturbations or machine malfunctions at 37°C could greatly impact the donor heart, resulting in loss of the graft, and, despite the aforementioned benefits, decision making regarding the suitability of the donor currently relies largely on a metabolic parameter – lactate accumulation. Also, while the OCS is transportable, it is larger, costlier, and requires more personnel than some of the cold perfusion device technologies.

1.3.2 Hypothermic Perfusion

Similar to static storage, hypothermic machine perfusion slows down metabolic processes in myocardium thus decreasing the amount of oxygen and energy needed by the heart. Flow rates and oxygen carrying capacity are therefore much lower than for normothermic perfusion and an oxygen carrier, such as hemoglobin, is not typically required to meet the metabolic demands of the heart. Paragonix (Braintree, MA), an organ preservation company created the SherpaPak™ Cardiac Transport System which optimizes cold static storage and showed reduced endothelial dysfunction, reduced apoptosis and more intact mitochondria than in cold, static storage (Michel et al. 2015). However, this is merely a storage device but their perfusion device (SherpaPerfusion™)

has received the CE mark. Previous studies done in our lab evaluated hypothermic machine perfusion using the LifeCradle® to preserve donor hearts in multiple models. In human hearts rejected for transplantation, both antegrade (flow through the aorta) and retrograde (flow through the coronary sinus) flow were evaluated compared to static preservation. In both machine perfusion models, the lactate/alanine ratio was reduced and high energy phosphate to inorganic phosphate ratios were increased compared to the static control (Figure 1.4) and compared to control hearts without ischemia thus illustrating that this technique not only maintains but also improves the energy state of the perfused myocardium (Cobert et al. 2014).

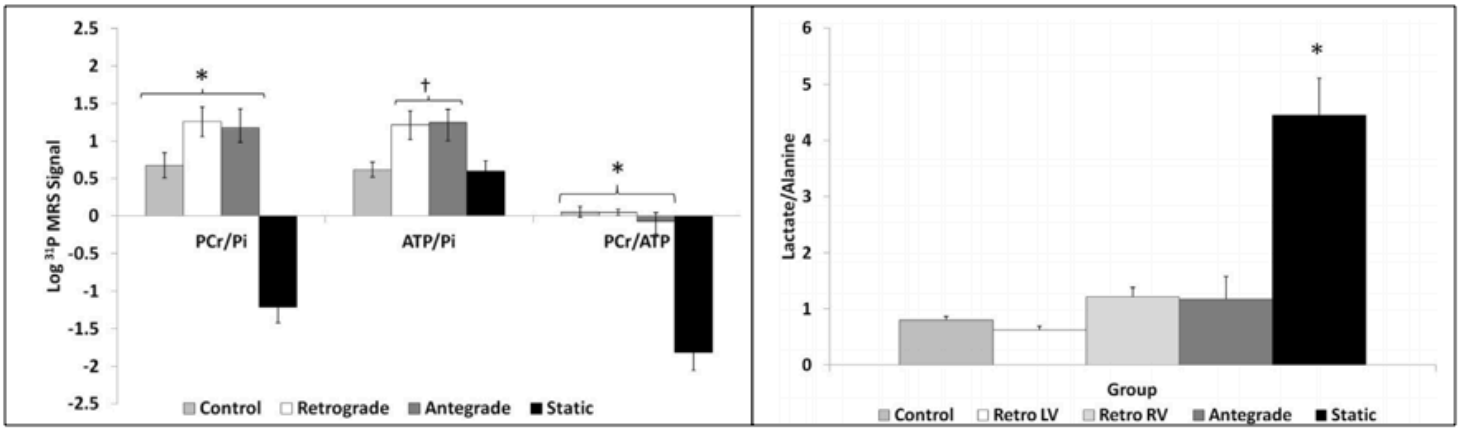

Figure 1.4: 12 hours hypothermic machine perfusion device study results comparing static preservation to antegrade & retrograde perfused hearts, and control hearts. Left Panel: Energetic Phosphate ratios. *,†-p<0.05 vs static groups. Right Panel: Lactate/Alanine ratio. *-p<0.05 vs all other groups.

In addition to improved metabolic factors, our lab showed that hypothermic machine perfusion improved cardiac function after implantation in a long-term preservation canine model. After nearly fifteen hours of ischemia, pre-load-recruitable stroke work, a

measure of cardiac contractility and ability to wean off cardiopulmonary bypass was improved with this technique compared to static storage (Figure 1.5) (Brant et al. 2016).

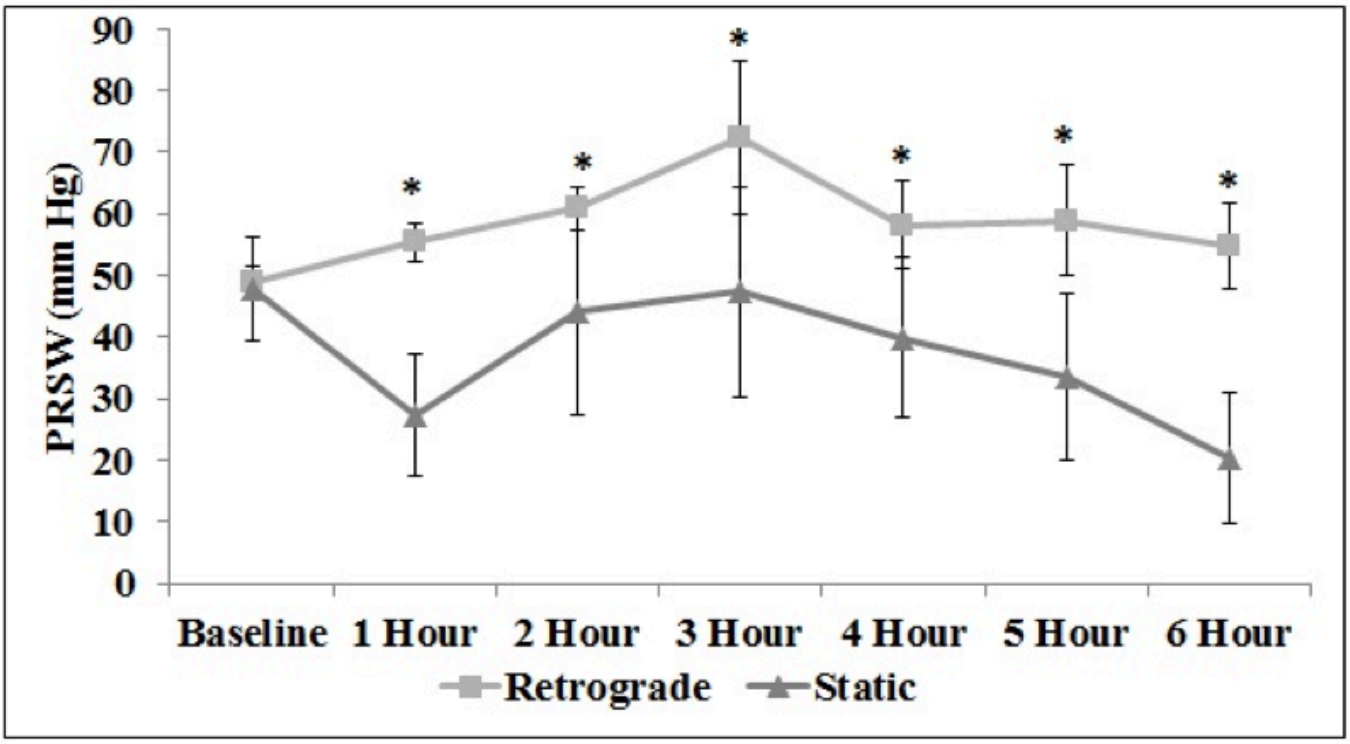

Figure 1.5: Cardiac Functionality after reperfusion as measured by Preload recruitable Stroke Work. Retrograde (aortic perfusion) perfused hearts versus hearts that underwent static preservation. *-$p<0.05$ vs static time point.

Our lab has also shown that hypothermic machine perfusion is promising for recovery of marginal donor hearts. Perhaps the most severe example is retrieval of organs from after so called “donation after circulatory determination of death” (DCDD). In these donors, cessation of pulse and pressure have been deemed the cause of death. In another canine study by our group, DCDD hearts showed improved recovery of function, reduced cell apoptosis, reduced creatine kinase and troponin release when perfused with the LifeCradle (Brant et al. 2014).

Experimental models suggest hypothermic machine perfusion is not only a more effective cardiac preservation method, but it also presents the opportunity to revive hearts that might have been previously rejected or not even been considered for transplantation, thus increasing the donor pool.

1.4 Perfusion Solutions

Though cardiac machine perfusion has proven more effective than static preservation in maintaining and improving cardiac viability, the ideal perfusion solution (perfusate) with which to perfuse the heart remains unknown.

1.4.1 Whole or Modified Blood

In vivo, the heart circulates blood. Whole blood is around 7.35-7.45 in pH and is composed of plasma and formed elements. The majority of plasma consists of water while proteins (albumin, fibrinogen, and globulins), nutrients, gases, electrolytes, and waste products make up the minority. The formed elements that make up the other half of whole blood include red and white blood cells and platelets. Whole blood functions as a transporter: it moves gases, proteins, iron, glucose, fatty acids, vitamins, enzymes and other molecules throughout the body delivering them to their correct locations. It also maintains homeostasis by regulating pH, temperature, and water retention and protects against pathogens and clotting. Delivering the same substance that the heart normally circulates seems like the most obvious choice of perfusate and has been used in perfusion models. In the aforementioned OCS normothermic device, at least one liter of blood from the donor is used to prime the perfusion device and the blood is subsequently passed through a leukocyte filter (which removes white blood cells to

mitigate adverse reactions) before entering the organ in a pulsatile manner (Macdonald et al. 2016).

Modified blood has also been investigated as a perfusate solution. White blood cells and platelets can be removed from donor blood through a centrifugation protocol involving numerous wash and spin steps. The remaining red blood cells can be added to an oxygenated crystalline and electrolyte buffer composed of dextran albumin and used as a perfusate (Sutherland and Hearse 2000). Edema is minimized and coronary flow mimics *in vivo* rates. However, haemolysis has been shown(Sutherland and Hearse 2000; Bell, Mocanu, and Yellon 2011) and remains a concern. In addition, the process of preparing this solution is expensive, time-intensive, and complex. Autologous blood diluted with a buffer solution in a normothermic model has also been shown to replenish ATP and reduce the release of markers of cardiac injury (Tolboom et al. 2015). Though whole blood and modified blood perfusates might be more physiological substrates for perfusion, they add another layer of complexity to an already complicated heart transplantation procedure.

1.4.2 Celsior and UWMPS

Preservation solutions are therefore a critical component to maintain the machine perfused heart. Surprisingly few data are available regarding the optimal solution for cold perfused heart. Heart preservation solutions are broadly classified as intra or extracellular based on whether the sodium and potassium concentrations are similar to the extracellular or intracellular environment. None of been specifically developed for perfusion preservation of donor hearts. Celsior (Genzyme Corp., Cambridge, MA) and

University of Wisconsin Machine Perfusion Solution (UW-MPS) (Trans-Med Corp, Elk River, MN) are extracellular solutions delivering a relatively low concentration of potassium and high concentration of sodium to the heart. UWMPS mimics the intracellular environment by delivering a high concentration of potassium and low concentration of sodium. The composition of Celsior
and UWMPS are shown in Table 1.1.

	CELSIOR	UW	UW-MPS	KHB
PH	7.3	7.4	7.4	7.4
GLUCOSE	5.5	--	10	5.5
ADENOSINE	None	5	None	None
POTASSIUM	15	125	25	4.7 (NK) 20 (CP)
LACTATE	None	None	None	1.2
PYRUVATE	None	None	None	0.12
SODIUM	100	29	100	118
FATTY ACIDS	None	None	None	0.35
BICARBONATE	None	None	None	22
GLUTAMATE	20	None	None	None
MAGNESIUM	13	5	None	1.2
LACTOBIONATE	80	100	None	None
HYDROXYETHYL STARCH	None	5% (50g/L)	5% (50g/L)	None
MANNITOL	60	None	30	None
RAFFINOSE	None	30	30	None
HISTIDINE	30	None	None	None
POTASSIUM PHOSPHATE (MONOBASIC)	None	25	25	1.2
DEXTROSE	None	None	10	None
CALCIUM CHLORIDE	None	0.5	0.5	1.2
MANNITOL	None	None	30	None
ALLOPURINOL	None	1	1	None
ADENINE	None	None	5	None
RIBOSE	None	None	5	None
SODIUM GLUCONATE	None	None	85	None
HEPES	None	None	10	None
GLUTATHIONE (REDUCED)	3	3	3	None

Table 1.1: Perfusion Solution Compositions. All values in mmol/L unless otherwise noted. NK=Normokalemia. CP=Cardioplegia.

Differing from other solutions celsior also contains glutamate which has shown anti-ischemic effects (Minasian et al. 2015). Celsior has been previously used in lung preservation while UWMPS was originally developed for pancreatic preservation (Wittwer et al. 1999; Wahlberg Ja Fau - Love et al. 1987). While both are hypothermic perfusion solutions, celsior differs in that it lacks an oncotic agent. UWMPS contains hydroxyethyl starch which regulates osmotic pressure and reduces edema. Both perfusates have been extensively investigated in porcine, canine, murine transplant models, and clinically as well as comparative analysis of the two versus each other(Li et al. 2016; Cobert et al. 2010; Mohara et al. 1999; Warnecke et al. 2002; Kajihara et al. 2006). A twelve hour canine transplantation study determined that Celsior better maintained mitochondrial structure than UWMPS and showed faster recovery of left ventricular pressure (Mohara et al. 1999). However, our lab has shown that UWMPS better controls edema and weight gain in a canine model using the LifeCradle (Figure 1.6) (Cobert et al. 2010). Celsior and UWMPS are the most common hypothermic machine perfusion solutions, but a general consensus on the best solution has not yet been reached.

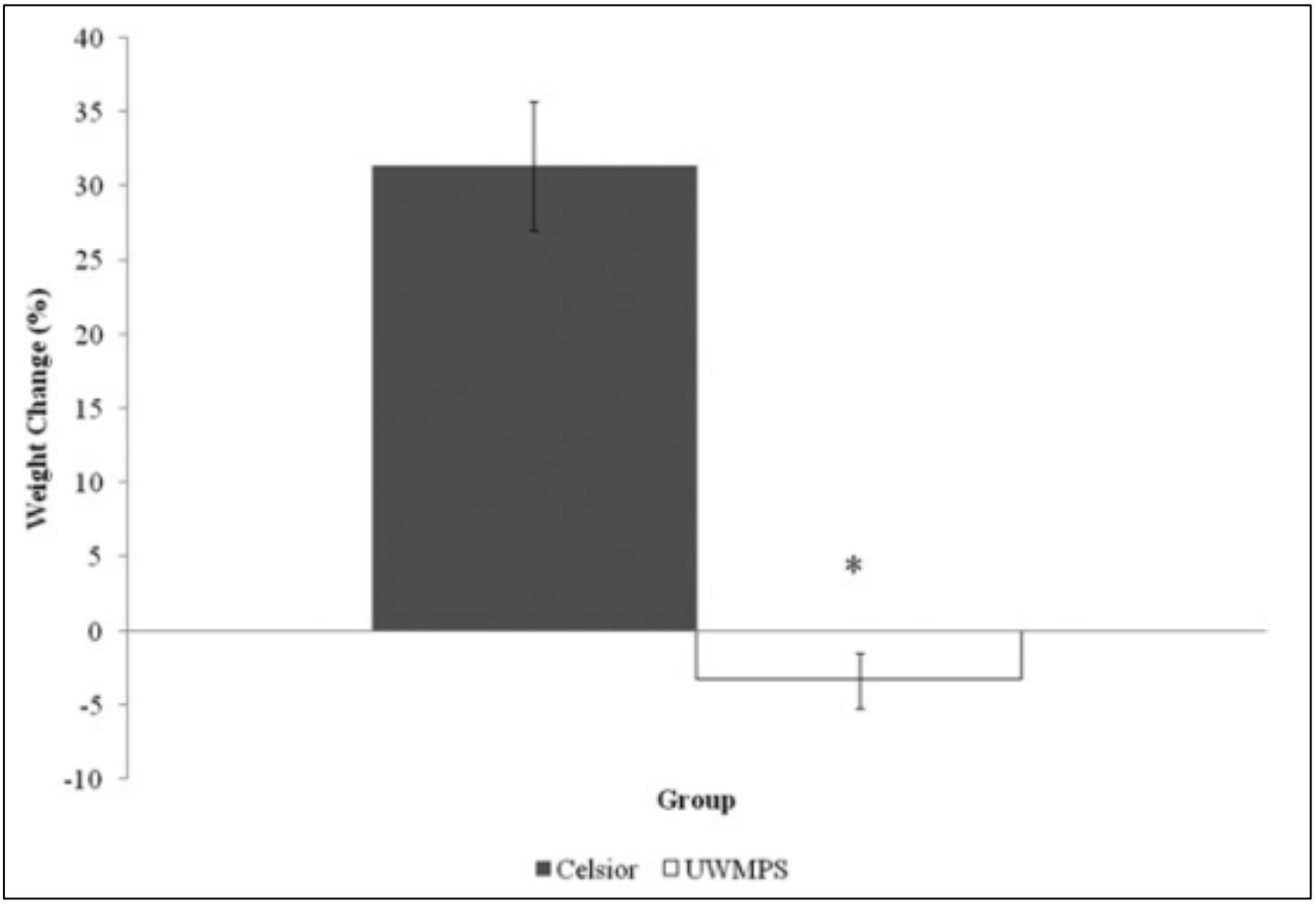

Figure 1.6: Hypothermic Machine Perfusion Comparing the effect of Celsior and UWMPS perfusion solutions on weight change in the myocardium.

1.4.3 Krebs-Heinslet Buffer

Krebs-Heinslet buffer (KHB) is a perfusion solution of physiologic electrolyte concentration also commonly used for isolated heart perfusion. It is composed of glucose, fatty acids, potassium, sodium, calcium, bicarbonate, magnesium, albumin and acetoacetate at varying concentrations shown in the table below. These components make it easy to modify the solution in a laboratory setting and vary the concentration of potassium to vacillate between high potassium and low potassium solutions (Minasian et al. 2010). This solution includes competing substrate which supplies the heart

energy and maintains electrolyte balance. KHB must be oxygenated during preparation and during delivery to the heart in order to adequately deliver oxygen. Southworth and group reported the low oxygen-carrying capacity of KHB buffer and the effects it had on heart function (Southworth et al. 2005). KHB has been demonstrated to have carrying capacity of oxygen that is ten times less than blood, but this group demonstrated that Krebs buffer increased the wall thickness of perfused hearts (Southworth et al. 2005; Kammermeier H Fau - Rudroff and Rudroff 1972). Though it is supposed to mimic a physiological buffer, it lacks certain factors like vasoconstrictors or enzymes secreted into the blood and circulated to the heart *in vivo.* Aims in my project will further investigate additives to KHB in an *ex vivo* perfusion model.

Optimization of perfusion solutions represents a crucial step in improving hypothermic machine perfusion as no ideal heart perfusate exists yet that is widely adopted. Interestingly, perfusion solutions represent a unique entrance into cardiac viability. They can serve as a delivery vehicle for numerous compounds and molecules that can improve cardiac viability. Determining the ideal substrates to deliver and how they affect the heart in a perfusion model represents an interesting avenue of research and will be discussed in this dissertation.

1.5 Myocardial Substrates

The heart consumes a large amount of energy and has a high oxygen demand. These are essential to maintaining cardiac functions like contractility and propulsion of blood throughout the body. The heart itself does not have large stores of ATP compared to other organs because of its high ATP hydrolysis rate—the pool of ATP in the heart turns over every ten seconds (Lopaschuk et al. 2010). Extra demand, external stress, or

surgical procedures could alter this rate as this rate reflects heart behavior at rest. Creatine phosphate also serves as another high energy phosphate in the heart and can be converted to ATP through a creatine kinase catalyzed reaction. Ketones, fatty acids, carbohydrates are the main substrates used to generate energy through their breakdown and the incorporation of their products into the tricarboxylic acid (TCA) cycle for use in oxidative metabolism. The heart is a metabolically flexible organ in that it can readily switch the substrate it consumes under different conditions including varying circulating substrate concentrations. Fatty acids are the preferred source of energy in a non-diseased, beating adult heart *in vivo.* Fatty acids are taken up from the plasma via transport proteins and undergo beta oxidation. During this process, fatty acids go through an oxidation reaction to yield acetyl-CoA, NADH and FADH2. Acetyl-CoA then enters the Krebs cycle for oxidative metabolism. A common fatty acid, palmitate, yields 8 moles of acetyl-coA whose incorporation into the TCA cycle and electron transport chain yields 108 moles of ATP (Weiss and Maslov 2004). It is regulated by oxygen supply status, the presence of other substrates and amount of fatty acids available, hormonal regulation, and alterations in TCA cycle activity. 60-90% of acetyl-CoA generated for the heart stems from fatty acids while the remaining percentage stems from pyruvate generation from lactate and glycolysis (Stanley, Recchia, and Lopaschuk 2005b). When the heart is under stress, like during exercise, fatty acid uptake and oxidation increase in response. However, the increased presence of a competing substrate, lactate, at certain concentrations, might decrease fatty acid uptake in favor of lactate.

Glucose is a commonly used carbohydrate in the heart. It is transported into

cardiac cycles through specific transporter (GLUT 1 and GLUT 4). After phosphorylation, glucose is either stored as glycogen for later use or undergoes glycolysis for more immediate utilization. Glycolysis yields 2 pyruvates and 2 ATP molecules—this accounts for only 4% of ATP generated in the heart (Weiss and Maslov 2004). Generation of TCA cycle intermediates by pyruvate is considered an anaplerotic reaction and occurs through carboxylation or transamination reactions. Carboxylation results in malate and oxaloacetate while transamination with glutamate forms alpha-ketoglutarate and alanine. Lactate production from pyruvate occurs under anaerobic conditions in the heart and is catalyzed by the enzyme, lactate dehydrogenase. Pyruvate is converted into acetyl-CoA through a decarboxylation reaction catalyzed by pyruvate dehydrogenase (Figure 1.7). This acetyl-CoA then enters the TCA cycle to fuel the Krebs cycle. If free fatty acids are present in high concentrations, then pyruvate and glucose uptake are significantly reduced (Wu, Peters Jm Fau - Harris, and Harris 2001; Huang et al. 2002). Ketones are also used by the heart, but they are only produced by the liver during fasting states or instances of low glucose circulation. When present, they undergo oxidation and also enter the TCA cycle to generate fuel through oxidative phosphorylation.

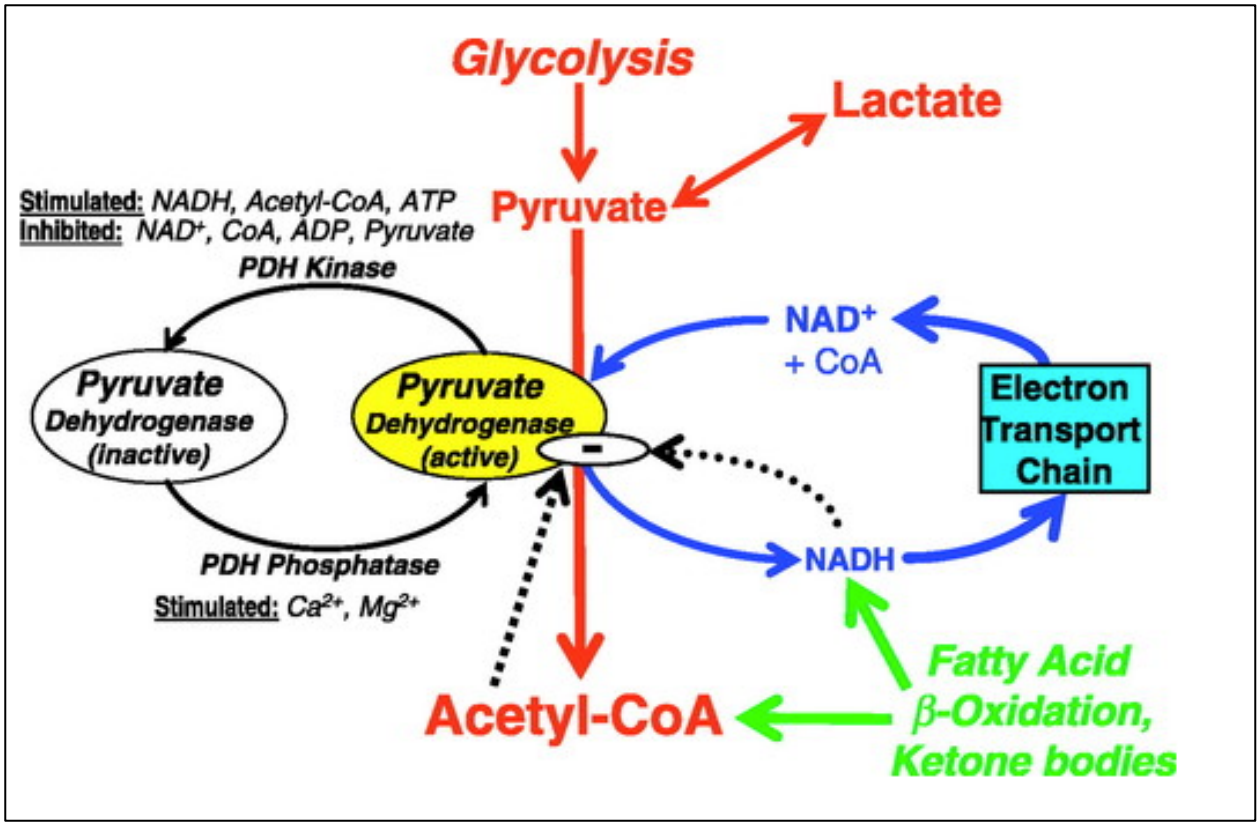

Figure 1.7: The generation of Acetyl-CoA by various energetic substrates (Stanley, Recchia, and Lopaschuk 2005b).

Heart issues like ischemia, heart failure, and diabetes can result in an alteration of substrates utilized by the myocardium. Overall issues include decreased ATP (which results in contractility problems) stemming from mitochondrial membrane fissures and electron chain transport deficiencies. In the case of diabetes, ischemia or fasting, concentrations of ketones are present, and their oxidation is increased due to inhibition of fatty acid oxidation. Pyruvate dehydrogenase is also inhibited in this state and pyruvate oxidation is decreased in favor of lactate oxidation. The aging heart has a lower rate of fatty acid uptake and oxidation as evidenced by a study comparing the hearts of 69 and 29 year old patients (Kates et al. 2003). The final common pathology in the diseased heart is end-stage failure. In a cardiomyopathy model, hearts removed

from the recipient (failing heart) showed a reduction in fatty acid oxidation due to reduced enzymatic activity in this oxidation pathway as further evidenced by reduced gene expression assays. Glycolytic enzymes and pyruvate dehydrogenase were also downregulated in a canine model (Sack et al. 1996; Lei et al. 2004). Understanding myocardial substrate utilization in the normal heart is critical to maintenance of the heart.

In addition to controlling the composition of oxidative substrates, other agents may alter substrate utilization by the myocardium. Substrates include insulin, which activates pyruvate dehydrogenase, and metabolically active drugs. An increasing number of recipients and donors have diabetes mellitus. Metformin has been shown to have beneficial effects even in patients without diabetes. Circulating metformin in donors or recipients could affect myocardial metabolism under those circumstances. While there are a myriad of possible drugs that can influence metabolism those involved with diabetes are amongst the most common and serve as a source of additional investigation in this research.

1.6 Nanoparticles targeting the heart

The heart transplant storage interval provides unique avenues to investigate delivery of molecules or substrates to the isolated organ *ex vivo*. Specifically, the perfusate solution serves, theoretically, as an excellent carrier for delivery of substrates or molecules in a localized manner. Exogenous drug, substrate, and gene delivery are potential therapeutic avenues for optimizing cardiac viability during perfusion. However, certain products, like miRNA or siRNA, require specific carrier to be taken up by cells.

To deliver gene products, a vehicle must be used in order to minimize degradation. Nanoparticles have been widely investigated for the delivery of drugs, small molecules, and more recently, nucleic acid products. Nanoparticles are spherical particles whose size is on the nanoscale and are used to deliver an encapsulated product to an organ, cellular compartment, or other site. The term encompasses a broad class of particles made of various materials including: dendrimers, liposomes, metallic nanoparticles and polymeric nanoparticles (Figure 1.8). Dendrimers are branched polymer structures

which contain the molecules to be delivered on their branches. Delivery molecules can also be placed in the core of the branched structure but must be immobilized there in

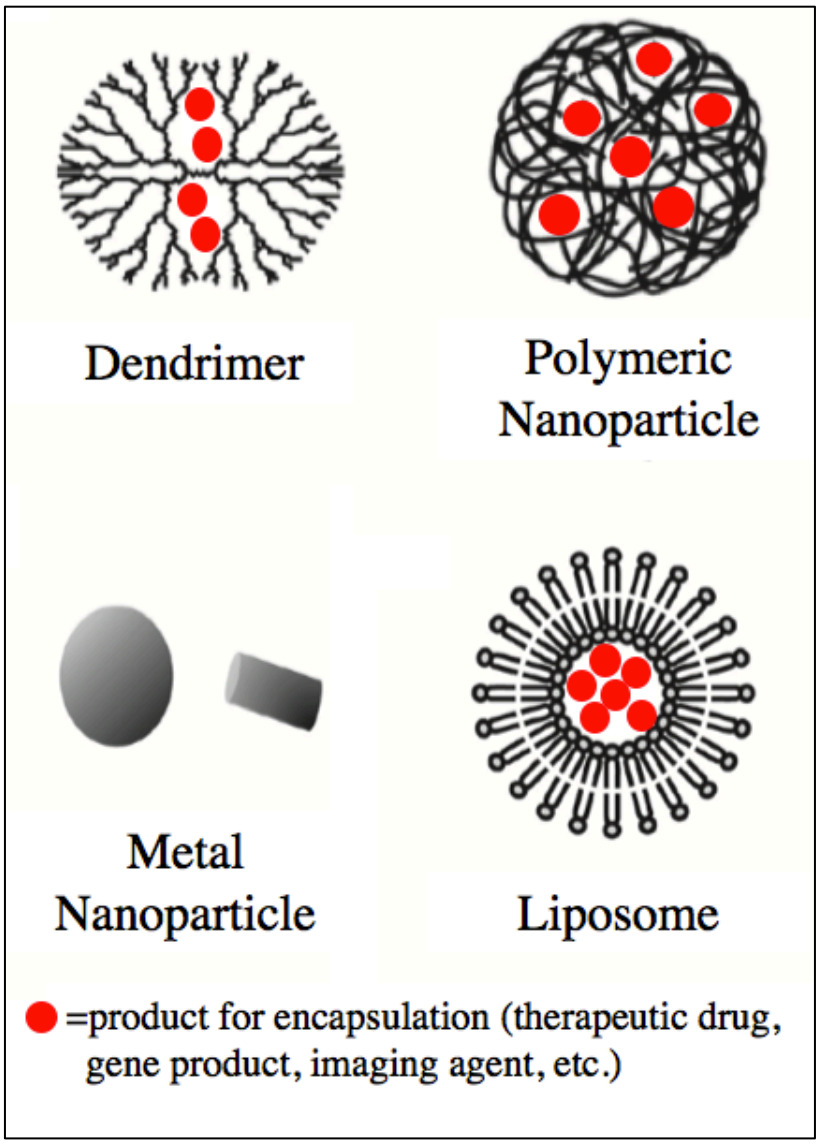

Figure 1.8: Particle Delivery Systems. Modified from Matoba et al (Matoba and Egashira 2014).

some manner in this type of particle. Toxicity to cells has been an issue central to dendrimers as delivery tools. Inorganic particles are most often made of metallic or ceramic materials. Gold, aluminum, and silica have been used to fabricate inorganic particles. Gold nanoparticles have been used for diagnostic and thermally-activate tumor dissipation(Hirsch et al. 2003). However, they are incapable of biodegradation.

Liposomes are composed of bilayers of phospholipids and can be loaded with both hydrophobic and hydrophilic compounds in their core. Their biostability is short though recent formulations have added functional groups in order to improve their stability. Polymeric nanoparticles are one of the most widely researched nanoparticle categories. They can be fabricated by a myriad of methods, are biodegradable, and are biocompatible. They possess the ability to circulate for long periods of time and the release profile of the encapsulated moiety can be tuned by selecting materials with desired degradation rates. Insoluble drugs can be encapsulated in the core while soluble drugs can be functionalized to the surface of the shell. Nanoparticles are advantageous because they have highly tunable properties. The degradation of the particle affects the release of the product inside and both of these properties can be sped up or slowed down based upon the material used to fabricate the nanoparticle. Common polymers used for nanoparticle formulations include: poly (lactic co glycolic acid) (PLGA), Poly (lactic acid) (PLA), poly (caprolactone) (PCL), poly (glycolic acid) (PGA), and poly(ethylenimine) (PEI). Both PLGA and PLA have been approved by the Food and Drug Administration (FDA) for human use. PLL and PEI are both cationic polymers whose positive charge allows for efficient nucleic acid packing and delivery. However, both polymers demonstrate high cytotoxicity and aggregation (Park, Jeong Jh Fau - Kim, and Kim 2006). Polymeric nanoparticles are advantageous because of their ability to be formulated with targeting ligands and polyethylene glycol (PEG) for enhanced circulation and uptake. Nanoparticles have been researched as vesicles to deliver targeted therapies to the infarcted heart (Devulapally et al. 2015; Dvir et al.

2011). Nanoparticle inclusion in a perfusion solution for heart transplantation represents a fusion of therapeutic and surgical care.

Distribution of particles in the tissue or to specific organs is dependent, among other factors, on size or the addition of targeting moieties (peptides, ligands, etc.) on the nanoparticles. Nanoparticles less than 20nm in diameter circulate for a longer period of time resulting in a lower accumulation in tissue and higher accumulation circulating through the vessels. Particles less than 5nm are cleared through the kidney and particles delivered intravenously tend to accumulate in the liver and spleen (Soo Choi et al. 2007; Ilium et al. 1982; Alexis et al. 2008). Particles between 20-100nm are able to avoid clearance from capillary beds and larger particles (200nm-4 microns) show better delivery efficacy via localized injections. Particles over 5 microns in diameter have been shown to form emboli in vessels while a similar embolic effect has been seen in smaller particles as well. Particles less than 100nm can aggregate into larger masses and have the same embolic outcome of blood vessel occlusion (Dvir et al. 2011). Cellular uptake of particles can occur by various size dependent manners. Phagocytosis encompasses the internalization of particles that are larger (on the micron scale). Phagocytosis does not occur in all cells and is found in phagocytic cells like dendrites, macrophages, and neutrophils. Pinocytosis of nanoparticles can occur in all cells and with particles that are less than one micron in size. In this uptake process, the cells membrane forms vesicles around the extracellular fluid and then internalizes these vesicles that contain a sampling of the fluid. This sampling indirectly results in the uptake of any solutes present in the extracellular fluid at that time including electrolytes or, in the desired case, nanoparticles. Particles that are 60-150nm in size can be taken up by receptor

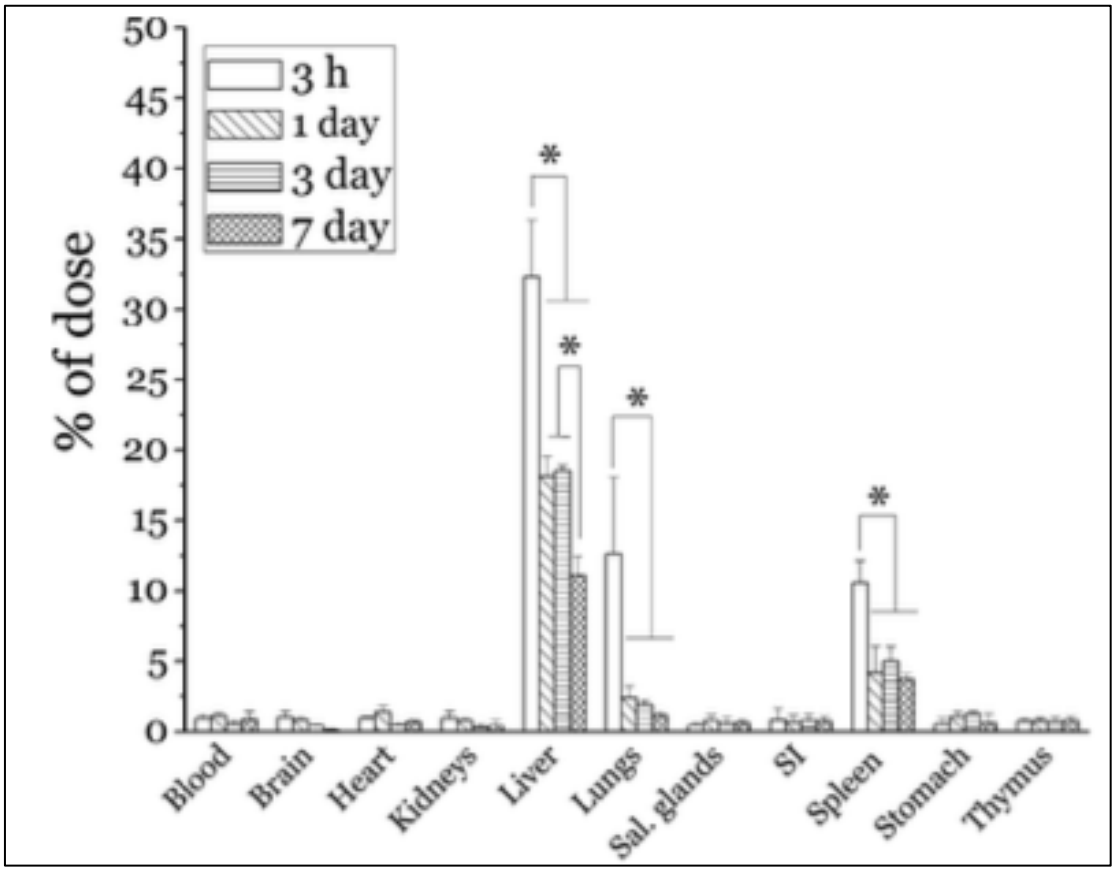

Figure 1.9: Biodistribution of polymeric nanoparticles in various organs after intravenous delivery after 3 hours, 1 day, 3 days, and 7 days (Mohammad and Reineke 2013).

mediated endocytosis. Particles are incorporated into the cytosol by association with a cellular membrane receptor. These particles are then taken up into the endosome of the cell where they either escape the endosome or are transferred to the lysosome. Lysosomal particles are degraded with the lysosome while particles that escape the endosome through diffusion are then able to either reach the nucleus or mitochondria. Once at their designated site of action, the contents of the nanoparticle can then carry out their desired effect. Any nanoparticle must be designed with the following abilities in mind: loading efficiency, cellular uptake, release from the endosome and into the cytoplasm, particle degradation to release the inner contents, and degradation and clearance of particle byproducts (Bishop, Kozielski, and Green 2015). In the heart,

nanoparticle internalization in cardiac cells is determined by mode of delivery of nanoparticles. Intravenous delivery is not an effective method when targeting the heart as systemic delivery has been shown to result in less than 5% of the delivered particles reaching the heart at various time points (3 hours, 1 day, 5 days, and 7 days) in a PLGA nanoparticle delivery system via tail vein injection, while the majority accumulates in the liver and spleen (Figure 1.9) (Mohammad and Reineke 2013).

Nanoparticles are a promising method of drug delivery due to their highly tunable properties. It is necessary to keep in mind that tuning these properties may result in varied interactions with the body. Toxicity of nanoparticles can stem from, but is not limited to, choice of nanoparticle material, surface charge, amount of particle delivered and particle geometry. Nanoparticles made from polyethylenimine (PEI) show great efficacy in encapsulating negatively charged molecules, however they have also been shown to exhibit high rates of cell death in cellular biocompatibility assays. In addition to causing occlusions, nanoparticles can trigger an inflammatory reaction through the release of cytokines and generation of reactive oxygen species. Spherical particles have been the chosen method of particle design in many instances because their symmetry allows for uniform flow and more rapid internalization (Petros and DeSimone 2010). Overall, nanoparticles demonstrate an effective delivery vehicle of therapeutics to cells and delivery to an isolated organ will be investigated in my dissertation.

1.6.1 Gene Delivery

Gene delivery is a promising treatment for many cardiac diseases and is an area of

intense investigation. Treatment of ischemia with vascular endothelial growth factor (VEG-F) 121 delivered by viral vectors in a porcine heart model resulted in angiogenesis and increased perfusion to regions of ischemia through creation of new vessels (Mack et al. 1998). However, antibody formation was observed indicating an inflammatory response. This method of viral gene delivery also required injection directly into the heart via the left anterior descending coronary artery in order for the gene product to reach its site of action without being degraded or causing systemic toxicity issues. Antioxidant gene therapy to reduce reactive oxygen species generation in cardiomyocytes has been investigated as treatment for myocardial reperfusion injury. Studies delivering the superoxide dismutase gene, a cardioprotective antioxidant, have been shown to reduce apoptosis, necrosis and decrease infarct size (Li et al. 2001; Yang et al. 2003; Li et al. 2017; Agrawal et al. 2004). Delivery of endothelial nitric oxide synthase (eNOS), a cardioprotective molecule, before and after induction of myocardial infarction showed decreased apoptosis and necrosis, decrease tumor gene expression, and increased contractility (Smith et al. 2005; Chen et al. ; Chen, Yin H Fau - Huang, and Huang 2007). All instances above used a viral vector for delivery. Though gene therapy is effective in the cardiac arena, long-term safety and efficacy data is non-existent. Viral vectors suffer from immune response issues and high cost of fabrication. Producing viral vectors for gene delivery would prove difficult to scale and must be balanced against the immune response they confer on the patient. Viral vectors often must be delivered locally to their site of action as attaching targeting ligands and modifying these vectors prove difficult.

1.6.2 MicroRNA

MicroRNA (miRNA) is another genetic product with therapeutic promise. miRNAs are short (20-25 nucleotides), non-coding nucleotide strands found endogenously with gene expression altering capabilities. They affect gene expression by either repressing mRNA translation or degrading mRNA. The 5' end of miRNA has the ability to bind to the miRNA recognition element (MRE) on any untranslated 3' region of mRNA. The MRE is only 5-8 nucleotides long, meaning complete complementarity of miRNA for mRNA is not required to exert its effect. One specific miRNA can bind to many mRNA strands and repress expression of an entire set of genes. Additionally, one miRNA can be found in many different locations. miRNA can localize to the nucleus and to the cytoplasm indicating that it can exert its effect in either compartment depending on the particular miRNA (Liao et al. 2010; Kotipalli A Fau - Gutti, Gutti R Fau - Mitra, and Mitra 2016). Many miRNAs have been found to play a role in cardiac function. These miRNAs can be divided into two categories: injury causing and cardioprotective. MiRNAs that are overexpressed in cardiac injury include miR-1, miR-29, miR-208, miR-320 (Qian et al. 2011; Kukreja, Yin C Fau - Salloum, and Salloum 2013; Bostjancic et al. 2010; Barringhaus and Zamore 2009). The presence of miR-1 and miR-29 are linked to increased apoptosis while transgenic mice for miR-320 showed increased infarct size and cardiomyocyte death in an ischemia/reperfusion model (Ren et al. 2009). Elevated miR-208 levels have been linked to a hypertrophic phenotype in cardiomyopathy (Callis et al. 2009). MiRNAs with a cardioprotective properties include miR-21, miR-24, miR-126, miR-133 and miR-499 (Kukreja, Yin C Fau - Salloum, and Salloum 2013; Fan et al. ; Dong et al. 2009; Barringhaus and Zamore 2009; Yu and Li 2010). miR-21, miR-24,

miR-133 and miR-499 have been showed to have anti-apoptotic affects while miR-126 shows an increase in angiogenesis in ischemia reperfusion injury by aiding in VEGF and FGF actions (Wang et al. 2008; Harris et al. 2014). Through downregulation or upregulation, the behavior of miRNA can be attenuated to lessen cardiac injury. Depending on the desired effect, miRNA mimics, nucleotide strands that mimic endogenous functions of miRNA, can be introduced to induce and increase the positive effect of the specific endogenous miRNA. MiRNA inhibitors (anti-miRs) can also be introduced if the desired effect is the downregulation or repression of endogenous miRNA to reduce a negative effect. miRNA mimics must suffer from a short half-life. Anti-miRs can be single stranded and still bind to endogenous miRNA to exert their inhibitory effect. Modifications to mimics to increase their stability might affect their function while modifications to anti-miRs are less difficult and can improve affinity(Gadde and Rayner 2016). Introducing miRNA to the heart represents a similar challenge as described with gene delivery. Naked delivery is not a viable option as most of the product would never reach its intended site due to degradation. Nucleic acid can survive in an extracellular environment for ten minutes and for one hour in an intracellular environment, yet half-life can be improved 3 to 6 fold when complexed with a polymer—protection via encapsulation is necessary for delivery(Chiou et al. 1994; Ha et al. 2011; Vaughan, DeGiulio, and Dean 2006). Large, negatively-charged molecules would also have trouble crossing cellular membranes and any that is passively taken up by scavenger-receptor mediated endocytosis would be degraded in the lysosome. Chemical modifications to nucleic acids have been investigated to reduce immune response and improve delivery, however how this might impair functionality of miRNA

has yet to be elucidated. Non-viral delivery of gene products via encapsulation of nanoparticles would mitigate the above issues. The delivery of miRNA during perfusion could have an advantageous effect on the heart. For the purpose of this study, miRNA will be used as a test product in determining nanoparticle delivery to the isolated organ.

The heart is a complex organ with many pathways for further exploration of transport milieu enhancement. Optimizing a perfusion solution to improve or maintain cardiac viability during transplantation. Described above, altering substrate or determining a delivery vehicle for miRNA products could exert the desired effect and will be investigated in this project. Overall, I hypothesize that the exogenous delivery of substrates and loaded nanoparticles during perfusion will increase oxidative metabolism, reduce injury, and maintain viability in donor hearts.

1.7 Specific Aims

1.7.1 Aim 1: Exogenous Substrate Delivery in Perfusate to Support Oxidative Metabolism

Most current machine perfusion solution are designed for static preservation and they do not optimize oxidative metabolism. Acetate, octanoate, β-hydroxybutyrate, and propionate all indirectly or directly contribute to the TCA cycle. Substrates will be investigated in a Langendorff rodent perfusion model. Blood gas analysis together with coronary flow will be used to investigate oxygen consumption and lactate values. Magnetic resonance spectroscopy and carbon-13 labeling will be used to investigate oxidative metabolism and gas chromatography/mass spectrometry will be used to investigate Tricarboxylic acid intermediate values and their isotopomer abundance*. I hypothesize that the delivery of these substrates in a perfusion solution will increase oxidative metabolism to alter viability during machine perfusion.*

1.7.2 Aim 2: Metformin and Insulin as Perfusate Additive to Alter Substrate Selection

Metformin has a cardioprotective effect on outcomes after cardiac surgery but insulin has been used in preservation solutions to improve glucose uptake (Rudd and Dobson 2011). The exact mechanism of this effect is unknown. The addition of these drugs could act as a switch for the heart and result in use of metabolically favorable substrates which may induce changes in myocardial substrate selection. Effects will be investigated in a rodent Langendorff non-recirculating perfusion model. Blood gas analysis will be used to investigate oxygen consumption and lactate values. Magnetic resonance spectroscopy and carbon-13 labeling will be used to investigate oxidative metabolism. Cardiac functionality will be evaluated using ventricular pressure

measurements. *I hypothesize that metformin alone or metformin and insulin in combination change the substrate the heart oxidizes during cardiac perfusion.*

1.7.3 Aim 3: Characterization of a Perfusion Method for Nanoparticle Delivery

This aim approaches the attenuation of machine perfusion from a second angle, improving cardiac viability by reduced cell death. In this aim, I focus on the construction and characterization of the nanoparticle delivery vehicle using polymeric materials. Characterization will be done to determine the size, polydispersity index, morphology, and zeta potential of the formed particles. Release and loading efficiency will be determined by bioanalyzer using the cardioprotective miRNA-499 for release validation. This aim also focuses on characterization of a perfusion model for *ex vivo* delivery of nanoparticles. Verification of localization of particles in a cardiac perfusion model will be characterized by the delivery of fluorescently labeled particles. The effect of nanoparticle perfusion on cardiac functionality will be characterized by myocardial oxygen consumption and lactate accumulation as determined by blood gas and coronary flow analysis. Phosphorus-31 magnetic spectroscopy will be used to characterize energy stores. *I hypothesize that a polymeric delivery vehicle can be used in an acute perfusion model to deliver therapeutics drugs or nucleic acid.*

Chapter Two

Exogenous Substrate Delivery to Support Oxidative Metabolism

2.1 Introduction

Current cardiac donor preservation involves a period of cold, static storage. While this method is meant to preserve the heart, it has been shown to cause ATP depletion, lactate accumulation, and myocyte damage (Peltz et al. 2008). This method does not adequately support myocardial metabolism and transplant recipient mortality is increased when donor ischemic intervals exceed three hours (Lund et al. 2016). Machine perfusion has emerged as an alternative for preservation of donor organs. Machine perfusion has been used clinically for the preservation of kidneys, but has only been investigated in a research setting for the preservation of hearts (Brant et al. 2016; Cobert et al. 2012; Peltz et al. 2008). Our laboratory has demonstrated the ability of cold machine perfusion at 5-10°C to maintain energy stores, minimize lactate accumulation, reduce myocardial injury, and improve functional recovery (Peltz et al. 2008; Rosenbaum et al. 2008; Cobert et al. 2014). Ongoing oxidative metabolism during machine perfusion serves as the energy source for the heart during machine perfusion. Fatty acids are the main substrate utilized by the heart under normal conditions. Fatty acids undergo oxidation which yields acetyl-CoA that then enters the tricarboxylic Acid

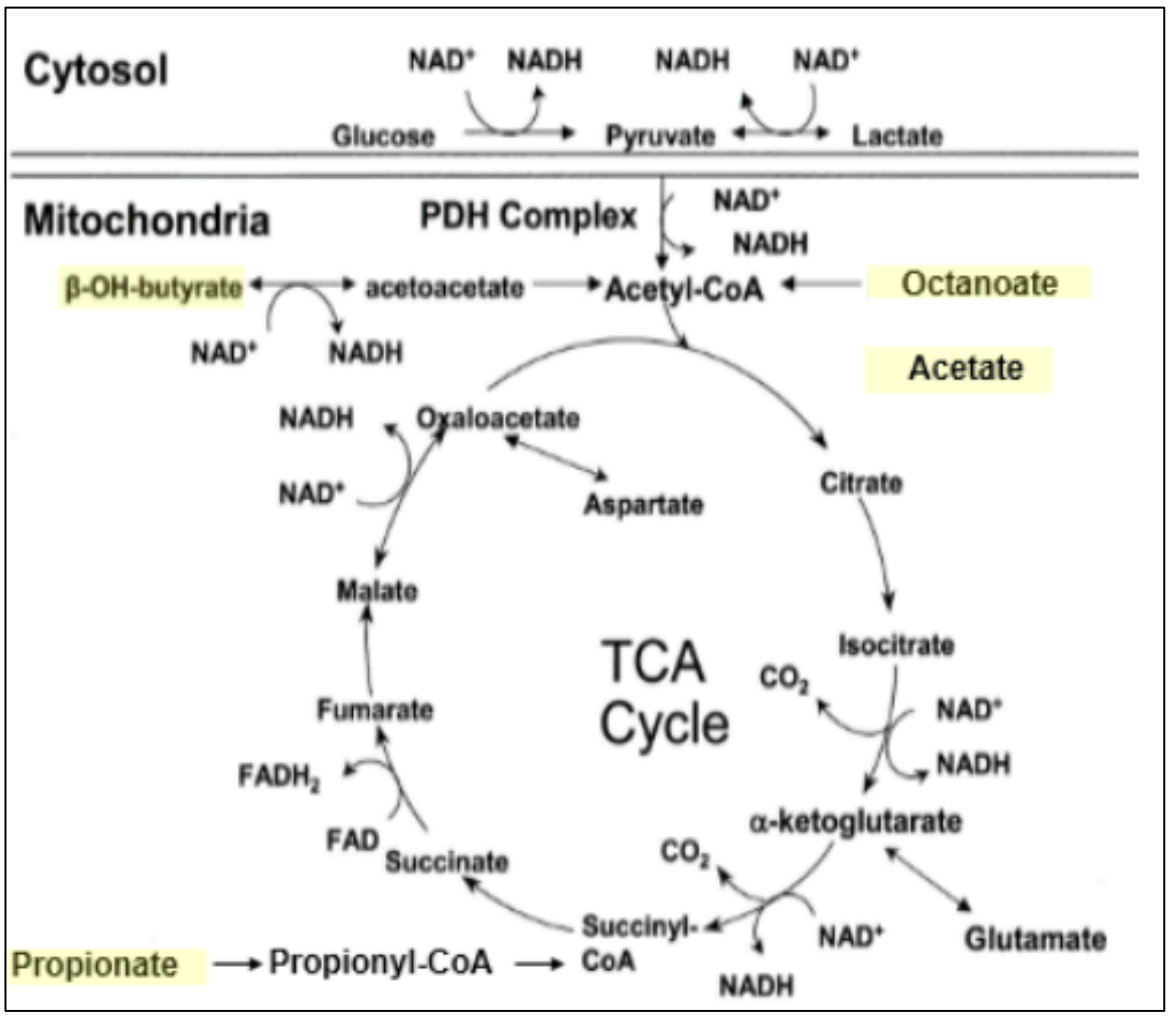

Figure 2.1: Substrate entry into TCA Cycle.

(TCA) cycle to generate the reducing equivalents for oxidative metabolism (Figure 2.1) (Houten and Wanders 2010). Ketones become the dominant substrate oxidized in the potassium arrested heart. Acetate is another simple substrate that is avidly oxidized by the heart (Stanley, Recchia, and Lopaschuk 2005b). Most preservation solutions contain glucose as a substrate. Our lab has previously demonstrated that although myocardial preservation is improved in hearts perfused with glucose containing preservation solutions, glucose is an ineffective substrate for supporting metabolism of the machine perfused heart (Cobert et al. 2012). However, these substances cannot replenish the TCA cycle directly and despite their oxidative potential, may eventually

lead to myocardial functional impairment due to loss of TCA cycle intermediates as previously suggested (Gibala, Young, and Taegtmeyer 2000; Reed et al. 1996). The TCA cycle intermediate pool size is 1-2 micromoles per gram of tissue while flux through the cycle is estimated at 1-2 micromoles per gram per minute (Brunengraber and Roe 2006). Intermediates can be depleted through cataplerosis, where, in this instance, the loss of intermediates stems from membrane leakage. Anaplerosis, or replenishment of these intermediates, is necessary to maintain the overall intermediate pool. Both glutamate and pyruvate are known anaplerotic substances because of their ability to replenish the cycle via alpha-ketoglutarate and pyruvate carboxylase (or malic enzyme) respectively. The intermediate pool can change drastically in various situations like increased stress, fasting, or through increased anaplerosis. Some substrates such as glucose and amino acids, can replenish the TCA cycle intermediate pool but may be limited in supporting myocardial oxidative metabolism. These factors seem to be important factors when designing optimal preservation solutions for the cold-perfused donor heart. I hypothesize that free fatty acids, ketones, and acetate would be preferred oxidative substrates during hypothermic machine perfusion preservation and that an anaplerotic substrate would be required to maintain the TCA-cycle intermediate pool under these conditions.

2.2 Methods

2.2.1 Animals

Male Sprague-Dawley rats weighing 250-450g were given access to food and water ad libitum and were used in a research protocol approved by the Institutional Animal Care and Use Committee at the University of Texas Southwestern Medical Center. All animals were treated in accordance with guidelines set forth in the Guide for the Care and use of Laboratory Animals (National Institutes of Health Publication No. 86-23, revised 1996).

2.2.2 Chemicals

^{13}C labeled compounds were obtained from Cambridge Isotope Laboratories (Andover, Mass), Sigma Aldrich (St. Louis, Missouri), and Isotec (Miamsburg, Ohio). β-hydroxybutyrate, acetate, and propionate were all uniformly ^{13}C labeled while octanoate was 2,4,6,8-^{13}C enriched. Labeled compounds were added to a custom batch of University of Wisconsin Machine Perfusion solution (UWMPS Trans-Med Corp, Elk River, MN, USA) prepared without glucose to create preservation solutions of varying concentrations as explained in the Experimental Groups section. See Table 2.1.

2.2.3 Cardiac Procurement

Rats were anesthetized with an intraperitoneal injection of 4% chloral hydrate. A sternotomy was performed to expose the chest cavity and 300 units/kg of heparin were administered by intrahepatic injection. The inferior vena cava and the superior vena

cava were ligated. The heart was removed, flushed with preservation solution through the aorta, and stored in ice-cold lactated ringers.

2.2.4 Perfusion Solution

Hearts were perfused through the ascending aorta with University of Wisconsin Machine Perfusion Solution. Its composition is illustrated in Table 2. A substrate free batch of UWMPS was used in the current study to allow for substrate modifications in our experiments. The potassium concentration maintains the heart in the depolarized, arrested state.

Compound	UW-MPS (mmol/L)
Sodium Gluconate	80
Sodium Hydroxide	.70 g/L
Total Sodium	100
Potassium Phosphate (monobasic)	25.0
Calcium Chloride (dihydrate)	0.5
Magnesium Gluconate (anhydrous)	5.0
HEPES (Free Acid)	10.0
Total buffer	35.0
Adenine (free base)	5
Dextrose (+)	10
Mannitol	30.0
Gluconate	85.0
Ribose, D(-)	5
Hydroxyethyl Starch	5% (50g/L)
Osmolarity	300 mosmol/kg
pH at 20°C	7.4

Table 2.1: UWMPS Composition

2.2.5 Perfusion Technique

Hearts were mounted on a Langendorff apparatus and perfused by retrograde perfusion through the ascending aorta for 6 hours with or without substrate modified UWMPS at 8 ± 2ºC at 0.5mL/min. Coronary flow, heart rate, and inflow and pulmonary artery perfusate pO_2 were measured every 30 minutes. Myocardial oxygen consumption (MVO_2) was calculated from aortic and pulmonary artery pO_2 differences, coronary flow, and measured temperature. MVO_2 was reported as µmol O_2/gram of dry weight/min(Reed et al. 1996). After the perfusion interval, the atria were removed, and ventricles were weighed. A small sample was placed in an oven for drying to determine dry weight. Specimen were weighed until a constant, stable value was obtained. The ratio between wet and dry weight was calculated to determine water content. Lactate excretion into the preservation solution was measured at each time increment and averaged for each animal. The remaining ventricular tissue was freeze-clamped with liquid nitrogen cooled tongs and stored in a -80^{oC} freezer.

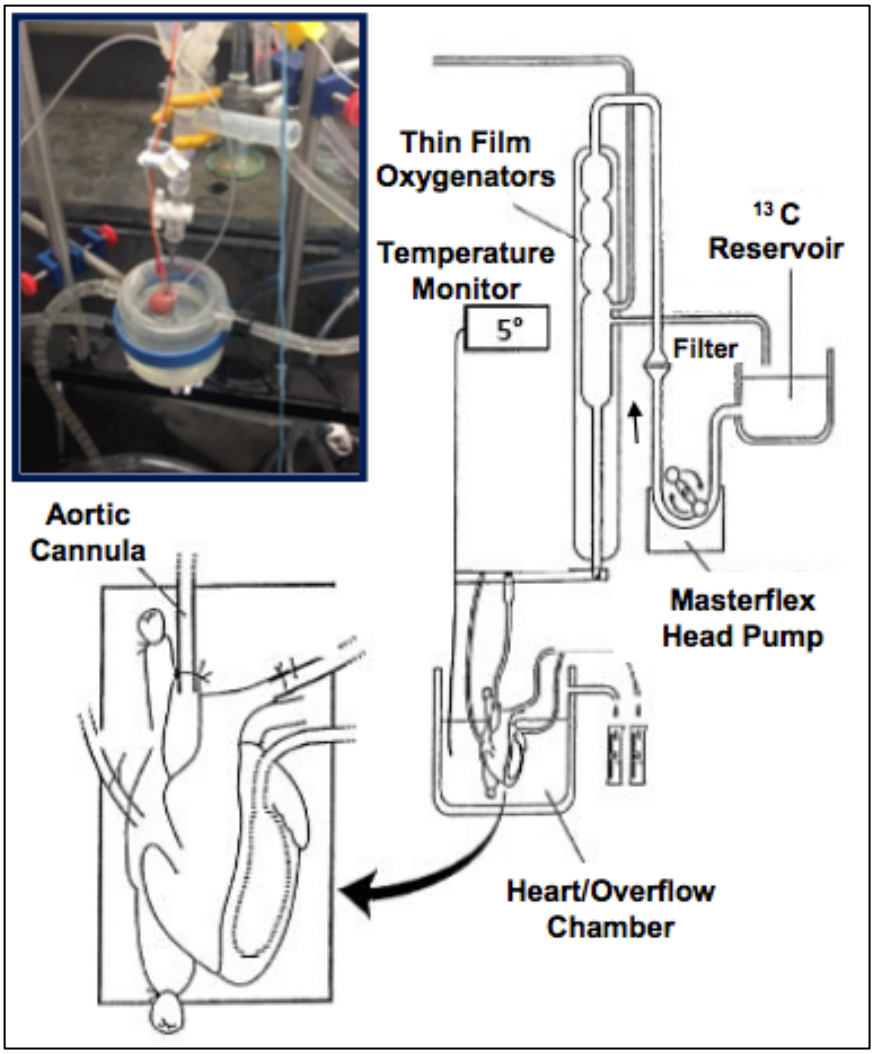

Figure 2.2: Non-Recirculating, Single-Chambered Langendorff Perfusion Apparatus

2.2.6 Tissue Extraction

Myocardial metabolites were extracted by grinding the ventricular tissue sample with mortar and pestle under cooled conditions, employing liquid nitrogen. The pulverized tissue was reconstituted in 4% perchloric acid. Samples for magnetic resonance spectroscopy (MRS) were freeze-dried in a speed vacuum and reconstituted in D_2O. Samples for TCA cycle intermediate analysis were stored at -80ºC.

2.2.7 Experimental Groups

Fourteen groups of rat hearts (n=4/group) including two control groups were studied. 1. The No Perfusion Group evaluated hearts that were recovered immediately after cardiectomy to determine baseline TCA-cycle intermediate concentrations and 2. The No Substrate Perfusion Group was used to evaluate MVO_2 and TCA-cycle intermediates in substrate free UWMPS. Four groups per substrate were analyzed at low and high concentrations of each substrate with and without the potentially anaplerotic species propionate (5mM): Acetate (2mM and 8mM), Acetate + Propionate (2mM and 8mM), β-hydroxybutyrate (0.25 and 2mM), β-hydroxybutyrate + Propionate (0.25 and 2mM) and Octanoate (0.5mM and2mM), and Octanoate + Propionate (0.5mM and 2mM). See Table 2.2.

Acetate	Acetate + Propionate	β-Hydroxybutyrate	β-Hydroxybutyrate + Propionate	Octanoate	Octanoate + Propionate
2mM	2mM	0.25mM	0.25mM	0.5mM	0.5mM
8mM	8mM	1mM	1mM	2mM	2mM

Table 2.2: Experimental Groups

2.2.8 Measurement of Substrate Utilization

Proton decoupled ^{13}C NMR was performed on heart extracts using a 14.1T Varian Inova spectrometer (Varian Instruments, Palo Alto, CA) operating at 600 MHz with a 1-second delay between 45º carbon pulses. Fourier transformation and peak fitting was performed on glutamate carbons using commercially available software (ACD/Labs, Toronto, Canada). Glutamate isotopomer analysis was used to determine the fractional

contribution of each ^{13}C-labeled substrate to oxidative metabolism. Glutamate is an indirect indicator of metabolism as it exists in equilibrium with the TCA cycle intermediate, α-ketoglutarate(Jeffrey et al. 1996). The third, fourth, and fifth carbon were used for this analysis as previously described to determine fractional contribution relative to the contribution of unlabeled, ^{12}C endogenous substrates(Burgess et al. 2001; Reed et al. 1996). Fractional contribution values were determined assuming non steady-state conditions(Malloy, Sherry, and Jeffrey 1990). Amounts of Acetyl-CoA generated by labeled and endogenous substrates were determined using fractional substrate utilization values and specific flux values (Malloy et al. 1996).

2.2.9 Measurement of TCA Cycle Intermediates

Gas Chromatography/Mass Spectrometry (GC/MS) was used to determine absolute concentrations of citrate, succinate, fumarate, and malate. Tissue samples were split, and standard amounts of each desired intermediate were added to one half of the sample (25nanomoles for succinate, fumarate, and malate; 50 nanomoles for citrate). Samples were then concentrated, reconstituted in Tri-Sil for derivatization, and analyzed by GC/MS to yield a spectrum seen in Figure 2.3. The samples with the spiked in standard and the sample without the spiked in standard were then compared to determine raw abundance values. TCA cycle intermediate concentrations were calculated from mass spectrum data using isotopomer analysis as previously described (Chatham, Bouchard, and Des Rosiers 2003) and the software program Metran (Antoniewicz Laboratory, University of Delaware). Isotopomer contribution was derived

from GC/MS data and reflected as a fraction of the total isotopomer abundance.

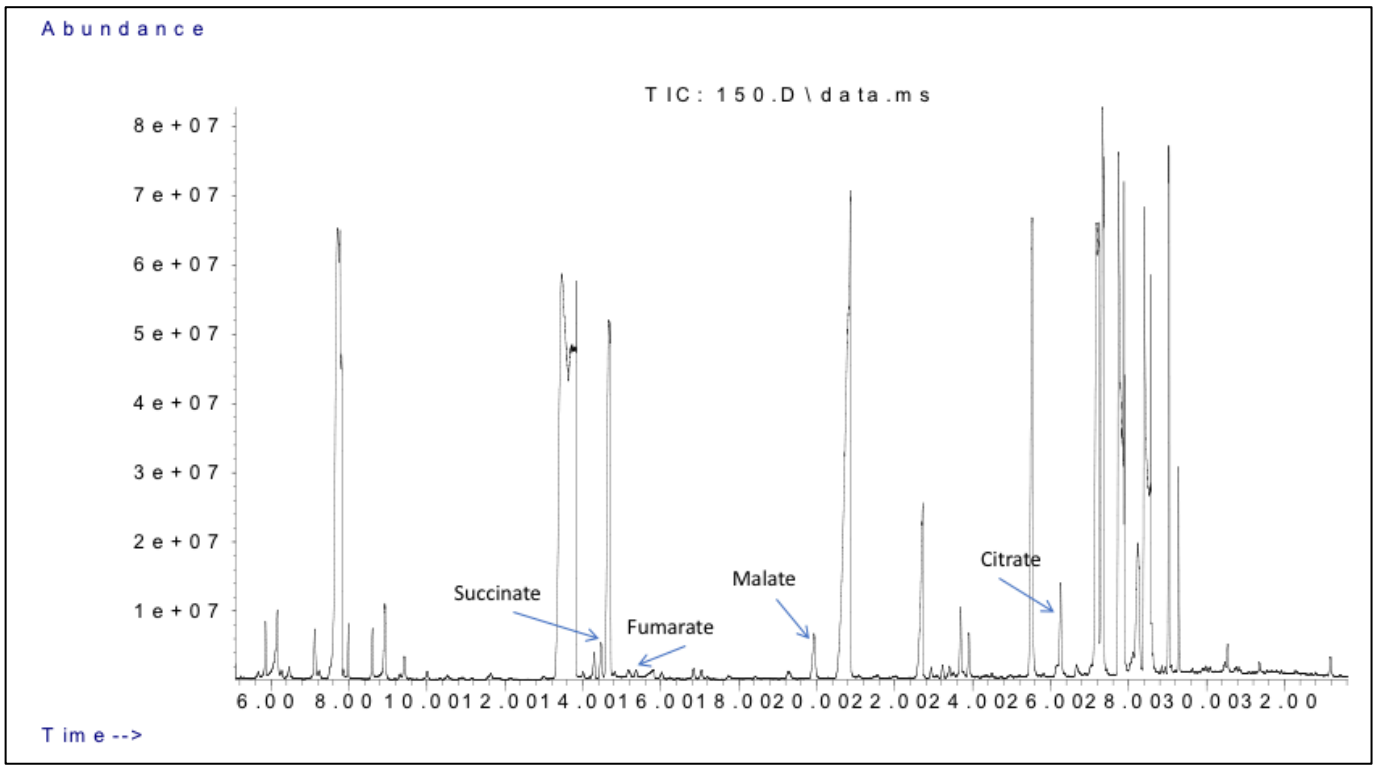

Figure 2.3: GCMS Spectrum showing TCA Cycle Intermediates.

2.2.10 Statistical Analysis

Results are reported as mean and standard error of the mean (SEM). Commercially available software (GraphPad Prism 6, La Jolla, CA) was used for analysis. Groups were compared by analysis of variance and two-sided t-tests as appropriate. A repeated measures analysis of variance was applied to samples compared over multiple time-points. A p-value less than .05 was considered significant.

2.3 Results

2.3.1 Myocardial Oxygen Consumption

Myocardial oxygen consumption (MVO_2) for each substrate concentration was calculated and compared to the substrate free perfusion control group. MVO_2 appeared higher for all substrate containing groups over the entire time interval, reaching statistical significance for a number of perfusion groups (Table 2.3). There was also a tendency for further increasing MVO2 by the addition of propionate though this only reached significance for the .25mM β-hydroxybutyrate containing groups.

	Control	Acetate		β-Hydroxybutyrate		Octanoate	
	No Substrate Added	2mM	8mM	0.25mM	1mM	0.5mM	2mM
No-Propionate	0.56± 0.03	0.941± 0.13	0.72± 0.05	0.76±0.10	1.06± 0.11*	0.95± 0.16	1.16± 0.07*
Propionate	---	1.35± 0.12*	0.86± 0.08	1.04± 0.11*†	1.43± 0.13*	1.08± 0.07*	1.34± 0.06*

Table 2.3: Myocardial Oxygen Consumption (μmol/g*min). *-p<0.05 vs no substrate control. †-0.05 <p vs no propionate group of same concentration.

2.3.2 **Substrate Selection and Acetyl-CoA Production**

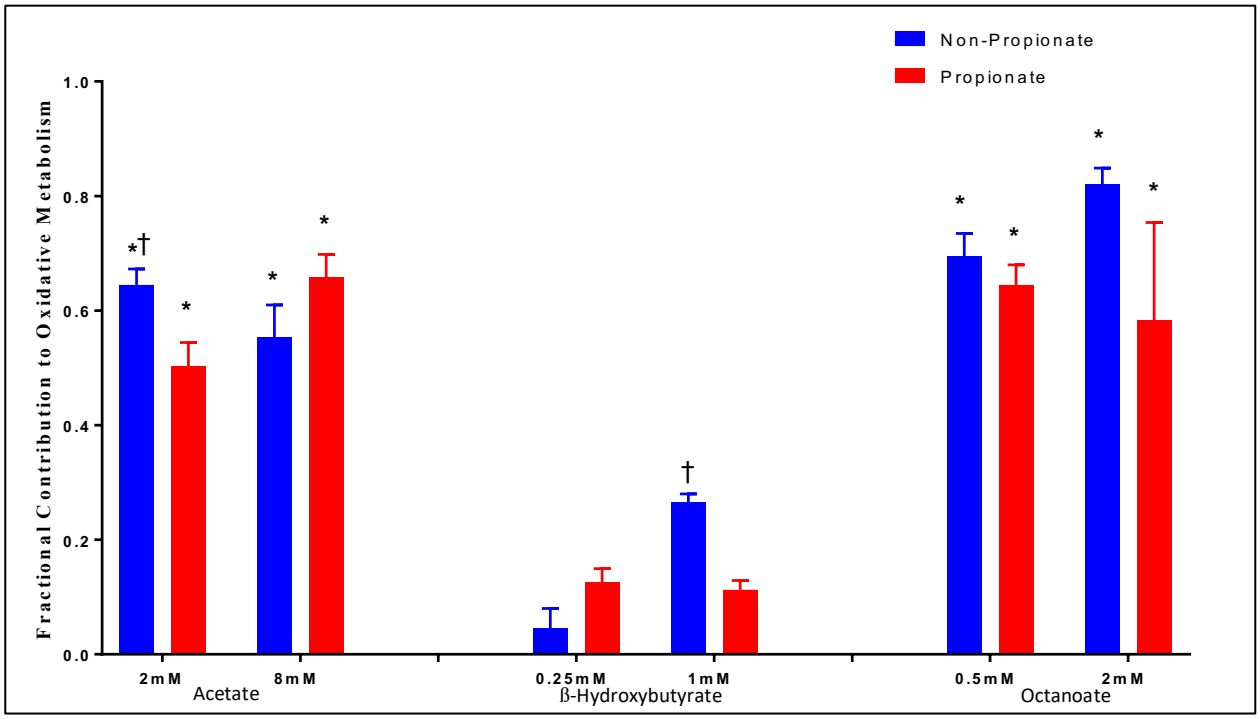

Figure 2.4: Fractional Contribution to Oxidative Metabolism. *- 0.05>p vs 0.25mM BHB. †-0.05>p vs concentration of same substrate of non-propionate group.

Fractional contribution of each substrate to oxidative metabolism was evaluated at non-steady state conditions (Figure 2.4). Both octanoate and acetate were preferred substrates contributing 50-85% to acetyl CoA oxidized through the TCA cycle. BHB was a minor contributor to oxidative metabolism with the substrate contributing 7-30% acetyl CoA though its contribution appeared to increase at the higher BHB concentration. Propionate significantly reduced ketone oxidation at higher concentrations of BHB and lower concentrations of acetate. However, the addition of propionate did not cause significant changes to any other groups.

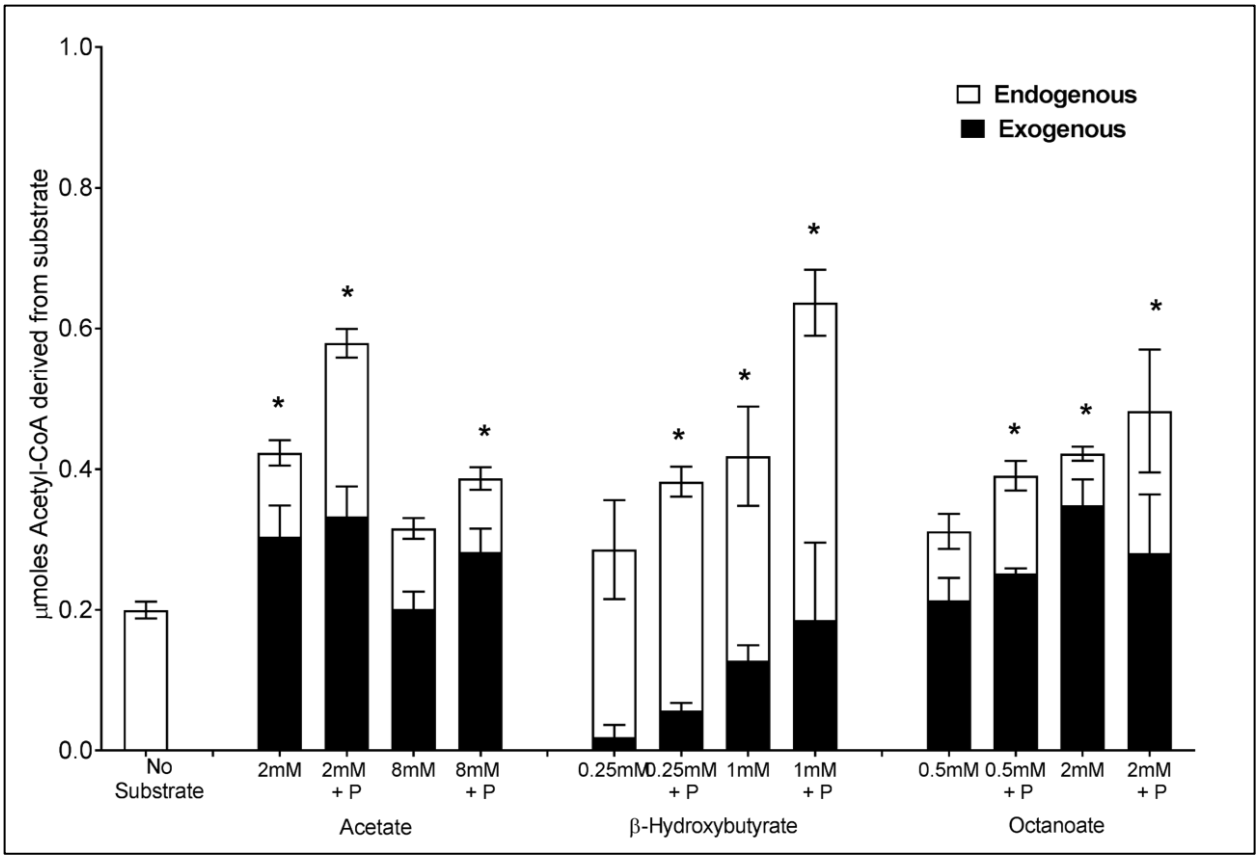

Figure 2.5: Acetyl-CoA Generated. *-p<0.05 vs no substrate control for total Acetyl-CoA derived from exogenous (substrate) and endogenous sources.

Total substrate oxidation rates (endogenous and exogenous) were higher for all substrate containing groups compared to the controls (Figure 2.5). These differences reached statistical significance for all groups except 8mM acetate, 0.25mM BHB, and 0.5mM Octanoate. In BHB groups, the majority of Acetyl-CoA was generated from oxidation of endogenous substrates. In both acetate and octanoate groups, Acetyl-CoA generation was dominated by the oxidation of exogenously introduced acetate or octanoate. Propionate did not significantly alter Acetyl-CoA production when added at each concentration within each substrate.

2.3.3 TCA Cycle Intermediates

2.3.3.1 Controls

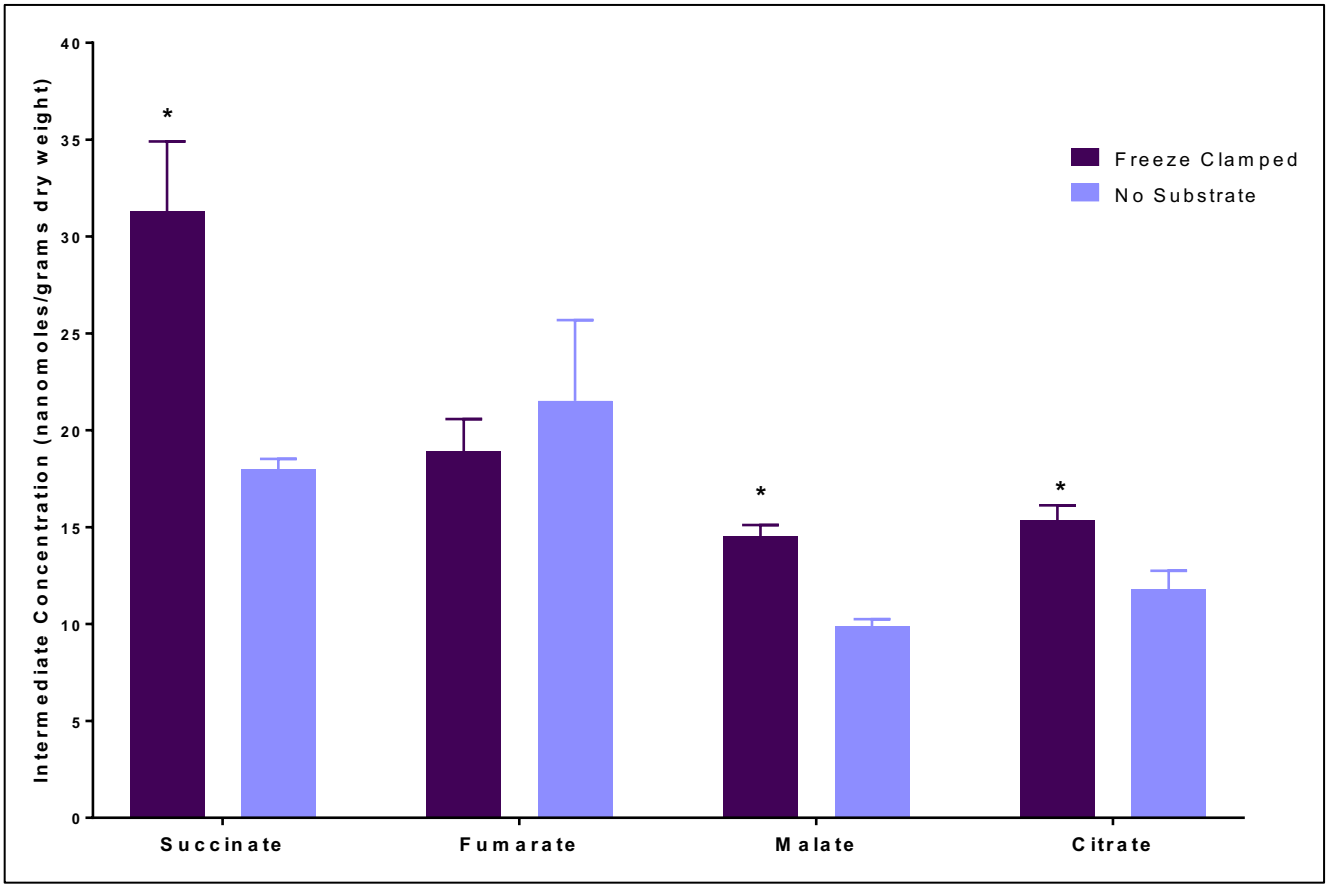

Figure 2.6: TCA Cycle Intermediates Values in controls. *-p<0.05 vs no substrate intermediate.

Succinate, malate and citrate concentrations were significantly reduced in hearts perfused without additives (15.99±0.91 and 8.81±0.59 respectively) than in groups that were immediately freeze clamped without perfusion (27.64±3.08 and 12.91±0.97) as shown in Figure 2.6. Fumarate concentrations were slightly higher in perfused hearts than in hearts that did not undergo perfusion, though, this difference did not reach statistical significance.

2.3.3.2 Succinate

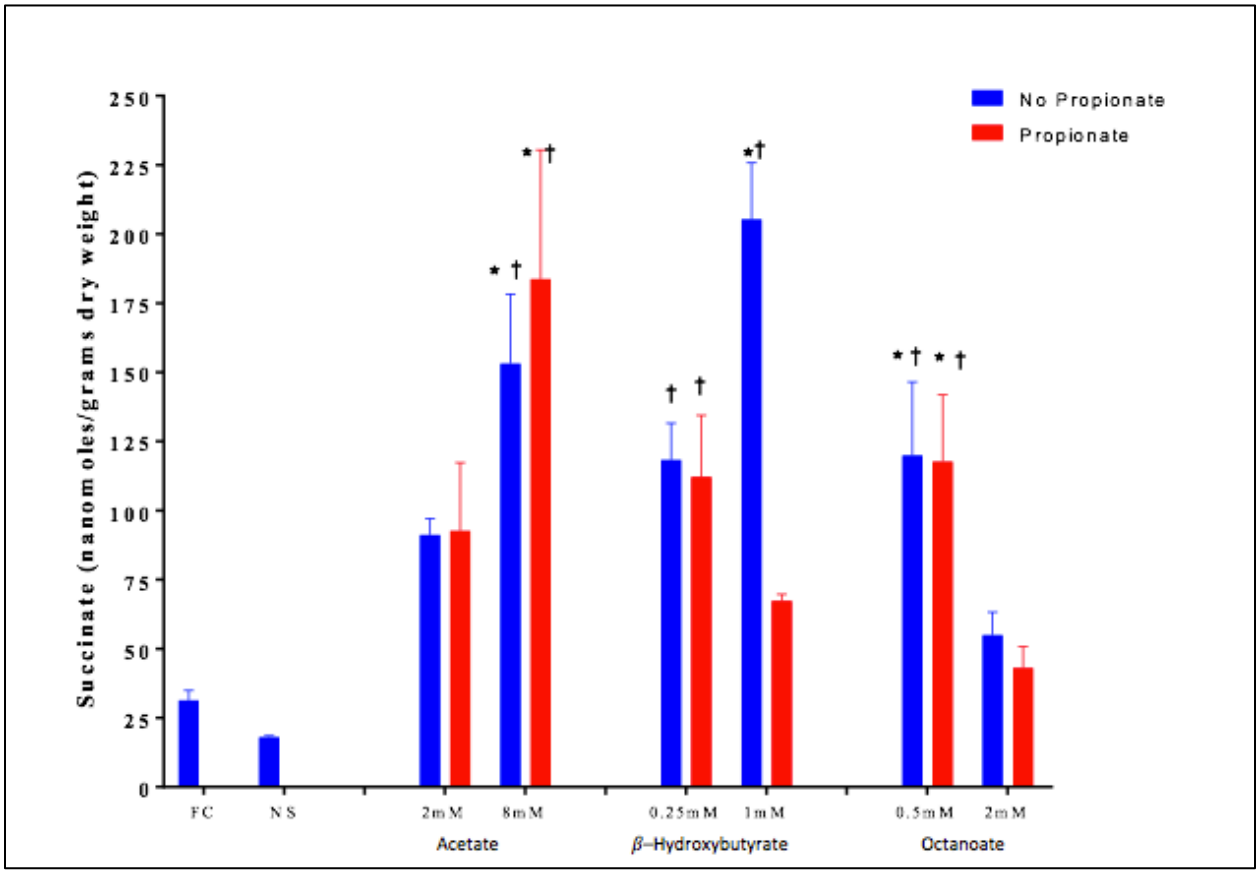

Figure 2.7: Succinate Levels Reported as Value ± SEM. FC= Freeze Clamped. NS=No Substrate. *-$p<0.05$ vs FC. †-$p<0.05$ vs NS.

Succinate concentrations were higher in all groups in comparison to the controls (Figure 2.7). 8mM acetate with and without propionate, 0.25mM BHB with and without propionate, 2mM BHB without propionate and 0.5mM Octanoate without propionate all

reached statistical significance. No consistent propionate trend was evident though the addition of propionate to 1mM BHB did significantly reduce succinate levels.

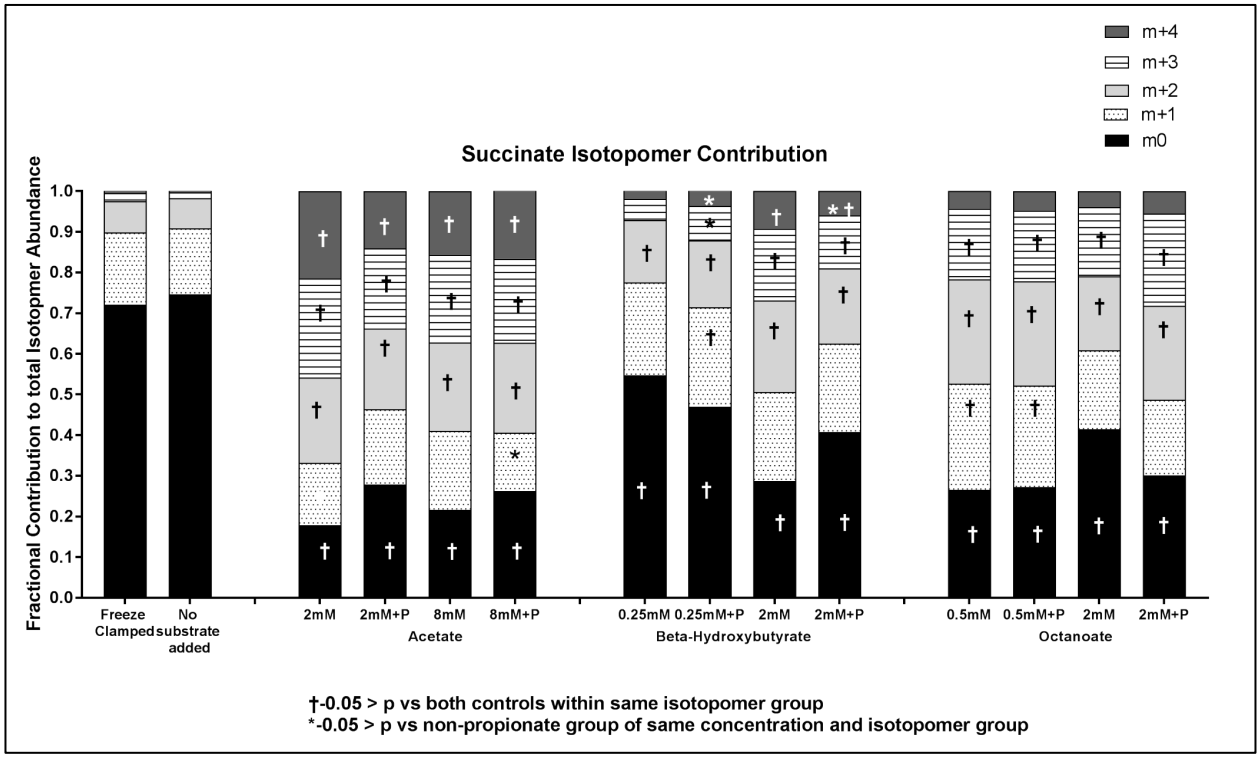

Figure 2.8: Succinate Isotopomer Contributions

The m0 isotopomer was the dominant isotopomer abundance present in both controls and was significantly higher than all substrate perfused groups at all concentrations (Figure 2.8). m+3 isotopomer abundance was also significantly higher in all acetate and octanoate groups. 0.25mM with propionate, and both 0.5mM groups were significantly higher than the control group in the m+1 contribution to overall isotopomer abundance. m+4 abundance was significantly higher in all acetate groups in comparison to both controls. Propionate addition did not result in a consistent trend in isotopomer abundance, though a few groups did reach significance: m+1 in 8mM acetate, m+3 and m+4 in 0.25mM BHB and m+4 in 2mM BHB.

2.3.3.3 Fumarate

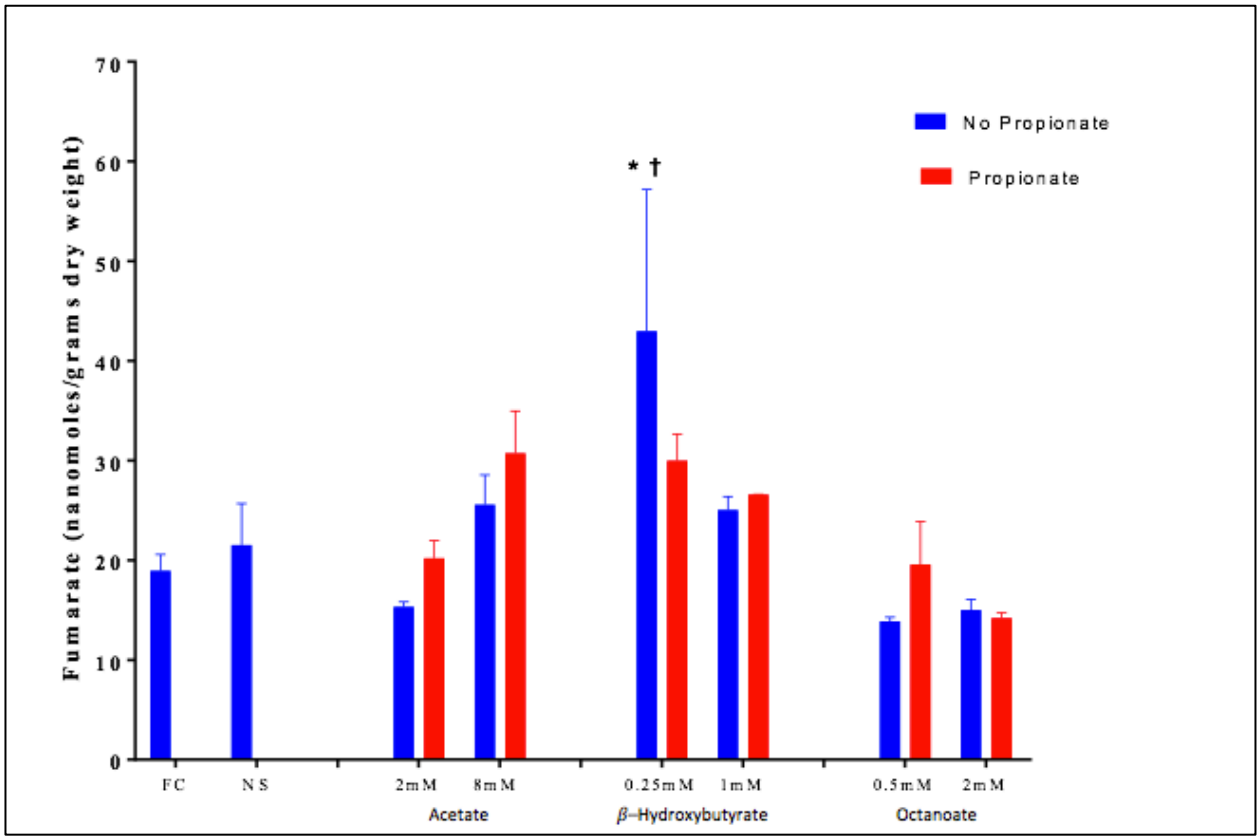

Figure 2.9: Fumarate Values reported as Value ± SEM. FC= Freeze Clamped. NS=No Substrate. *-$p<0.05$ vs FC. †-$p<0.05$ vs NS.

No fumarate values were significantly higher than the controls except in the 0.25mM group (Figure 2.9). The addition of propionate at this concentration also resulted in the reduction of fumarate.

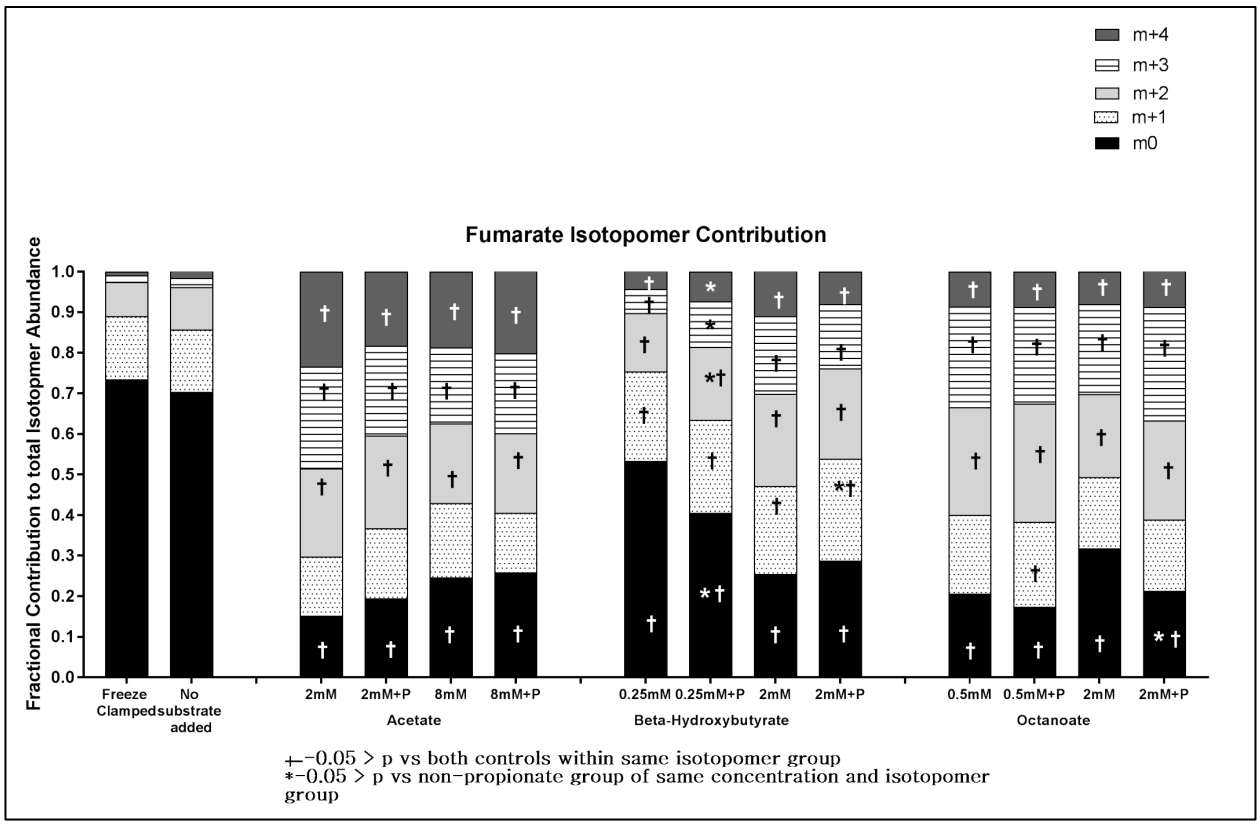

Figure 2.10: Fumarate Isotopomer Contribution.

The m0 isotopomer was the dominant isotopomer abundance present in both controls and was significantly higher than all substrate perfused groups at all concentrations (Figure 2.10). m+1 isotopomer abundance was significantly elevated in all BHB groups and in the 0.5mM Octanoate with propionate group. M+2 abundance was significantly elevated in all substrate groups. M+3 and m+4 abundance was significantly higher in all acetate and octanoate groups. Propionate differences were not consistent and did not result in an overall trend.

2.3.3.4 Citrate

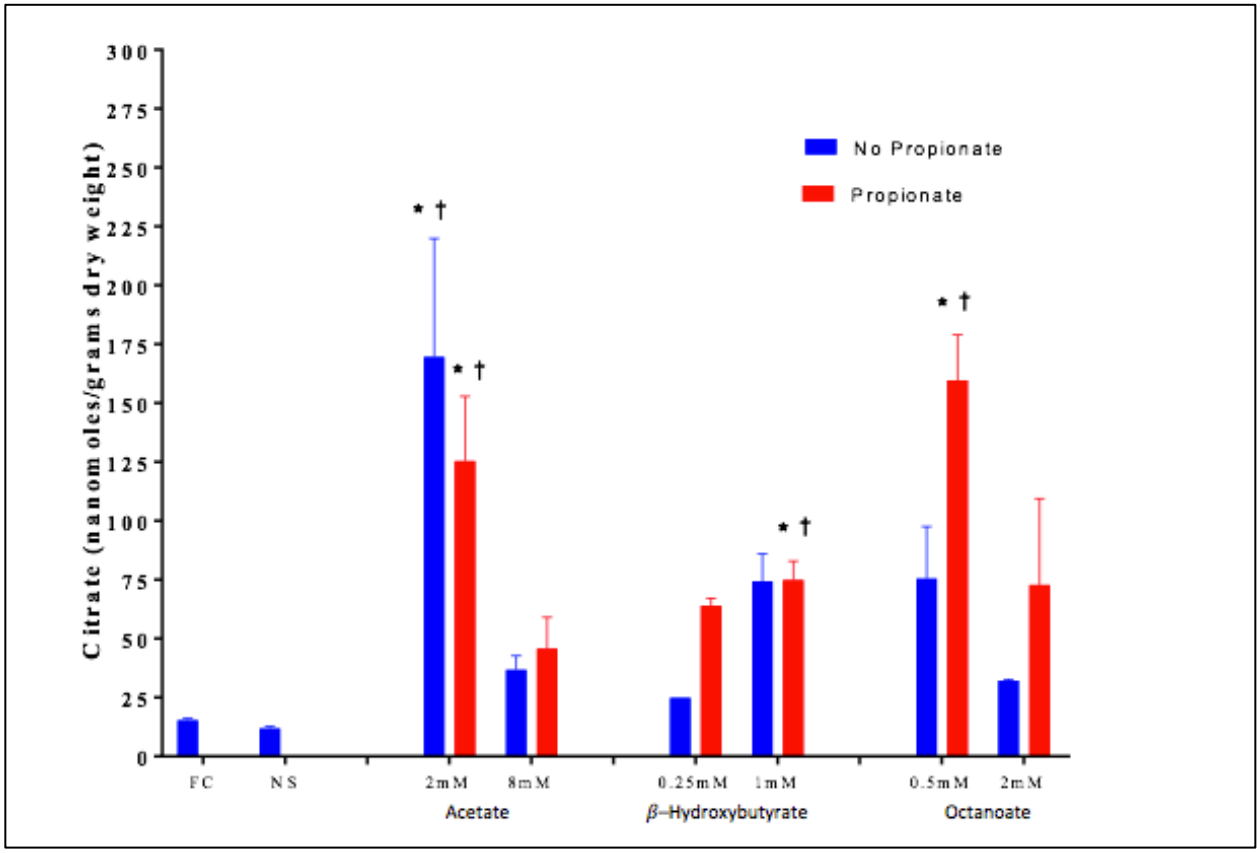

Figure 2.11: Citrate Values reported as Value ± SEM. FC= Freeze Clamped. NS=No Substrate. *-p<0.05 vs FC. †-p<0.05 vs NS.

Citrate concentrations were elevated in all substrate groups and these increases reached statistical significance in both 2mM acetate groups, 1mM BHB with propionate group, and the 0.5mM Octanoate with propionate group. See Figure 2.11.

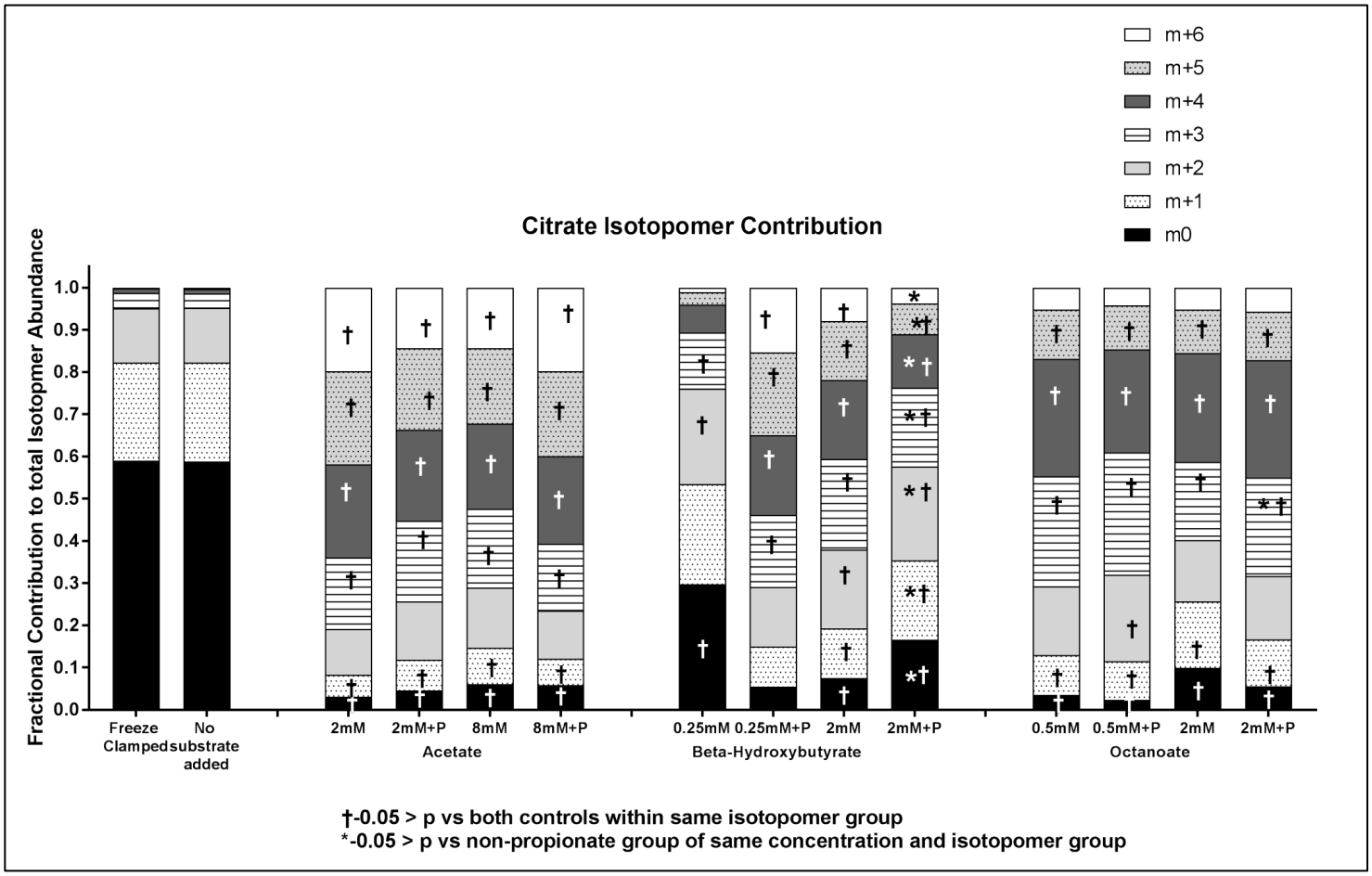

Figure 2.12: Citrate Isotopomer Contribution

The m0 isotopomer was the dominant isotopomer abundance present in both controls and was significantly higher than all substrate perfused groups at all concentrations. m+1 group isotopomer abundance was higher in both 2mM BHB groups and in all acetate and octanoate groups. M+2 abundance was statistically significantly increased in both 2mM BHB groups and in 0.5mM Octanoate with propionate. All acetate and octanoate groups were significantly higher in m+3 and m+4 abundance. M+5 abundance was significantly higher in all groups in comparison to the controls while all acetate groups were higher in m+6 abundance. The addition of propionate caused a significant increase in m0, m+1, and m+2 abundance in 2mM BHB. The addition of

propionate caused a significant decrease in m+3, m+4, m+5, and m+6. No other propionate trend was evident. See Figure 2.12.

2.3.3.5 Malate

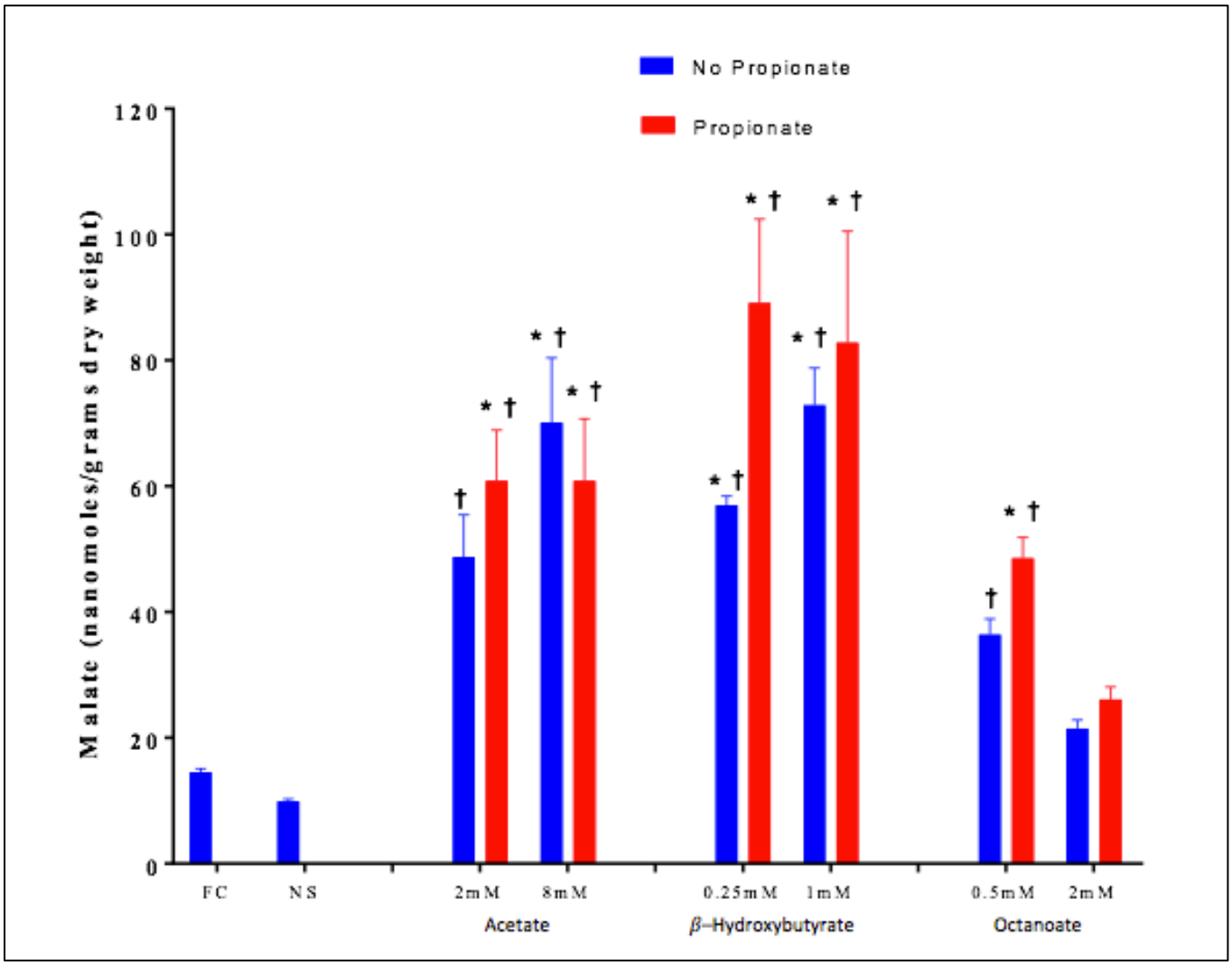

Figure 2.13: Malate Values reported as Value ± SEM. FC= Freeze Clamped. NS=No Substrate. *-p<0.05 vs FC. †-p<0.05 vs NS.

Malate concentrations were elevated in all groups and this increase reached statistical significance in all acetate and BHB groups and in both 0.5mM octanoate groups. The addition of propionate increased malate production in 0.25mM BHB groups, but a consistent trend resulting from the addition of propionate was not evident. See Figure 2.13.

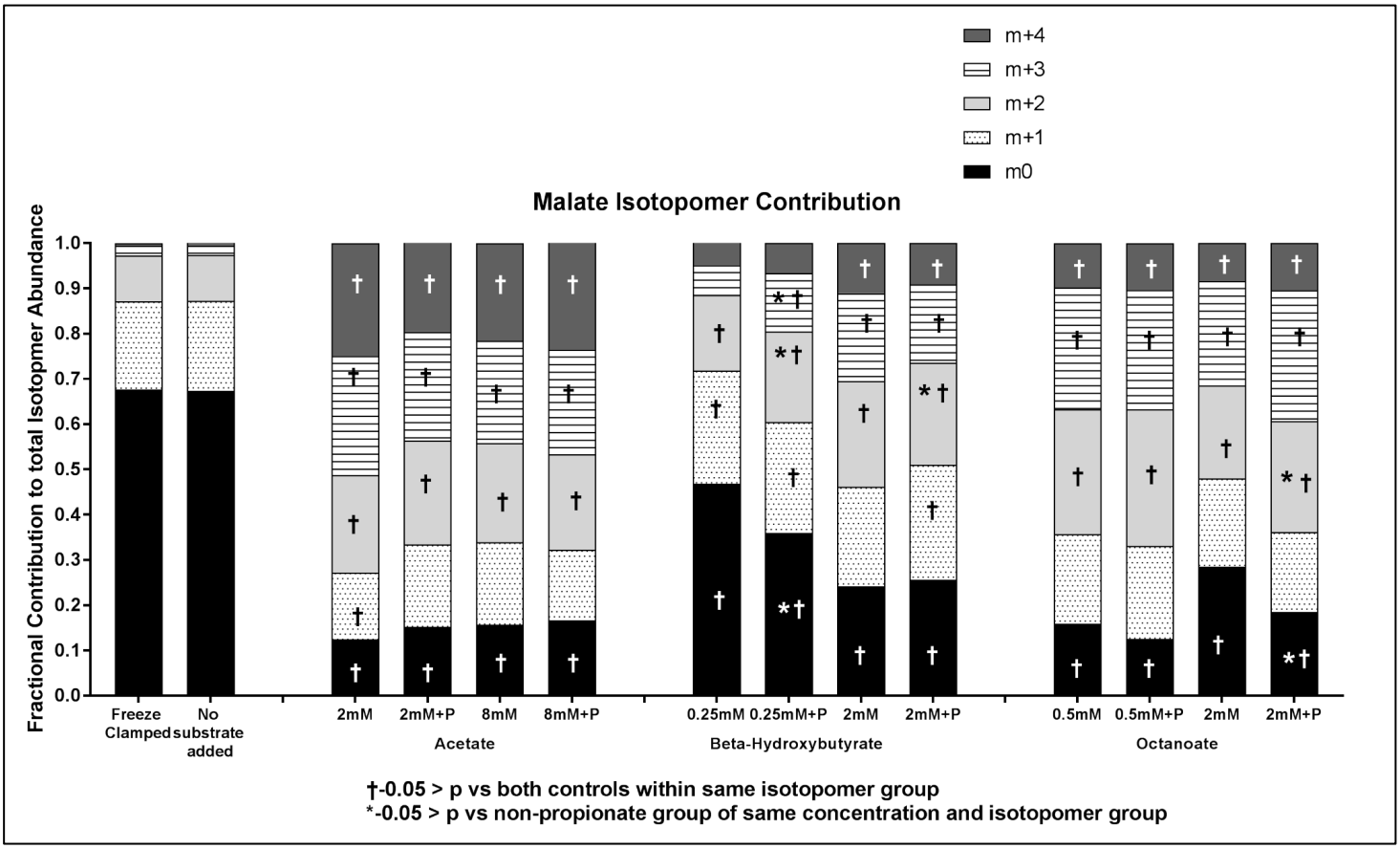

Figure 2.14: Malate Isotopomer Contribution

M0 abundance was significantly reduced in all substrate groups in comparison to both controls whereas m+2 abundance was significantly increased in all substrate groups. All acetate and octanoate groups showed increased m+3 and m+4 abundance. A few groups (2mM Acetate and both 0.25mM BHB groups) were statistically different in m+1 abundance. No consistent propionate trend was evident. See Figure 2.14.

2.4 Discussion

The TCA cycle generates the reducing equivalents NADH and FADH for ATP generation in the electron transport chain. The myocardium is able to utilize a number of substrates to generate acetyl-CoA to condense with oxaloacetate, form citrate and maintain the TCA cycle. A number of TCA cycle intermediates exist in equilibrium with other molecules, and depending on conditions, could be depleted over time and thus affect myocytes' potential for oxidative metabolism. Certain substrates, such as glucose, pyruvate, lactate, and some amino acids, can replenish these intermediates and also generate acetyl-CoA. Other substrates only provide acetyl-CoA for oxidative metabolism and generation of adenosine triphosphate (Nagoshi et al. 2011).

Hypothermic machine perfusion preservation has proved to be superior to conventional static storage and is used clinically for kidney transplantation, particularly for marginal donors and donation after circulatory death (Van Caenegem et al. 2016). Compared to other organs, oxygen consumption and energy requirements of the cold perfused heart are high and depletion of nutrient stores may reduce the benefits of this preservation technique (Preusse Cj Fau - Winter et al. 1985). Myocardial substrate preferences under these conditions are not known but seem important to optimize preservation of the donor organ. Free fatty acids and ketones are the preferred myocardial substrate during normokalemic and hyperkalemic perfusion, respectively though these seem to be influenced to some extent by the redox state of the heart (Peltz et al. 2004). In the current experiments, both octanoate and acetate were avidly oxidized and the ketone, β-hydroxybutyrate, was only a minor substrate, suggesting that myocardial substrate preferences in the cold perfused, potassium arrested heart are

different than during clinical conditions. Interestingly, MVO_2 appeared to be higher in hearts perfused in presence of an exogenous readily oxidized substrate. Intuitively, MVO_2 should be driven by the metabolic demand of the organ. These data, however, suggest that MVO_2 is dependent on the availability of readily oxidized exogenous substrate and myocytes likely restrict MVO_2 when substrate is limited. Our results also suggest that while reducing metabolism is desirable under static, anaerobic storage conditions, optimizing organ metabolism may be favored in the perfused organ when oxygen supply is not limited. Both acetate and octanoate were effective in supporting myocardial metabolism. Contrary to normothermic, hyperkalemic perfusion, ketone oxidation under these conditions was reduced, a difference that can only partially be explained by the unfavorable redox state of β-hydroxybutyrate (Laughlin and Heineman 1994).

Maintenance of the TCA Cycle intermediate pool sizes is dictated by the balance between cataplerosis, the removal of intermediates through disposal or biosynthesis pathways, and anaplerosis, the replenishment of these intermediates. In the absence of anaplerotic substrate, TCA cycle intermediates lost through these disposal pathways may result in depletion of TCA cycle intermediates, potentially leading to a reduction in TCA cycle flux and reducing equivalents for oxidative phosphorylation (Owen, Kalhan Sc Fau - Hanson, and Hanson 2002). In the current study, after 6 hours of hypothermic machine perfusion in the absence of any substrate, some TCA cycle intermediate concentrations (succinate, citrate, malate) were lower in the perfused heart without substrate compared to hearts from the intact organism suggesting that the intermediate pool can be depleted over time, a finding previously noted by other investigators in

normothermic, beating heart experiments (LaNoue, Nicklas, and Williamson 1970; LaNoue, Bryla, and Williamson 1972). Additionally, oxygen consumption and flux of endogenous and exogenous substrate appeared to be lower compared to substrate containing groups, even when these were only a minor contributor as in the β-hydroxybutyrate groups. Whether this reduction in metabolism was due to intermediate depletion, limited endogenous substrate or both is unclear but does indicate that the presence of a readily oxidizable substrate is important for machine perfused donor hearts. Lactate production (Appendix) was low and MVO_2 remained stable in all perfused groups implying that this reduced metabolism was not due substrate depletion and conversion to anaerobic glycolysis in hearts perfused without substrate.

In substrate containing groups, MVO_2 and TCA cycle flux seemed to be consistently increased compared to perfused hearts without substrate. Increased contribution of exogenous substrate was correlated with increased flux and MVO_2. Optimal concentrations of substrate were different. Both acetate and octanoate were avidly oxidized. BHB contributed less than 50% of acetyl-CoA units oxidized though its oxidation seemed to increase at the higher BHB concentration. Interestingly, independent of the exogenous substrate oxidation, concentrations of TCA cycle intermediates were higher in the presence of exogenous substrate. These data suggest when TCA cycle flux is increased, anaplerosis is favored even in the absence of an exogenous substrate that can be converted to a citric acid cycle intermediate. This is consistent with other observations that suggest an increase in anaplerosis and TCA cycle intermediates when MVO_2 is increased (Malloy et al. 1996; Li et al. 2011). The contributors to anaplerosis in substrate perfused hearts in our study are not known but

the trend towards increases in the M0 fraction in succinate suggest either unlabeled propionate or unlabeled glutamate as potential contributors to anaplerosis in this study.

It is interesting that unlike during normothermic perfusion, exogenous propionate did not seem to be a major anaplerotic substrate. Reasons are not entirely clear but may involve uptake inhibition via a negative feedback mechanism at higher intermediate concentrations as others have suggested (Siliprandi, Lisa, and Menabò 1991; Brunengraber and Roe 2006; Russell and Taegtmeyer 1991; Halarnkar and Blomquist 1989). Briefly, propionate is converted into propionyl CoA by the enzyme thiokinase. Propionyl CoA carboxylase catalyzes the reaction from propionyl-CoA to methyl-malonyl CoA. A Vitamin B-12 dependent reaction occurs next to yield succinyl CoA, a precursor to succinate in the TCA cycle (Schowen 1993).

Endogenous generation of propionyl-CoA from endogenous odd chain fatty acids and its eventual incorporation into the TCA cycle could affect the uptake of exogenous propionate by oversaturating enzymes used in the conversion pathway. Substrate competition for Coenzyme A may also play a role. Acetate, ketone and octanoate oxidation are Coenzyme A dependent processes. All utilize acetyl-CoA synthase, an enzyme used in both fatty acid oxidation and propionate metabolism in the heart (Gibala, Young, and Taegtmeyer 2000). The addition of propionate to already acetate/octanoate perfused groups would have no effect if the enzyme is saturated (Sundqvist et al. 1984). Furthermore, the effects of hypothermia on propionate metabolism in this model are not known.

This study has a number of limitations. Clinically, perfusion preservation may be used for prolonged ischemic intervals beyond the six-hour time period in these

experiments. It is possible that endogenous contributors to TCA cycle can be depleted thus affecting limiting the metabolic potential of exogenous substrate that cannot replenish the intermediate pool directly. Also, exogenous substrates that can replenish the TCA cycle might be superior though our prior studies did not suggest any increases in MVO_2 when perfused with glucose or pyruvate containing UWMPS, and, while pyruvate was avidly oxidized, glucose was not (Cobert et al. 2012). The ketone body in our experiments, β-Hydroxybutyrate, at the concentrations studied did not appear to be a major contributor to myocardial oxidative metabolism. Acetoacetate may be preferentially oxidized due to a favorable redox state but is unlikely to be useful because of its instability (Schonfeld P Fau - Bohnensack et al. 1983).

In conclusion, my studies indicate that myocardial metabolism during hypothermic perfusion of hearts can be optimized. The free fatty acid octanoate and acetate were preferred myocardial substrates under these conditions. Even though none of the substrates studied can replenish the TCA cycle directly, concentration of citric acid cycle intermediates and TCA cycle flux were increased in the presence of exogenous substrate. These data have important implications when designing the optimal preservation solutions for machine perfused donor hearts.

Chapter Three

Metformin and Insulin as Perfusate Additive to Alter Substrate Selection

3.1 Introduction

Diabetes mellitus is a major cause of cardiovascular morbidity and mortality. Treatment of Type 2 diabetes may involve diet, oral agents and insulin. Insulin sensitizing agents, such as the biguanide metformin, appear to improve outcomes in diabetic patients with coronary artery disease and heart failure (Group 2009; Panunti, Kunhiraman, and Fonseca 2005). These effects may be unrelated to improved glycemic control and seem to involve alterations in myocardial metabolism. Metformin has many actions throughout the body (appendix), with a not yet fully investigated effect on the heart. Metformin acts through the upregulation of the AMPK and P13K/AKT pathway and downregulation of the PAI-1 pathways (Batchuluun et al. 2014) (Figure 3.1). This all results in cardioprotective effect.

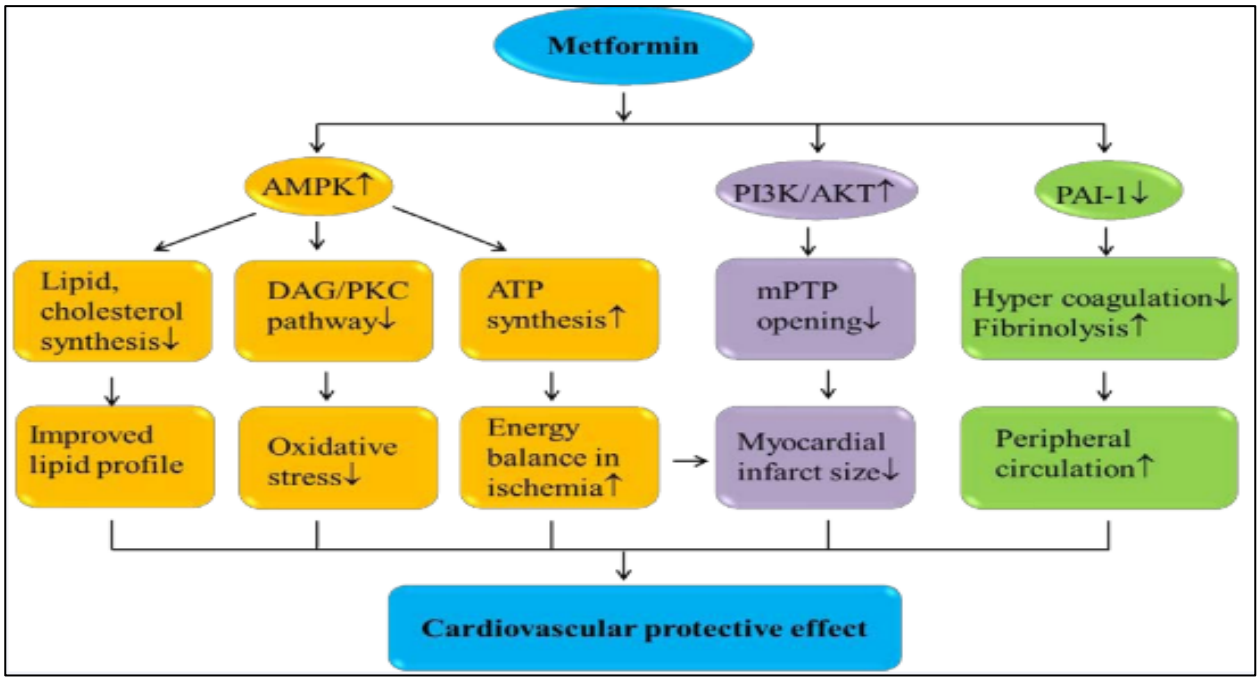

Figure 3.1: Cardioprotective pathways affected by Metformin (Batchuluun et al. 2014).

Interestingly, metformin may also improve cardiac morbidity in patients without diabetes mellitus, a finding supported by clinical studies and experimental models of myocardial infarction or ischemia (Calvert et al. 2008; Jadhav et al. 2006). During cardiac surgery, diabetic and non-diabetic patients frequently require insulin infusions to manage hyperglycemia. Conditions encountered in cardiac surgery may result in vast alterations in myocardial metabolism. We previously demonstrated that potassium cardioplegia, for example, shifts myocardial substrate preferences toward ketone oxidation and away from fatty acid oxidation (Peltz et al. 2004). The effects of metformin and insulin on myocardial substrate selection under these conditions are incompletely understood but may explain improved outcomes in patients with coronary artery disease undergoing cardiac surgery. I hypothesized that metformin and insulin therapy influence myocardial substrate selection by reducing fatty acid oxidation during conditions encountered in cardiac surgery. I investigated this hypothesis in a rodent model of simulated coronary artery bypass grafting.

3.2 Materials and Methods

3.2.1 Animals

Male Sprague-Dawley rats weighing 300-550g were given access to food and water at libitum and were used in a research protocol approved by the Institutional Animal Care and Use Committee at the University of Texas Southwestern Medical Center. All animals were treated in accordance with guidelines set forth in the Guide for the Care and use of Laboratory Animals (National Institutes of Health Publication No. 86-23, revised 1996).

3.2.2 Chemicals

Carbon-13 (^{13}C) labeled compounds were obtained from Cambridge Isotope Laboratories (Andover, Mass) and Isotec (Miamisburg, Ohio). Unlabeled mixed free FA were acquired from Martek Biosciences (Columbia, Md). All other unlabeled chemicals for buffer components were purchased from Sigma Chemical Corp (St. Louis, Mo). Metformin hydrochloride powder and Insulin (Humulin R, 100 units/mL) were obtained from the University of Texas Southwestern Medical Center pharmacy.

3.2.3 Surgical protocol

Rats were anesthetized with an intraperitoneal injection of 4% chloral hydrate (1ml/100 g). After median sternotomy and an intrahepatic injection of heparin (1000 U/kg), the inferior and superior vena cavae were ligated. The heart was rapidly excised, cooled in lactated ringers (4ºC), and mounted on a Langendorff apparatus. A fluid-filled left ventricular balloon was inserted and adjusted to a left ventricular pressure of 10 mm Hg.

3.2.4 Experimental Groups

Rat hearts (n=8 per group) were analyzed across three experimental conditions: normokalemia (NK), cardioplegia (CP), and repeated cycles of ischemia/potassium cardioplegia simulating metabolic conditions encountered during coronary artery bypass grafting (BP). Within each condition, four groups were compared based on the perfusion buffer additives: 1) Control, 2) Metformin (buffer + metformin 500μM), 3) Insulin (buffer + insulin 10U/L), and 4) Combined metformin-insulin. The concentration of 500 μM was chosen based upon previous preliminary dose dependency experiments (appendix).

	Groups	Concentrations
Normokalemia (n=16)	Control	--
	Metformin	500mM
	Insulin	10 U/L
	Metformin + Insulin	500mM, 10U/L
Cardioplegia (n=16)	Control	--
	Metformin	500mM
	Insulin	10 U/L
	Metformin + Insulin	500mM, 10U/L
Bypass (n=16)	Control	--
	Metformin	500mM
	Insulin	10 U/L
	Metformin + Insulin	500mM, 10U/L

Table 3.1: Experimental Groups.

Hearts in all groups were stabilized by perfusion for twenty minutes with unlabeled normokalemic Krebs buffer. NK hearts were subsequently perfused for thirty minutes with substrates containing specific ^{13}C-labeling patterns. CP hearts, after

stabilization, were perfused with cardioplegia buffer supplemented with the same ^{13}C-labeled substrate concentrations. After stabilization, BP hearts were perfused for three minutes of cardioplegia buffer containing unlabeled substrates followed by twenty-two minutes of ischemia to simulate intermittent administration of cardioplegia during cardiac surgery. The cycle was repeated for a total of four times and a final dose of cardioplegia was administered. Hearts were subsequently reperfused with ^{13}C-labeled substrate containing normokalemic buffer. See Table 3.1.

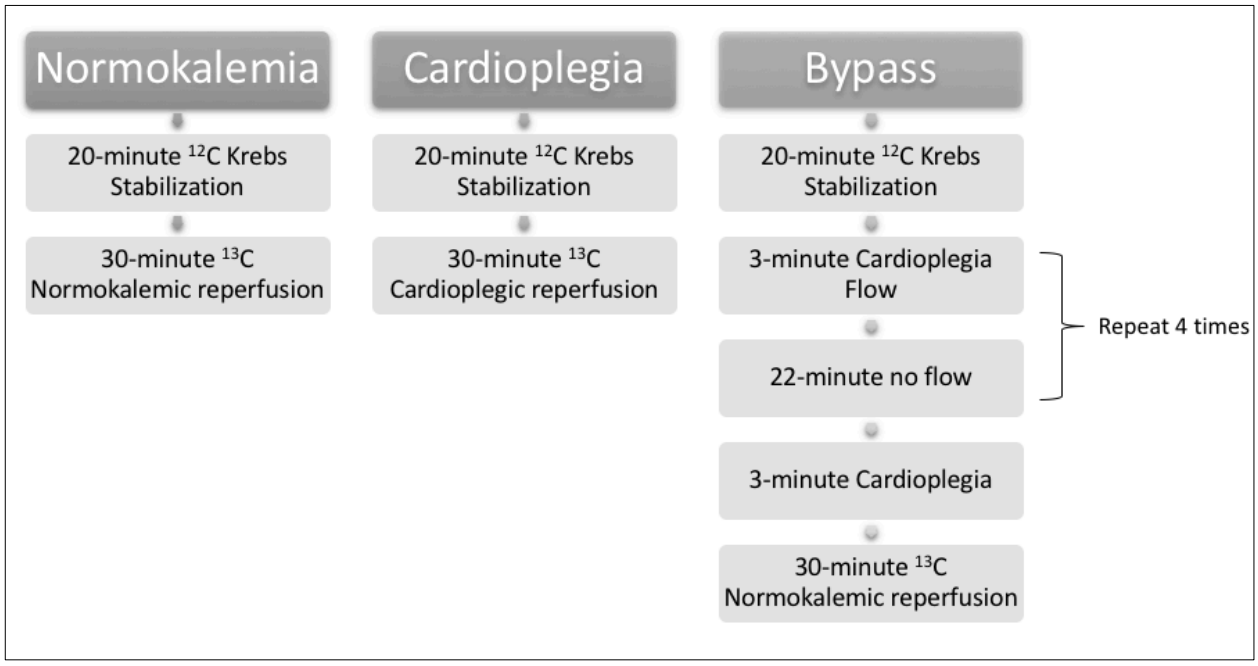

Figure 3.2: Experimental protocols for Normokalemia, Cardioplegia, and Bypass groups.

3.2.5 Perfusion Protocol

Hearts were perfused retrograde from a height of 100 cm H_2O with modified Krebs-Heinslet buffer containing unlabeled (^{12}C) substrates for a 20-minute stabilization period. The stabilization buffer composition was as follows: 25mM $NaHCO_3$, 115mM NaCl, 4.7 mM KCl, 1.2 mM $MgSO_4$, 1.2 mM NaH_2PO4, 1.2 mmol $CaCl_2$, and 0.75% fatty acid free bovine serum albumin. The buffer was oxygenated with a 95% O2 and 5%

CO2 mixture. For delivery of cardioplegia, the buffer was modified by increasing the potassium chloride concentration to 20mM and decreasing the NaCl concentration accordingly. Physiologic concentrations of unlabeled fatty acids (.35mmol), acetoacetate (.17mmol), lactate (1.2mM), pyruvate (.12mmol) and glucose (5mmol) were provided in the perfusion buffer. Specific ^{13}C labeling substrate labeling patterns (Figure 3.3) at the same concentrations were used for the experimental perfusion period at each condition as detailed. Each of these substrates is oxidized and enters the TCA cycle (Figure 3.4). In each group, in some hearts, glucose and fatty acid labeling patterns were reversed to assess the influence of additives on glucose oxidation. These substrates generated

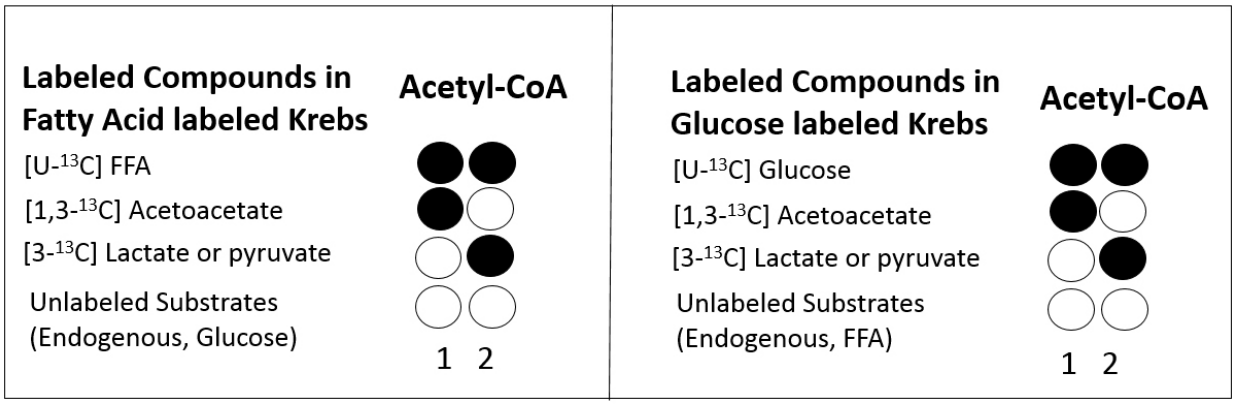

Figure 3.3: Acetyl-CoA labeling patterns for each substrate. Circle 1 represents the first carbon on acetyl-CoA and circle 2 represents the second carbon. FFA, free fatty acids.

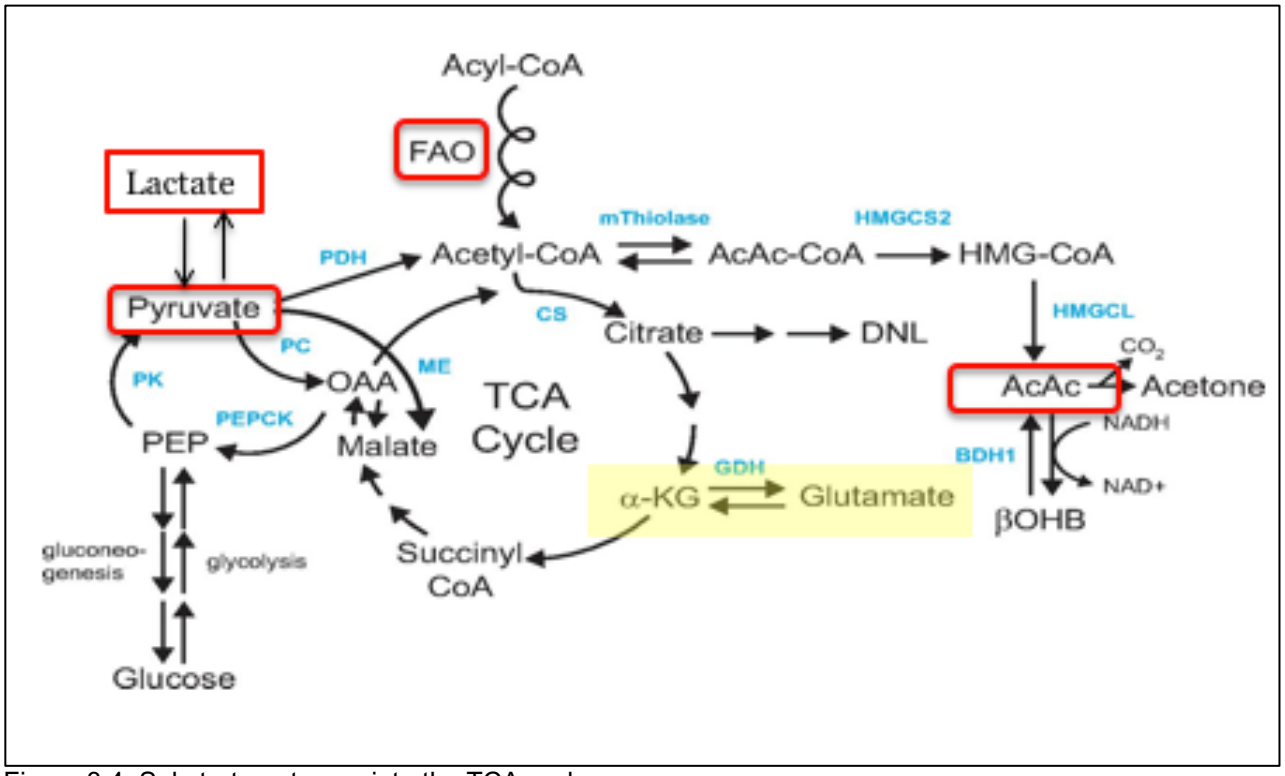

Figure 3.4: Substrate entrance into the TCA cycle

Blood pressure and heart rate were monitored continuously. Some hearts were paced to achieve a minimum average rate-pressure product of 24,000 per group. Myocardial oxygen consumption (MVO_2) was calculated at ten minute intervals or as detailed in the experimental protocol from the arteriovenous pO2 difference and coronary flow rate and reported as µmol O2 per gram wet weight per minute (Jeffrey et al. 1996). The double chambered (^{13}C and ^{12}C solution) perfusion apparatus is shown in Figure 3.5.

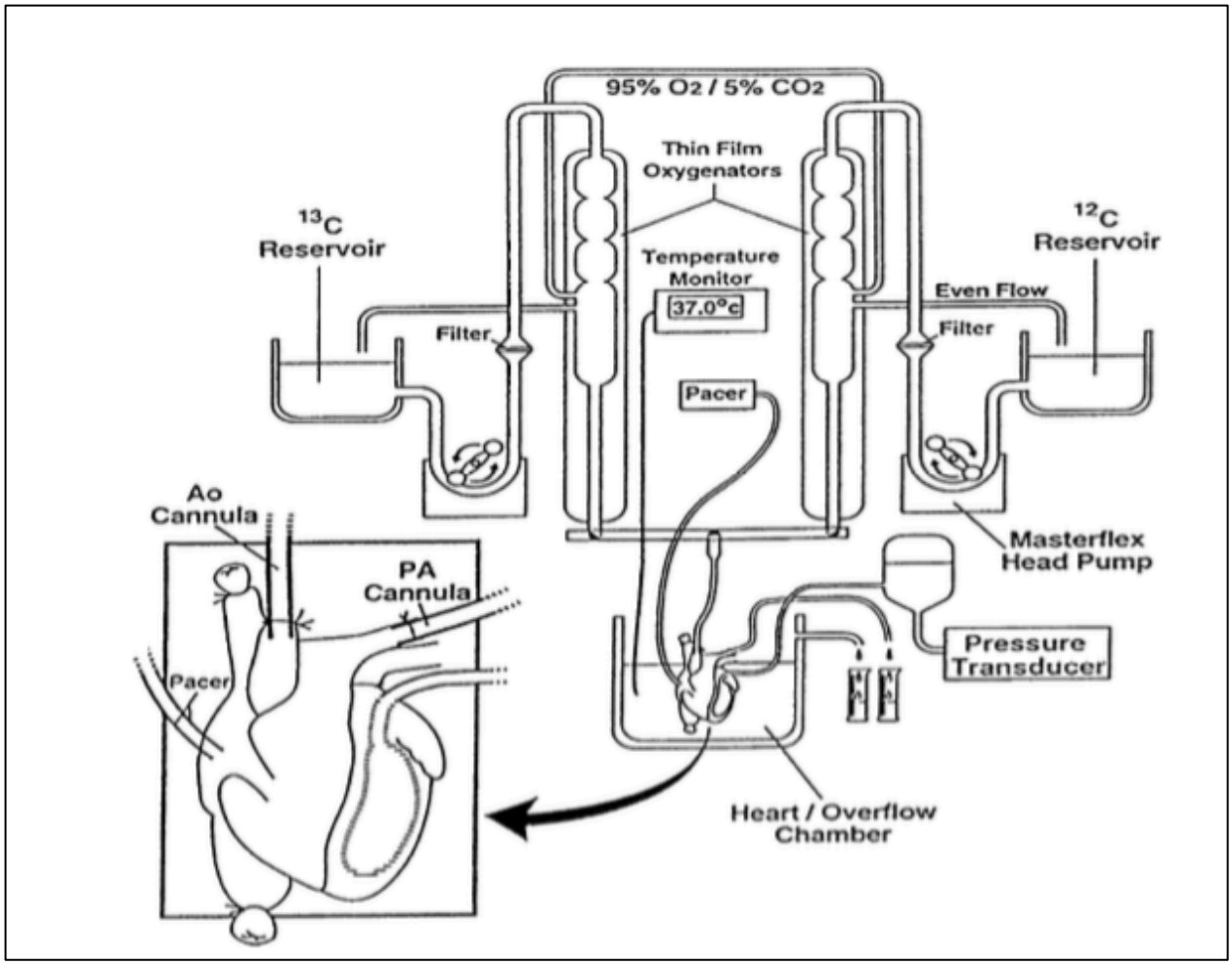

Figure 3.5: Double-Chambered Langendorff Apparatus

3.2.6 Tissue Extraction

After the perfusion interval, ventricular tissue was sampled and freeze-clamped in liquid nitrogen cooled tongs and stored in a freezer maintained at -80^{oC}. Tissue metabolites were extracted by grinding the ventricular tissue sample with mortar and pestle under cooled, liquid nitrogen. The pulverized tissue was reconstituted in 4% perchloric acid. Samples for MRS analysis were freeze-dried in a speed vacuum overnight and reconstituted in 1.08mM EDTA in D_2O at a pH of 7.0-7.4.

3.2.7 Magnetic Resonance Spectroscopy

Proton decoupled ^{13}C MRS was performed on heart extracts using a 14.1T Varian Inova spectrometer (Varian Instruments, Palo Alto, CA) operating at 600 MHz with a 1-second delay between 45º carbon pulses. Fourier transformation and peak fitting was performed on glutamate carbons using commercially available software (ACD/Labs, Toronto, Canada).

3.2.8 Measurement of Substrate Utilization

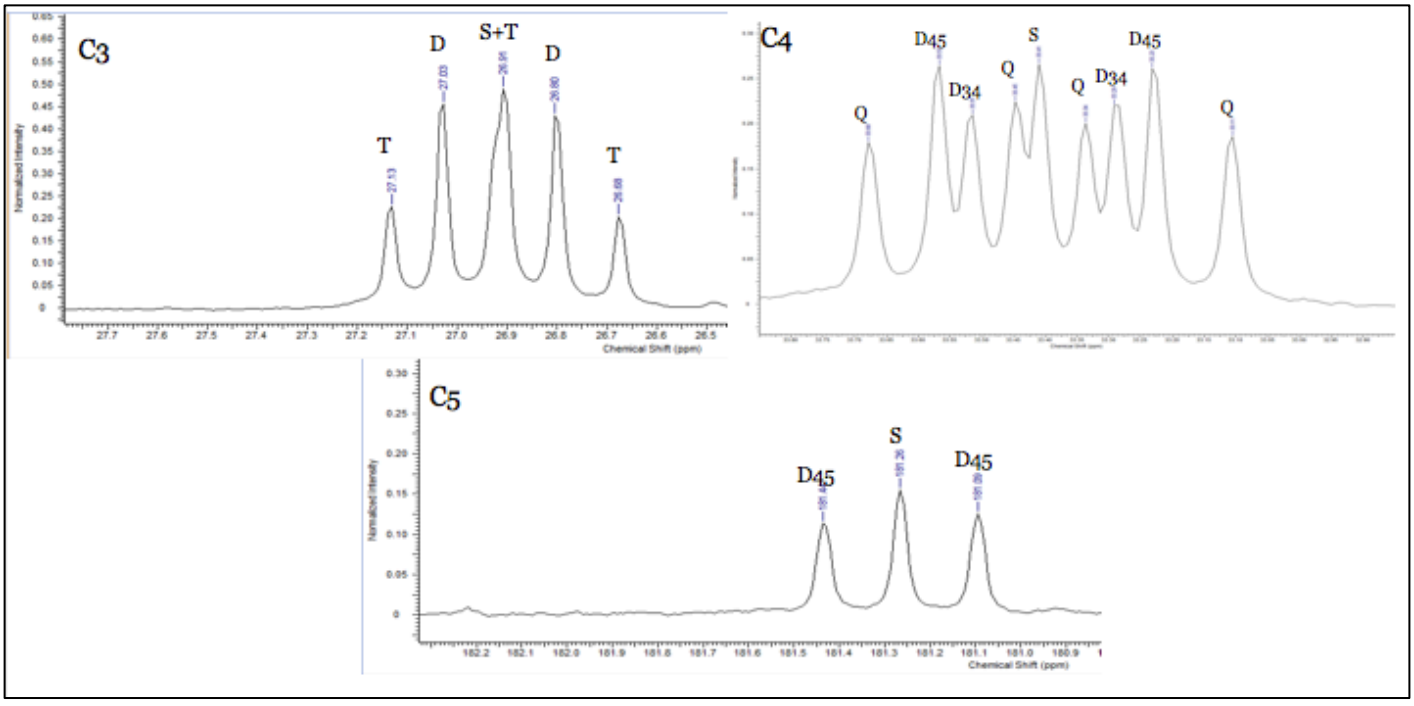

Figure 3.6: Representative spectra highlighting the C3, C4, and C5 carbons glutamate and the peaks they yield. S: Singlet, D: Doublet, T: Triplet, D34: Doublet from 3rd and 4th carbon, D45: Doublet from 4th and 5th carbon

Each ^{13}C labeled substrate generates a specific acetyl-CoA labelling pattern that can be traced through the tricarboxylic acid (TCA) cycle (see Appendix figure). Glutamate isotopomer analysis was used to determine the fractional contribution of each ^{13}C-

labeled substrate to oxidative metabolism assuming non-steady state conditions (Peltz et al. 2004; Burgess et al. 2001; Malloy, Sherry, and Jeffrey 1990). Spectra generated from ^{13}C MRS were analyzed for the abundance of their glutamate peaks (Figure 3.6). Based upon labelling patterns, certain peaks correspond to certain substrates. The much larger intracellular glutamate pool can be used to characterize oxidative metabolism since it exists in rapid equilibrium with the TCA cycle intermediate, α-ketoglutarate (Jeffrey et al. 1996). The 3rd, 4th, and 5th carbon are used for glutamate isotopomer analysis to determine the amount of lactate/pyruvate, ketones, and fatty acids present in each heart. Using the areas under the peaks to yield relative abundance and the previously discovered equations (Figure 3.7), fractional contribution was calculated (Burgess et al. 2001; Malloy et al. 1996). Briefly, the fractional contribution from the doublet peaks generated from the 3rd and 4th carbon and the ratio of the abundance of the 4th carbon and the 3rd carbon were used to calculate the contribution of lactate/pyruvate to oxidative metabolism. The abundance from the quartet peaks and the ratio of abundance from the peaks generated by the 4th and 3rd carbon was used to calculate the contribution of free fatty acids to oxidative metabolism. The singlet and doublet abundance at the fifth carbon and the contribution from free fatty acids was used to calculate the fractional contribution derived from ketones.

$$F_{Ketones}=C5S/C5D*F_{FFA}$$
$$F_{Lactate/Pyruvate}=C4D34*(C4/C3)$$
$$F_{FFA}=C4Q*(C4/C3)$$
$$F_{Unlabeled}=1-F_{Ketones}-F_{lactate/Pyruvate}-F_{FFA}$$

Figure 3.7: Fractional Contribution Equations

Fractional utilization data were combined with MVO_2 data to determine substrate oxidation rates as previously described (Malloy et al. 1996).

3.2.9 Statistical Analysis

Results are reported as mean and standard error of the mean (SEM). Commercially available software (GraphPad Prism 7, La Jolla, CA) was used for analysis. Substrate values were analyzed by one-way analysis of variance (ANOVA). Differences between groups, when present, were determined by Tukey's test for multiple comparisons. For data compared over multiple time points, a repeated-measures analysis of variances was applied. A p-value $< .05$ was considered significant.

3.3 Results

3.3.1 Cardiac Function and Myocardial Oxygen Consumption (MVO_2)

	Control	Metformin	Insulin	Metformin + Insulin
Stabilization	4.9 ± 0.6	4.9 ± 0.8	3.3 ± 0.2	4.2 ± 0.7
Cardioplegia 1	1.2 ± 0.4*	1.2 ± 0.7*	0.9 ± 0.1*	0.7 ± 0.3*
Cardioplegia 2	1.8 ± 0.3*	1.2 ± 0.4*	0.9 ± 0.1*	1.6 ± 0.1*
Cardioplegia 3	2.2 ± 0.2*	1.3 ± 0.3*	1.0 ± 0.1*	1.4 ± 0.2*
Cardioplegia 4	2.4 ± 0.3*	1.6 ± 0.2*	1.4 ± 0.1	1.1 ± 0.2*
Cardioplegia 5	2.5 ± 0.6*	2.3 ± 0.3*	1.0 ± 0.1*	1.0 ± 0.4*
Reperfusion (10 mins)	3.5 ± 0.7	4.3 ± 0.5	3.2 ± 0.5	3.8 ± 0.8
Reperfusion (20 mins)	4.3 ± 0.7	3.9 ± 0.3	3.2 ± 0.2	4.1 ± 0.9
Reperfusion (30 mins)	3.3 ± 0.8	4.1 ± 0.3	3.1 ± 0.4	4.0 ± 0.9

Table 3.2: Oxygen consumption (μmol/g/min) in bypass model. Values shown as mean ± SEM at stabilization, cardioplegia interval, and reperfusion 260 time points. *P < .05 versus stabilization time point within additive group. P = significant between group

There were no functional differences between any groups during the stabilization period for any of the three conditions studied. Rate-pressure product after repeated cycles of ischemia and cardioplegia, simulating coronary artery bypass grafting were not different at any time point amongst groups (Figure 3.9) The achieved rate pressure product for all groups after reperfusion was lower than the stabilization value for most

time-points but this difference was not statistically significant. MVO_2 during the periods of ischemia and cardioplegia was lower for most time points compared to the stabilization MVO_2. See Table 3.2. There were no statistically significant differences in oxygen consumption values at stabilization or at each reperfusion time point across all bypass groups. Myocardial efficiency, defined as rate-pressure product/MVO_2 was also not consistently different between groups (Figure 3.10**)** Both rate pressure product and myocardial efficiency demonstrated an expected value of zero during cardioplegic and ischemic intervals as the heart was not beating in both instances.

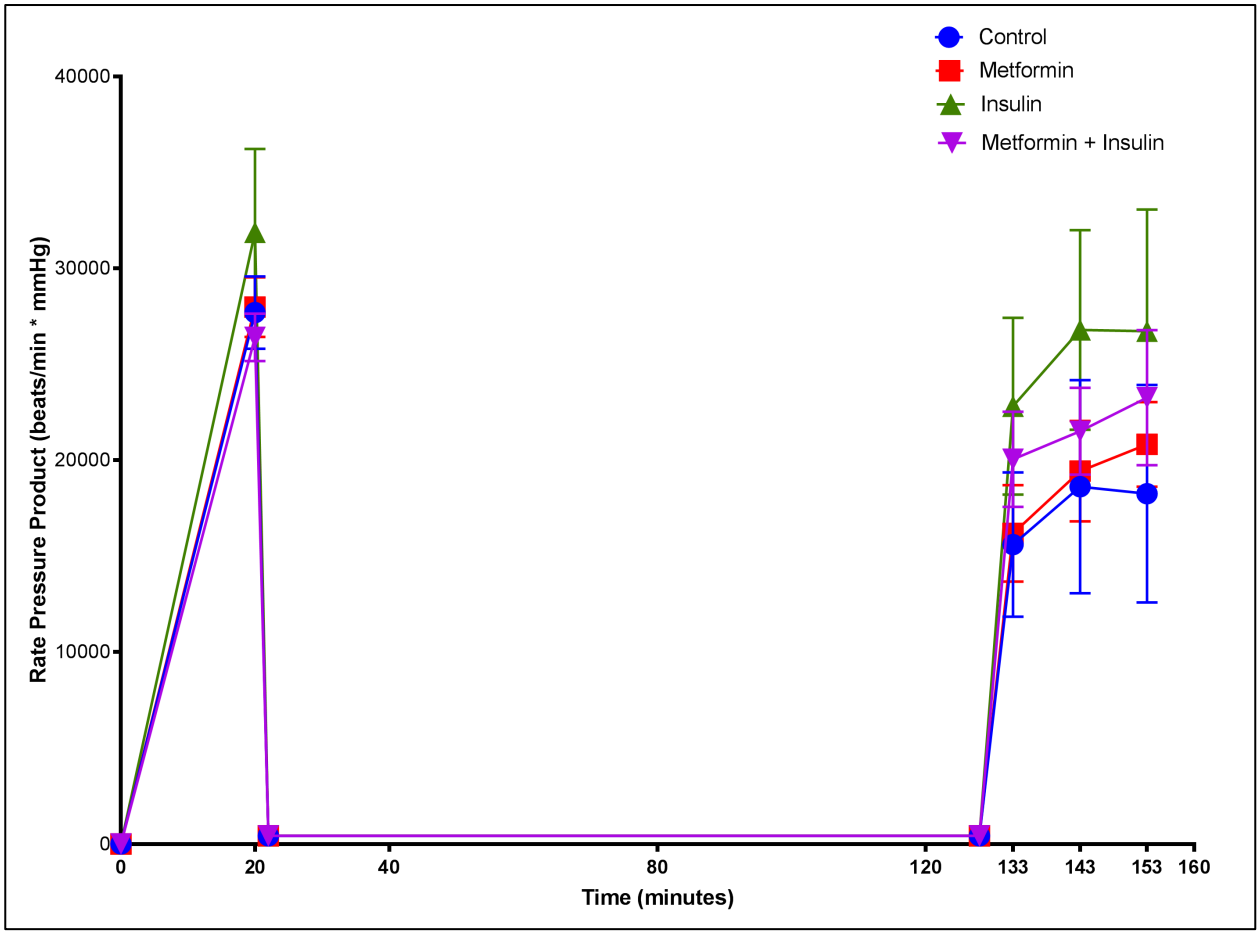

Figure 3.8: Rate pressure product in bypass during stabilization and three reperfusion time points. Values shown as mean ± standard error of the mean. P = nonsignificant for all time points.

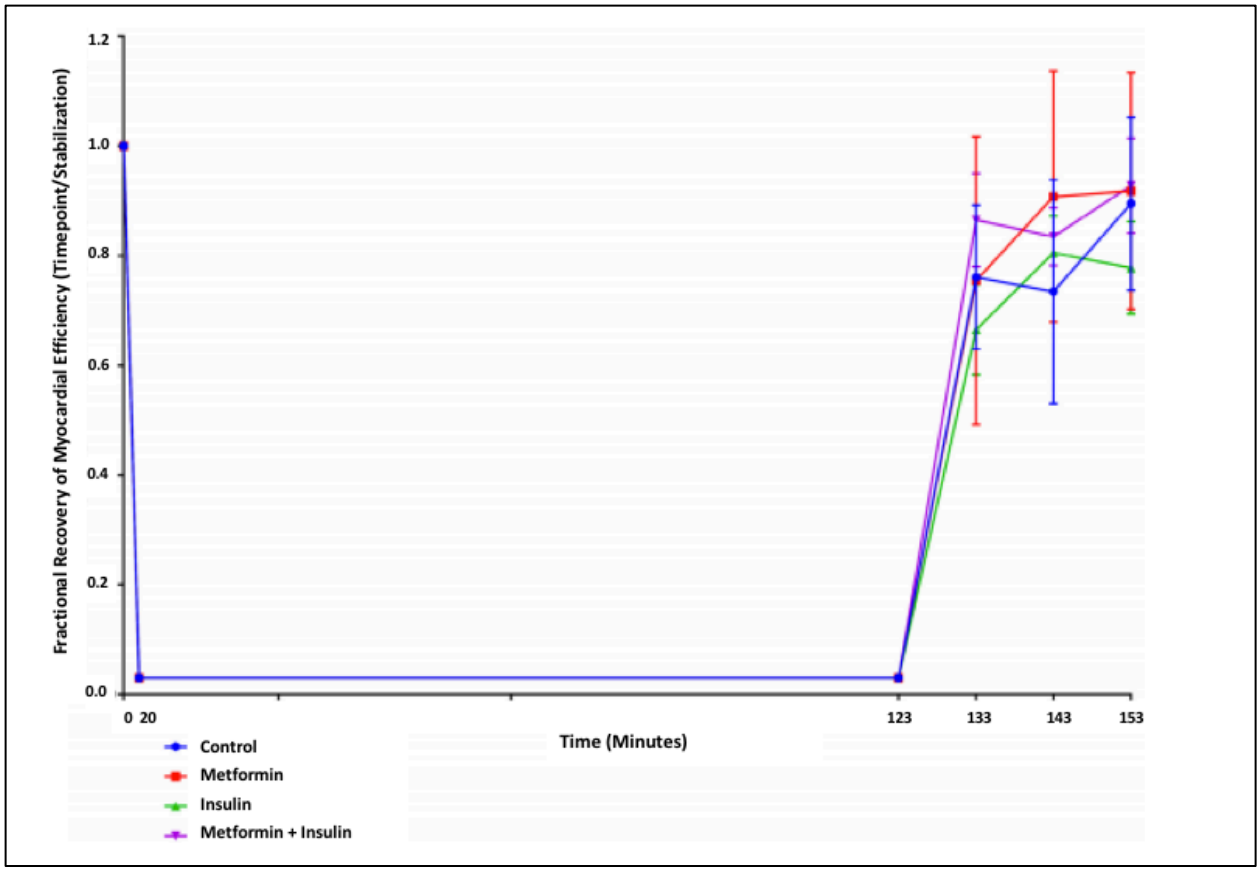

Figure 3.9: Myocardial efficiency in bypass condition. Data are represented as fractional recovery from stabilization period for each additive. There were no differences among groups after stabilization. Values displayed as mean ± Standard error of the mean. P= non-significant between additive groups or between individual time points within each group.

3.3.2 Myocardial Substrate Oxidation: Normokalemia

Fractional substrate oxidation during NK perfusion demonstrated some notable differences between groups. In the insulin only group, there was near complete absence of ketone oxidation with a corresponding increase in oxidation of lactate/pyruvate ($p < .05$). The combination of metformin and insulin seemed to suppress fatty acid oxidation with a corresponding increase in lactate/pyruvate, as well. See Figure 3.11. These differences persisted when fractional utilization data were combined with MVO_2 to calculate acetyl-CoA concentrations derived from each substrate. See Figure 3.12.

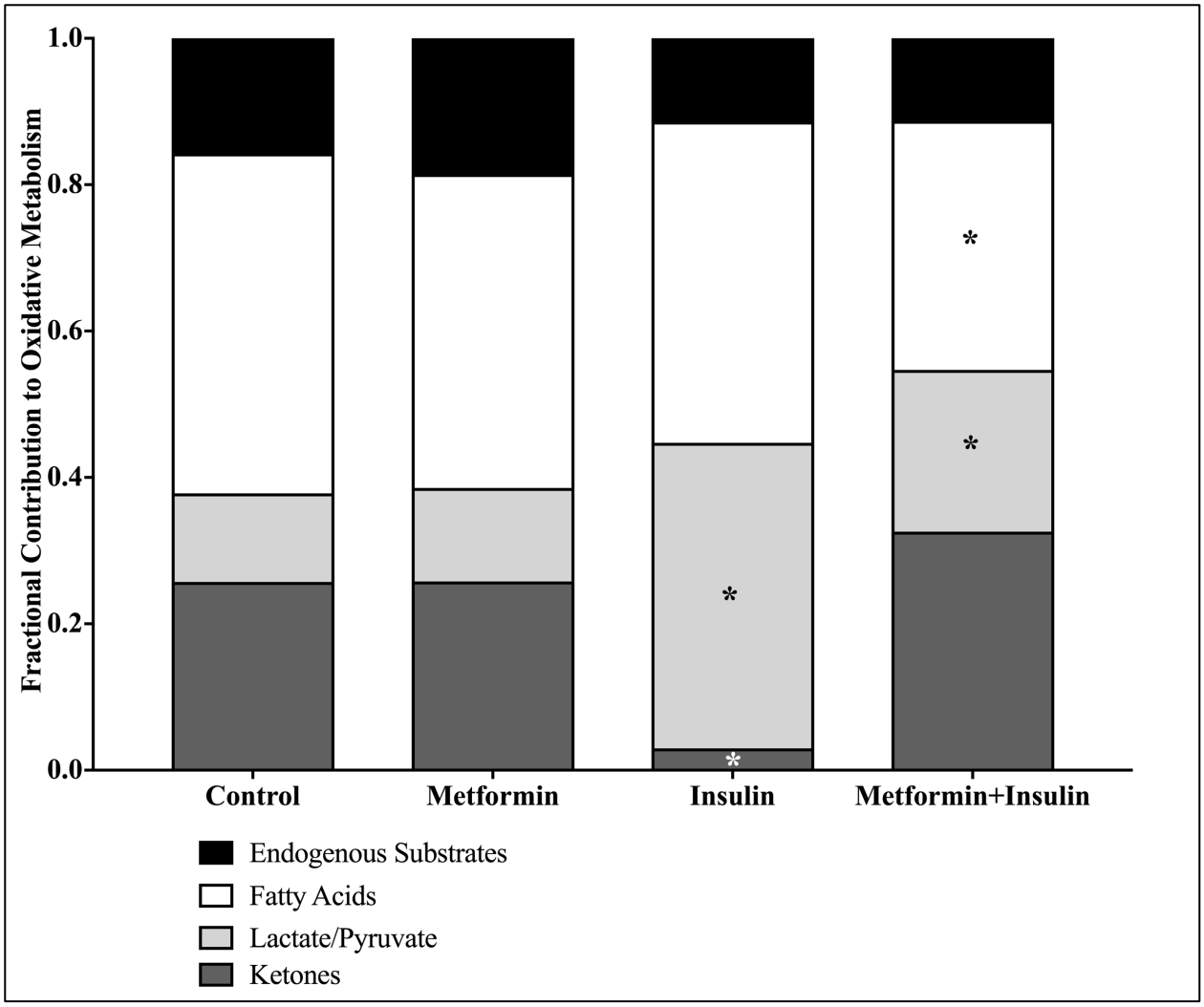

Figure 3.10: Fractional substrate use in normokalemia condition. Values shown as means. *P < .05 versus all other groups within substrate.

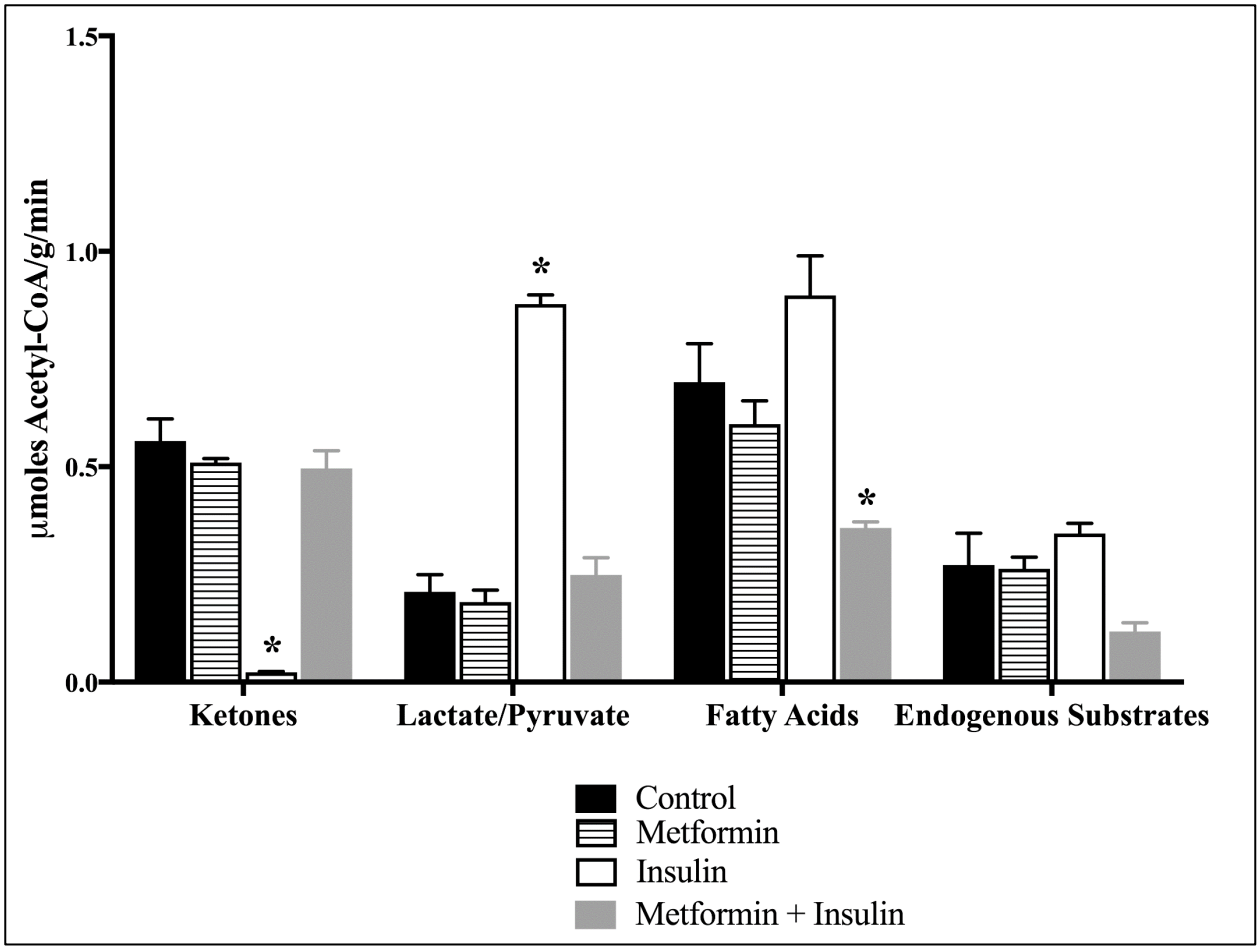

Figure 3.11: Amount of acetyl-CoA derived from each energy substrate during normokalemia. Values shown as mean ± standard error of the mean. *P < .05 versus all other groups within substrate.

3.3.3 Myocardial Substrate Oxidation: Cardioplegia

Perfusion of hearts with potassium modified buffer to simulate a period of cardioplegia demonstrated the expected shift away from fatty acid oxidation towards ketones in all but the metformin only group. When metformin was added to cardioplegia, fractional fatty acid and ketone oxidation were reduced with a corresponding increase in oxidation of exogenous substrates and lactate/pyruvate. See Figure 3.13. When these data were combined with MVO_2, only the reduction in ketone derived acetyl-CoA remained significant. See Figure 3.14.

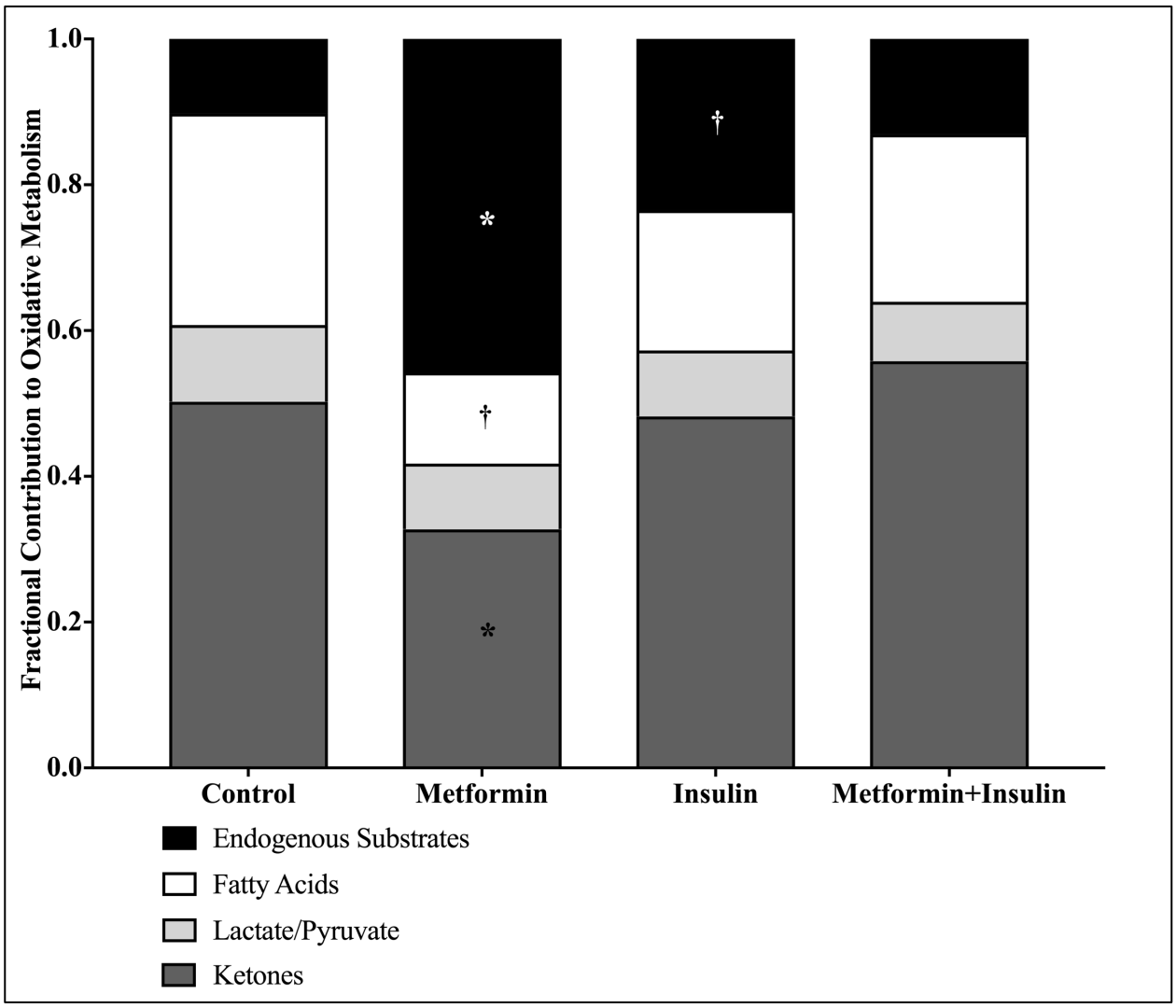

Figure 3.12: Fractional substrate use in cardioplegia condition. Values shown as means. *P < .05 versus all other groups within substrate. †P < .05 versus control within substrate.

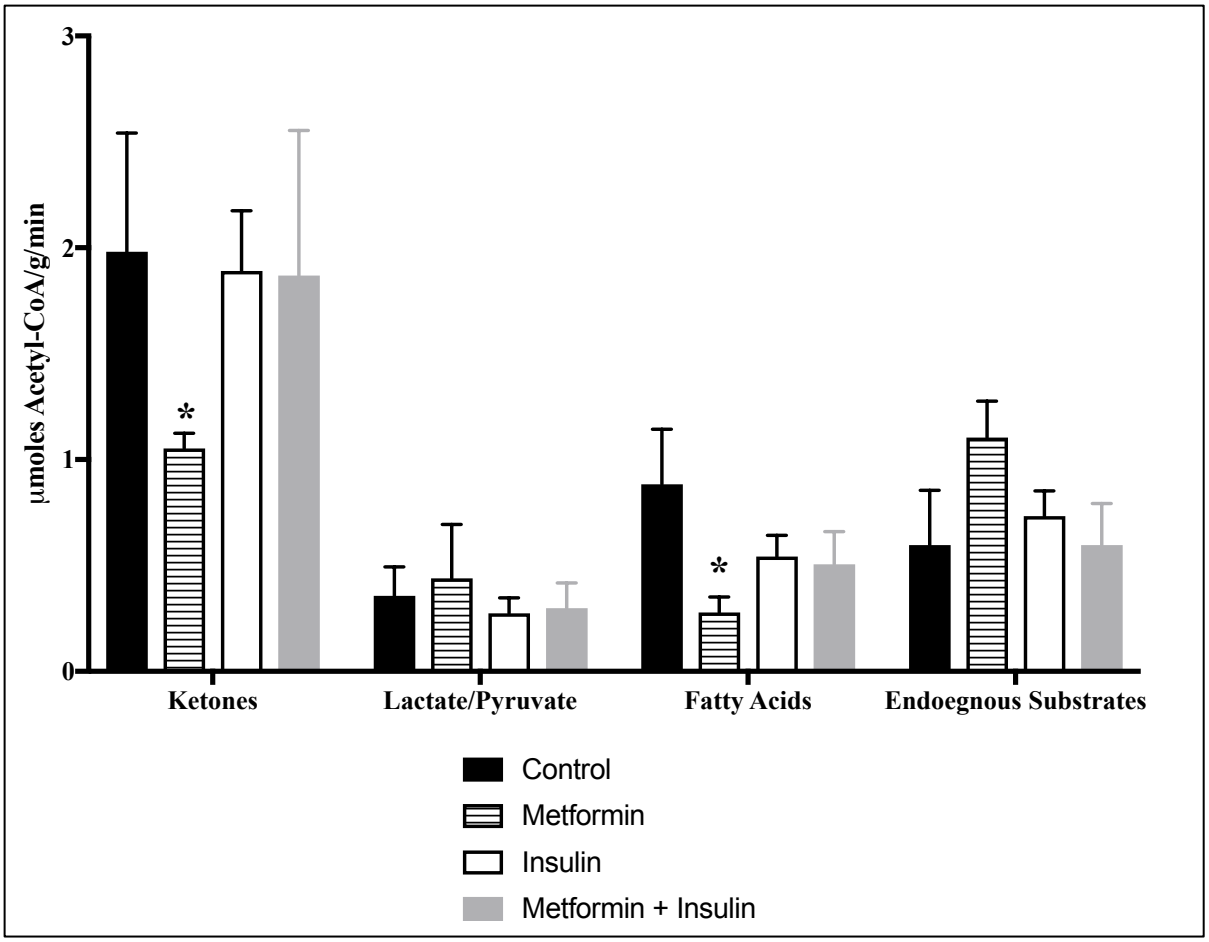

Figure 3.13: Amount of acetyl-CoA derived from each energy substrate during cardioplegia. Values shown as mean ± standard error of the mean. *P < .05 versus all other groups within substrate

3.3.4 Myocardial Substrate Oxidation: Bypass

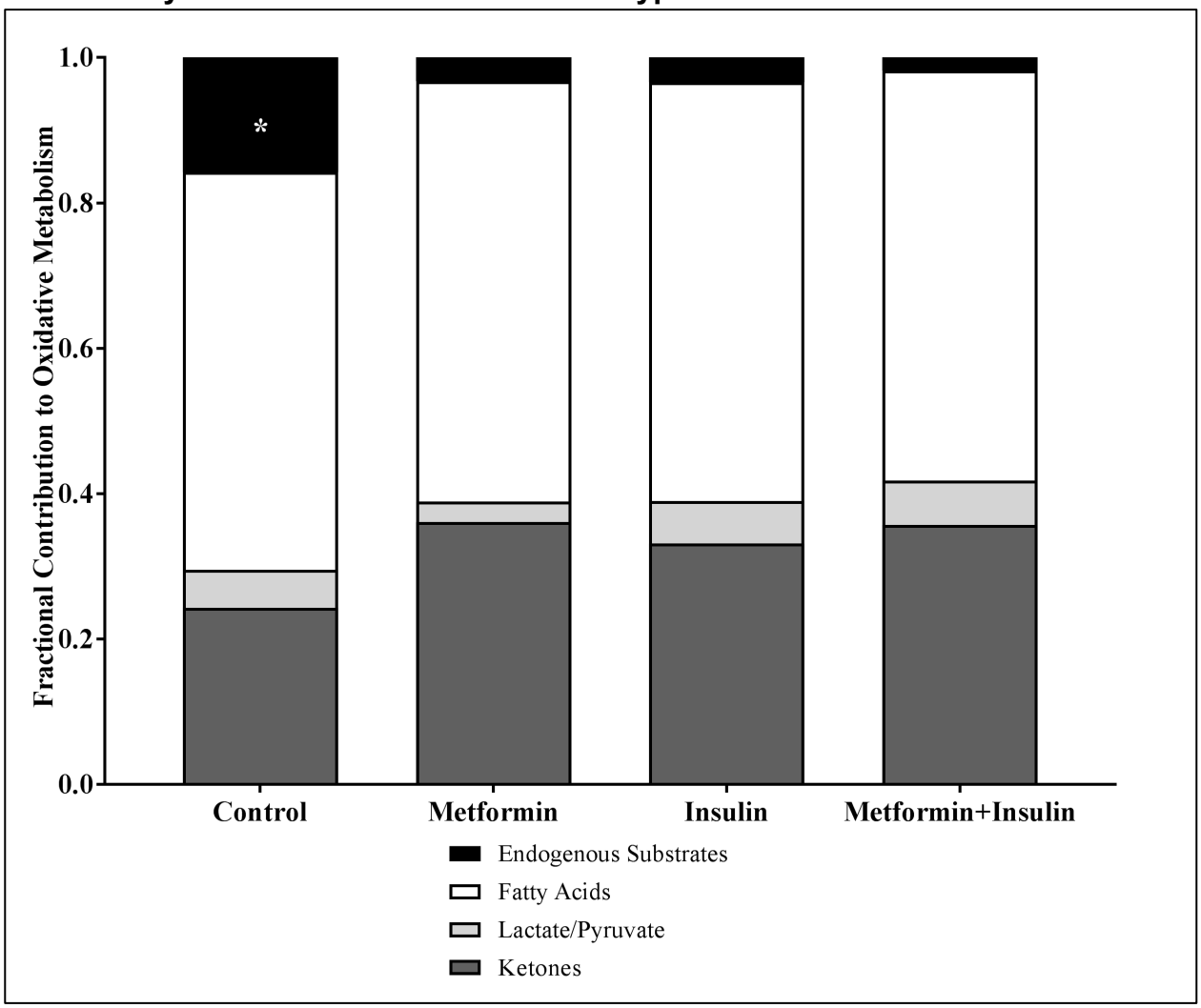

Figure 3.14: Fractional substrate use in bypass condition. Values shown as means. *P < 0.05 versus all other groups within substrate.

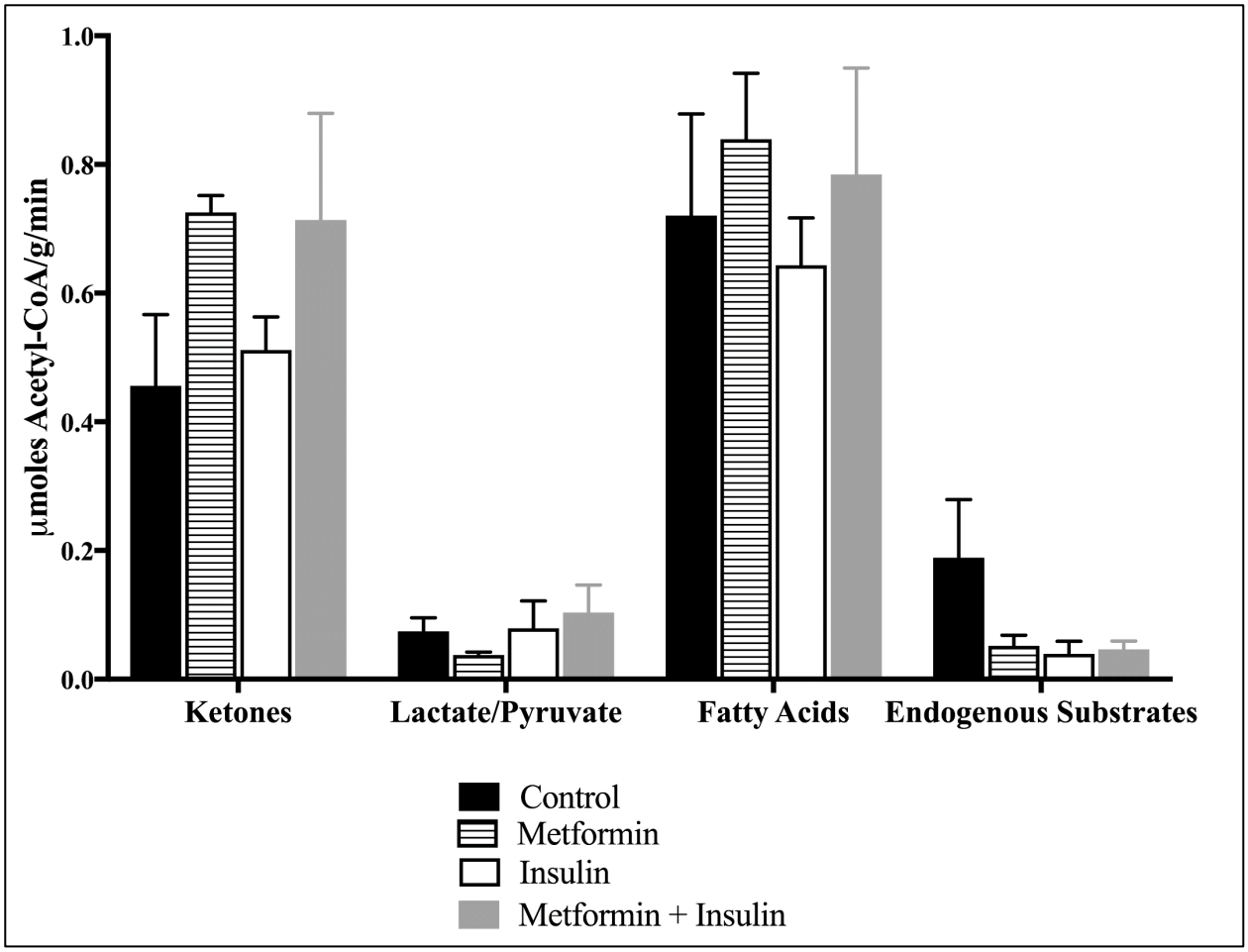

Figure 3.15: Amount of acetyl-CoA derived from each energy substrate during bypass. Values shown as mean ± standard error of the mean. P = nonsignificant

After 30 minutes reperfusion, fatty acid oxidation contributed over 50% of all acetyl-CoA to TCA cycle flux in all groups. Fractional utilization of fatty acids was higher for all BP groups compared to NK groups ($p<.05$). The only notable finding within BP groups was in increase in endogenous substrate – a difference that did not persists after adjusting for MVO_2. See Figure 3.15 and Figure 3.16.

3.3.5 Glucose Oxidation

Oxidation of exogenous glucose was investigated by switching the labeling pattern for all experiments to U-^{13}C labeled glucose and unlabeled mixed fatty acids. The lactate, pyruvate and acetoacetate labelling patterns remained the same (Figure 3.3). Glucose oxidation was virtually non-existent for all groups, independent of the perfusion conditions. Evidence of glucose oxidation was rare and less than 1% for all groups. In most groups, no MRS evidence of glucose oxidation was detected – suggesting that the unlabeled fraction represented metabolism of endogenous substrates only.

3.4 Discussion

The ability of myocardium to utilize a variety of substrates is considered a protective mechanism of the nondiabetic heart. Depending on substrate availability and physiologic conditions, myocardium can utilize all major fuels (fatty acids, glucose, ketones, lactate/pyruvate). Under normal conditions, fatty acids represent 60-70% of the supplied energy sources to the heart (Stanley, Recchia, and Lopaschuk 2005a). This percentage shifts to 40% during stressed conditions, while 20% of the energy source is derived from glucose (Wisneski et al. 1985; Allard et al. 1997). During ischemia, a switch in substrate selection from fatty acids to glucose may be beneficial because of the ability to generate ATP by glycolysis. The reverse is true under normoxic conditions when oxygen delivery is not limited which in part may explain why free fatty acids are the preferred myocardial substrate under these conditions (Christe and Rodgers 1995). Cardiac dysfunction in diabetic patients in part may be explained by the dependence on nonesterified free fatty acid oxidation (Gropler 2009). This reliance on fatty acid metabolism results in buildup of toxic lipid metabolites that predispose the heart to free radical injury, particularly during periods of ischemia and reperfusion (Christe and Rodgers 1995; Calvert et al. 2008). The effect of metformin on myocardial fatty acid oxidation remains unclear. Some investigators have suggested that metformin increases fatty acid oxidation in the heart although other investigators have suggested that fatty acid oxidation after metformin treatment is unchanged or even reduced (Shoghi et al. 2009; van der Meer et al. 2009; Saeedi et al. 2008). These effects may in part be mediated by metformin induced alterations in the myocardial redox state (Musi et al. 2002; Leverve et al. 2003). We previously have demonstrated the myocardial

redox state is an important determinant of relative substrate oxidation rates (Peltz et al. 2004). In the current experiments, metformin alone did not affect fatty acid oxidation under NK conditions suggesting that its influence on substrate utilization under normal circumstances is limited. In the presence of insulin, however, metformin reduced fatty acid oxidation with a corresponding increase in lactate/pyruvate oxidation. During CP, the presence of metformin results in potentially important alterations in myocardial substrate selection by reducing fatty acid and ketone utilization and shifting towards oxidation of lactate/pyruvate and endogenous substrates. Metformin alone or in combination with insulin did not significantly affect substrate selection after reperfusion in BP groups. Insulin resulted in near complete elimination of ketone oxidation with a corresponding increase in lactate/pyruvate flux during NK conditions. It had no significant influence on substrate selection either during CP or BP conditions. The mechanisms of action of metformin remain incompletely understood but drug treatment seems to potentiate the effects of insulin without increasing circulating insulin levels. Glycemic control in patients receiving metformin is improved by reducing gluconeogenesis in the liver and possibly increased peripheral glucose utilization (Mues et al. 2009).

Metformin's effect on metabolism appears to differ among various tissues. In hepatocytes, experimental and clinical data suggest metformin inhibits gluconeogenesis and glucose oxidation (Molavi et al. 2007). Metformin also appears to inhibit complex I of the respiratory chain and stimulates anaerobic glycolysis in both muscle and hepatocytes (Brunmair et al. 2004). Other investigators have noted that this increase in glycolytic flux does not result in increased glucose oxidation suggesting that anaerobic

glycolysis and glucose oxidation pathways are compartmentalized within cells (Collier et al. 2006; Ofenstein et al. 1999). Similar findings have also been suggested in human studies (Christensen et al. 2015). Together these data may explain observations in our experiments during NK conditions. Unopposed metformin therapy may inhibit pyruvate dehydrogenase flux and enhance anaerobic glycolysis. When insulin is added to the perfusate, PDH stimulation results in a shift away from fatty acid oxidation, stimulation of PDH, and increased oxidation of lactate and pyruvate. This same effect is not observed in CP conditions where the reduction in ketone and fatty acid oxidation is associated with an increase in endogenous substrate oxidation and no change in lactate/pyruvate oxidation. These findings may in part be explained by alterations in the myocardial redox state in CP as previously suggested (Peltz et al. 2004).

Interestingly, none of the combinations of additives appeared to alter myocardial substrate utilization in BP hearts after reperfusion. Fatty acid oxidation under this condition was increased compared to NK and not influenced by either insulin or metformin. These data would suggest, any beneficial effects of metformin or insulin are dependent on administration prior to reperfusion.

This study has several limitations. Most notably, we chose to investigate non-diabetic animals. Findings in a diabetic model may be quite different. Metformin has been shown to reduce instances of breast, lung and colorectal tumor formation in diabetic patients (Zhang et al. 2013; Kong et al. 2015; Kim et al. 2015). More recently, a study by Peled et al showed a reduction of malignancies (specifically skin cancers, mortality, and cardiac allograft vasculopathy in this study) in diabetic patients after heart transplants (Peled et al. 2017). However, the mechanism by which metformin exerted

these protective effects was not investigated. Long-term administration of metformin and insulin are planned to further elucidate these mechanisms, but we felt it was important to determine acute effects of these therapies on normal animals first, especially since benefits had been reported in the nondiabetic population, as well (Jiralerspong et al. 2009). Additionally, no functional differences could be detected among groups. This is perhaps not surprising considering normal hearts were used in this study. Nevertheless, it is remarkable that despite a total ischemic interval of nearly ninety minutes, myocardial function in this non-working model returned essentially to baseline.

Because the effects of metformin on myocardial metabolism are primarily noted in the potassium arrested heart, a condition encountered during hypothermic perfusion preservation, metformin may be considered as an additive under these conditions. The ability to shift substrate selection away from ketones and towards a more energetically favorable source could be beneficial for long-term preservation of donor hearts.

Chapter Four

Characterization of a Perfusion Method for Nanoparticle Delivery

4.1 Introduction

Cardiac viability during perfusion is an important factor during heart transplantation. Nanoparticle mediated delivery of therapeutic agents, gene products, or miRNA has not been investigated in this model. This aim seeks to demonstrate feasibility of nanoparticle-modified perfusion solutions for machine perfusion. Various delivery systems have been investigated including viral vectors, liposomes, and polymeric systems (Park, Jeong Jh Fau - Kim, and Kim 2006). Though efficient in delivery, viral vectors could possibly elicit an immune response. Non-viral delivery systems include lipid-based particles or polymeric particles. Common polymers used for gene delivery include Poly(l-lysine) (PLL), polyethylenimine (PEI), polycaprolcatone (PCL), and poly lactic co glycolic acid (PLGA). PLL and PEI are both cationic polymers whose positive charge allows for efficient nucleic acid packing and delivery. However, both polymers demonstrate high cytotoxicity and aggregation (Kafil and Omidi 2011). While PLGA and PCL are not cationic, they are commonly studied polymers for delivery. A triblock copolymer containing PLGA has demonstrated effective DNA delivery despite not being cationic (Jeong, Kim Sw Fau - Park, and Park 2004). Furthermore, PLGA is biocompatible and approved by the FDA for drug delivery. Complexing nucleic acids with a cation prior to encapsulation in PLGA represents a possible avenue for investigation. Cations like protamine, a small positively charged peptide derived from fish sperm, are able to complex with nucleic acid like messenger RNA (mRNA) and

small interfering RNA (siRNA) (Kauffman, Webber, and Anderson 2016). This complex in itself forms a sort of particle that can then be further emulsified into a PLGA nanoparticle. PCL is another polymer with a longer degradation time that has been previously used for encapsulation and for the delivery of messenger RNA (Palama et al. 2015). This aim seeks to address the formulation and characterization of a novel nanoparticle for the encapsulation of a therapeutic miRNA. miRNA-499 will be used to study the release and loading efficiency. MiRNA-499 exerts its effect on many pathways and is thought to play a cardioprotective role. It inhibits DYRK2, PDCDC4, PACS2, and DRP1 all resulting in anti-apoptotic effects stemming from inhibition of mitochondrial dependent apoptosis (Appendix). Previous work has shown that an antagomir, an inhibitory molecule, against miR-499 resulted in an increase in apoptotic cells in an ischemic injury mouse model while a miR-499 transgenic mouse reduced apoptotic cell occurrence (Zhang et al.). This suggests an important role for miR-499 in reducing injury during cardiac perfusion and it will be used to verify loading and release. Next, I identify the ideal perfusion conditions for nanoparticle delivery and is intended to demonstrate that the addition of nanoparticles to a perfusion solution does not negatively affect cardiac function.

4.2 Methods

4.2.1 Materials

Acid-terminated Poly (lactic-co glycolic acid) at a 50:50 ratio of lactide:glycolide at molecular weight range of 24,000-38,000 was procured from Evonik (Millipore Sigma, St. Louis, MO). miRNA-499 mimic (13000 g/mol) was custom synthesized from mirVana (a Thermo Fisher Scientific subsidiary, Waltham, MA). The miRNA isolation kit and RNA Storage solution were also procured from mirVana. Spermidine, dichloromethane, and the surfactant polaxomer 407 (a triblock polymer composed of polyethylene glycol and poly (propylene glycol) were also procured from Millipore Sigma. 10% buffered formalin and sucrose for tissue fixation were also obtained from Millipore Sigma. Rhodamine 6G (excitation wavelength of 528nm and emission wavelength of 551nm) was purchased from Sigma Aldrich.

4.2.2 Nanoparticle Fabrication

Preliminary studies investigated PCL and PVA as a possible polymer and surfactant combination. However, PLGA and P407 were eventually chosen due to a combination of literature review and preliminary fabrication experiments (Appendix). Nanoparticles were fabricated using a previously described double emulsion solvent evaporation

(Figure 4.1) procedure with a few modifications (Nakano et al. 2016).

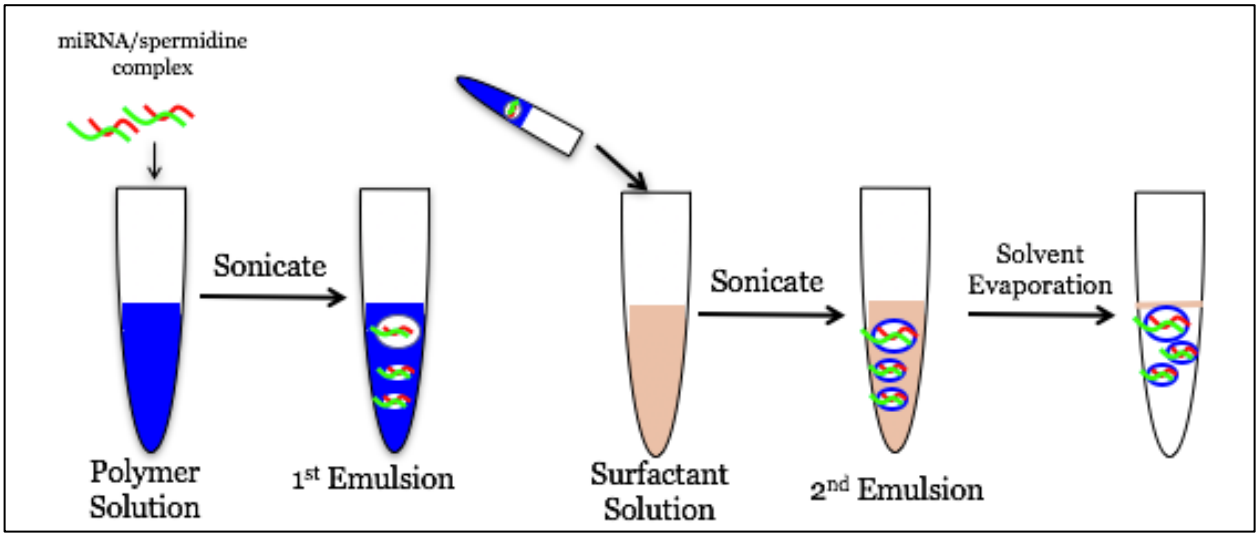

Figure 4.1: Double Emulsion Solvent Evaporation.

5-20 nanomoles of miR-499 mimic were reconstituted in RNAse free TE buffer to form the primary aqueous phase. Spermidine was added to the miRNA solution at a ratio of 15:1 (Spermidine phosphate group: miRNA nitrogen groups) and complexed for 30 minutes on a rotary shaker. This complex was then added dropwise under vortex to a 3% solution of PLGA in dichloromethane (oil phase) to form the first emulsion. This emulsion was sonicated on ice for a one-minute burst at 70% amplitude, followed by thirty seconds of no sonication. This burst-rest protocol was repeated five times for a total of five minutes of sonication. The first emulsion was then added dropwise under sonication to a 5% solution of polaxomer 407 (secondary aqueous phase) to yield a 6:1 (Surfactant solution: PLGA emulsion). This was then sonicated using the same burst-rest protocol described above to yield a total of five non-continuous minutes of sonication. This emulsion was then allowed to stir for at least six hours for evaporation of dichloromethane. Particles were then filtered using centrifugal filters to exclude

particles and free polymer particulates greater than 450nm in size. The remaining particles were then spun down for 30 minutes at 15000rpm and washed with TE buffer. Spinning and washing was repeated three times to remove any excess polymer or free miRNA. Particles were then freeze-dried for storage or further analysis.

Dye-loaded particles were made similarly for localization processes. Rhodamine 6G was dissolved in dichloromethane along with PLGA. This solution was then added in a dropwise manner under sonication to surfactant solution using the same burst protocol described above. Particles were then stirred, washed, and freeze-dried in the same manner.

4.2.3 Dynamic Light Scattering Characterization

A NanoBrook ZetaPals (Brookhaven Instruments, Holtsville, NY) machine was used to measure size, zeta potential, and polydispersity index using dynamic light scattering and Brownian Motion principles. Briefly, particles were reconstituted in PBS and loaded into a cuvette and loaded into the ZetaPals machine. A laser shines through the sample and the scattered light is measured by a detector. This detector uses scattered light information to measure diffusion of the particles. The diffusion value can then be plugged into the Stokes-Einstein equation to calculate hydrodynamic diameter (Figure 4.2).

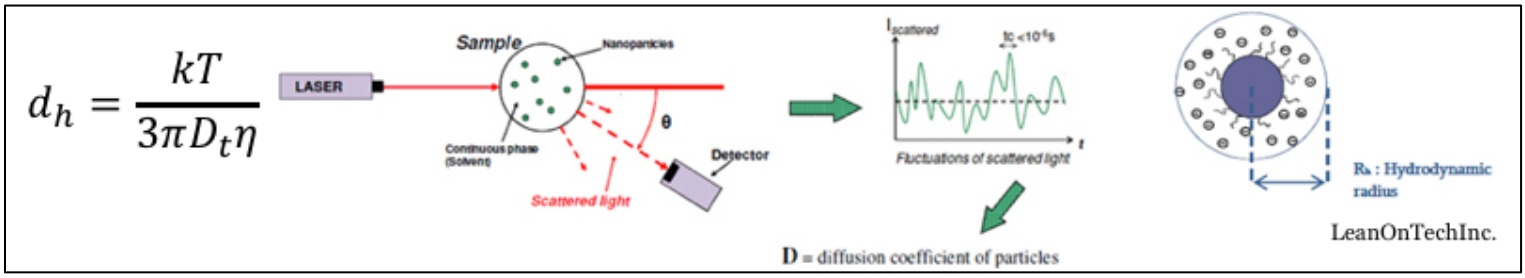

Figure 4.2: Stokes-Einstein equation (dh= hydrodynamic diameter, Dt=diffusion as a function of time, k=Boltzmann constant, T=absolute temperature, η=viscosity) and dynamic light scattering technique.

Polydispersity, a measure of uniformity ranging from 0 to 1 (uniform to non-uniform), is also calculated by ZetaPals and is calculated as the ratio of the mass average molecular weight (M_w) to the number average molecular weight (M_n). Zeta Potential was calculated to give a measure of the charge between the surface of the particle and the liquid. It is an indirect measure of particle stability and their propensity to aggregate.

4.2.4 Release and Loading Efficiency

Loading and release were determined using an Agilent bioanalyzer. Preliminary experiments were done to detect miRNA release by High-Pressure Liquid Chromatography. However, miRNA fragmentation occurred in interaction with the column and was difficult to quantify nucleotide fragmentation amounts. First, miR-loaded nanoparticles were prepared for an extraction procedure using the mirVana extraction kit. Briefly, particles were lysed in lysis buffer, followed by wash and centrifuge steps to yield only our small RNA product, miR-499. MiR-499 in solution was then stored in a -80°C freezer until analysis. One microliter of the sample was loaded into an Agilent bioanalyzer chip and automated gel electrophoresis was run to determine the amount of miR-499 sample present in solution. Loading efficiency was

then calculated using the equation in Figure 4.3.

$$Loading\ Efficiency = \frac{miRNA\ added - miRNAextracted}{miRNA\ added}$$

$$Release\ at\ Time\ Point = \frac{miRNA\ at\ timepoint}{miRNA\ added} + \text{previous timepoint}$$

Figure 4.3: Loading and Release Equations

Release was determined using a similar protocol. However, samples were taken at various time points (1hr, 6hrs, 12hrs, and 24hrs) by spinning down nanoparticles and sampling the supernatant. These samples were then run on an RNA chip to quantify exact amounts of miRNA loaded in solution. Release was determined using the specified equation in Figure 4.3.

4.2.5 Morphology

Particles for scanning electron microscopy (SEM) were sampled from a nanoparticle suspension, deposited onto a glass coverslip and allowed to dry in a desiccator overnight. This coverslip was then affixed to a metal stub using carbon paper for SEM imaging. Particles on the stubs were then sputter coated with gold using a Cressington 108 Sputter Coater (Cressington Scientific Instruments, Watford, UK). Stubs were loaded into the sealed chamber. Pressure inside the chamber was allowed to stabilize at 0.02 mBar and then argon gas was leaked into the chamber at a flow rate of 5 psi. Vacuum pressure inside the chamber was allowed to stabilize at 0.05 mBar. The coater then flushed the chamber twice with argon gas and then proceeded to coat the sample in gold at 40 mAmps for thirty seconds. After sputter coating, sample loaded stubs were

then imaged using a Zeiss Sigma VP SEM (Carl Zeiss Microscopy, LLC; Thornwood, NY). Imaging and sputter coating equipment were provided by the UT Southwestern Electron Microscopy Core Facility.

4.2.6 Cardiac Procurement

Rats were anesthetized with 4% chloral hydrate intraperitoneal injection. A sternotomy was performed to expose the chest cavity and 300 units/kg of heparin were administered by intrahepatic injection. The inferior vena cava and the superior vena cava were ligated. The heart was removed and stored in ice-cold lactated ringers.

4.2.7 Perfusion Models

Hearts were mounted on a Langendorff apparatus and perfused by retrograde perfusion through the ascending aorta with substrate free UWMPS with glucose added (0.99 grams per liter) at 8 ± 2ºC. Various perfusion models were tested and are shown in Figure 4.4. A total of four groups were investigated: Recirculating 6-hour Perfusion Control (no added nanoparticles), Recirculating 6-hour Nanoparticles, Non-Recirculating 3-hour Perfusion Control (no added nanoparticles), Non-Recirculating 3-hour Perfusion with a burst infusion of nanoparticles. Both recirculating perfusion and non-recirculating perfusion were evaluated for their ability to promote particle uptake but minimize aggregation. In all models, all hearts were stabilized with UWMPS without nanoparticle additives for thirty minutes, measurements were taken, and then nanoparticles introduced in the relevant models. In the recirculating models, nanoparticles were added after thirty minutes and allowed to recirculate via the waste chamber flowing back into the solution chamber. In the non-recirculating model (Figure 4.4), nanoparticles were

infused into the perfusate through a syringe portal above the aortic cannula. Waste was not recycled back into the solution chamber in this model. Both recirculating and non-recirculating controls were void of nanoparticles for the entire perfusion interval. Coronary flow and inflow and pulmonary artery perfusate pO_2 were measured every 30 minutes. Oxygen consumption (MVO_2) was calculated from aortic and pulmonary artery pO_2 differences, flow rate, and oxygen solubility and reported as μmol O_2 per gram dry weight. After the perfusion interval, a small cardiac tissue sample was placed in an oven for drying to determine dry weight. Samples were weighed until a constant, stable value was obtained. The ratio between wet and dry weight was calculated to determine water content. Lactate inflow and outflow was measured at each time increment and reported as lactate inflow subtracted from lactate outflow. Hearts from each group were set aside

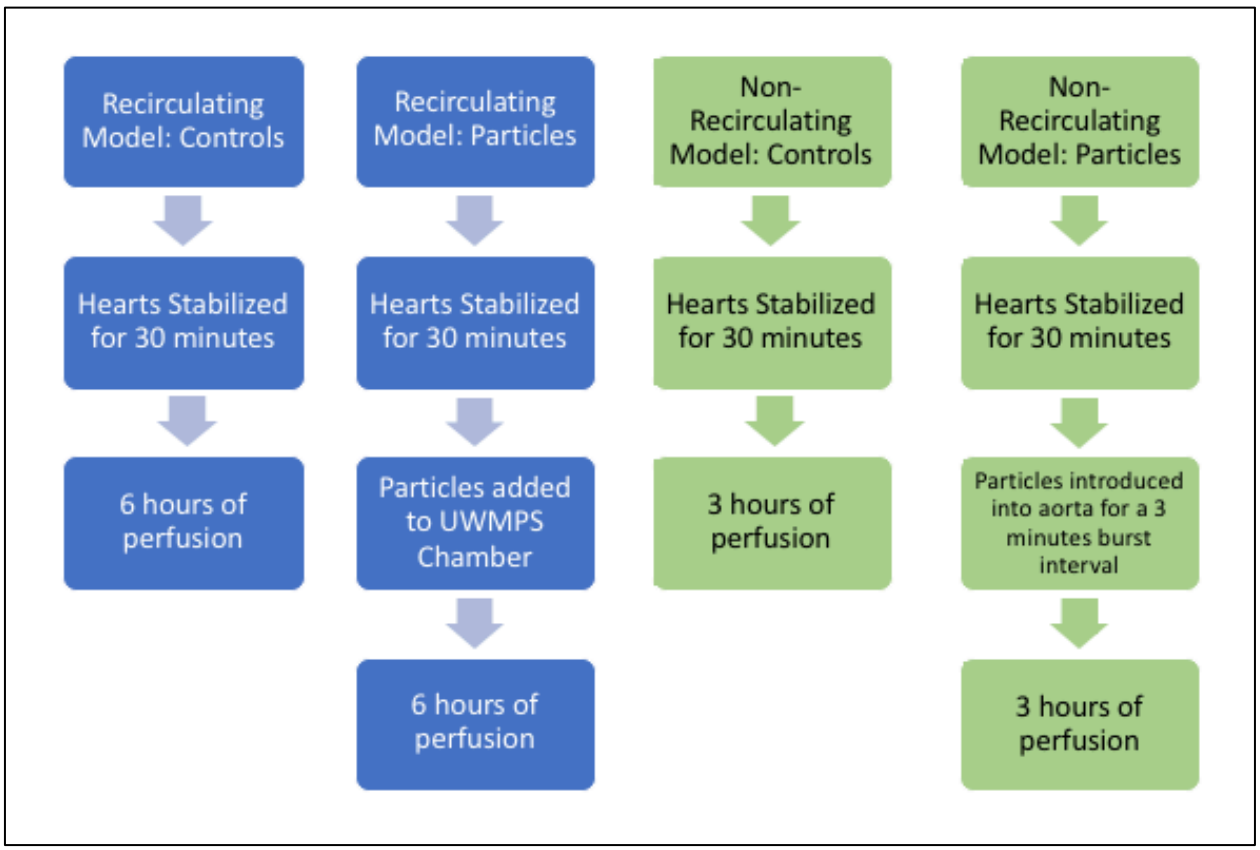

Figure 4.4: Nanoparticle Perfusion Methods. 6-hour Recirculating groups are in blue and 3-hour non-recirculating groups are in green.

for fixation and uptake studies while the remaining hearts were freeze-clamped in liquid nitrogen cooled tongs and stored in a -80^{oC} freezer. In addition to the groups mentioned above, preliminary studies investigated nanoparticle perfusion with UWMPS at 37$^{\circ C}$, perfusion with normokalemic and cardioplegic Krebs-Heinslet buffer at 37$^{\circ C}$, and tail vein injection for 24 hours. These groups reduced coronary outflow over two to three hours suggestive of capillary aggregation and toxicity and therefore were only investigated by confocal microscopy for particle uptake.

4.2.8 Uptake and Localization

Hearts set aside for uptake and localization studies were fixed in formalin for 24 hours, followed by fixation in 10% sucrose and then 18% sucrose. Hearts were then cryoembedded for a four-chamber view of the heart and stained with Hoechst Nuclear dye by the University of Texas Southwestern Histology Core. Tissue slices were imaged by confocal microscopy at the UT Southwestern Live Cell Imaging Facility using a Zeiss LSM 880 Airyscan confocal microscope (Carl Zeiss Microscopy, LLC; Thornwood, NY). 20X and 63X oil objectives were used with multi-channel imaging at 433nm and 533nm to image the blue (DAPI) and red (rhodamine 6G) wavelengths simultaneously. Both still images and z-stacks were acquired at a line scanning values of 8 and 4 respectively. Images were analyzed and using ImageJ Software.

4.2.9 Tissue Extraction

Hearts set aside for NMR studies were freeze-clamped in liquid nitrogen cooled tongs and stored in a -80^{oC} freezer. Tissue metabolites were extracted by grinding the tissue sample with mortar and pestle under cooled, liquid nitrogen. The pulverized

tissue was reconstituted and extracted in 4% perchloric acid and neutralized with potassium hydroxide. Samples for MRS analysis were freeze-dried in a speed vacuum and reconstituted in 1.08mM EDTA in deuterium oxide at a pH of 7.0-7.4 for loading into NMR tubes to analysis.

4.2.10 Magnetic Resonance Spectroscopy

Proton (^{1}H) spectra were acquired on a 14.1 Tesla Varian spectrometer at 600 MHz over a spectra width of 8000 Hz. Lactate and alanine peaks were measured to generate lactate to alanine ratios. The lactate to alanine ratio serves as a measure of aerobic and anaerobic metabolism. Phosphorus (^{31}P) spectra were also acquired on the 14.1 Tesla Varian spectrometer at an operating frequency of 243 MHz over a spectral width of 36000 Hz. Inorganic phosphate (Pi), gamma adenosine triphosphate (γ-ATP), and phosphocreatine (PCr) were measured to identify high energy phosphate stores in the perfused hearts. PCr/Pi, γ-ATP/Pi, and PCr/γ-ATP ratios were used to characterize the energy state of the myocardium. Spectral analysis, peak-fitting, and peak integration were performed using ACD Spectra Software.

4.3 Results

4.3.1 Nanoparticle Characterization

MiRNA loaded particles were characterized for their size, polydispersity index, zeta potential, morphology, release and loading efficiency.

Size (nm)	376 ± 98
PDI	.16 ± .06
Zeta Potential	-29 ± 4.6
Encapsulation Efficiency (%)	65 ± 12

Table 4.1: Nanoparticle Characterization.

SEM images show particle size and a spherical shape (Figure 4.5).

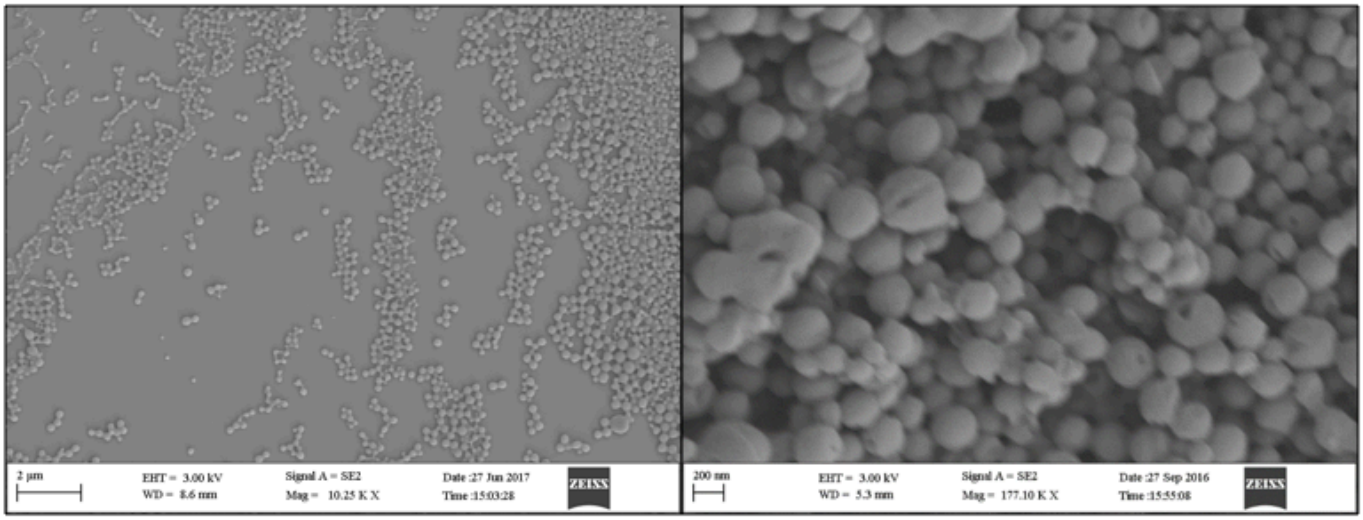

Figure 4.5: miR-499 loaded nanoparticles by SEM imaging.

Release and loading efficiency were characterized by bioanalyzer. Representative spectra in figure shows the output from small RNA analysis performed by this machine.

The generated peak abundance gives an indication of the abundance of a specific miRNA by detailing its nucleotide count and concentration. The spectra in Figure 4.6 shows the internal standard at 4 nucleotides and the miRNA of interest at 21 nucleotides. The peak at 40 nucleotides represents background noise in the sample. Total miRNA amount can be extrapolated from the reported concentration and original volumes used in fabricating nanoparticles. 2.72% of miRNA is released over the course of four days with 0.3% being released in a 6-hour interval (Figure 4.7).

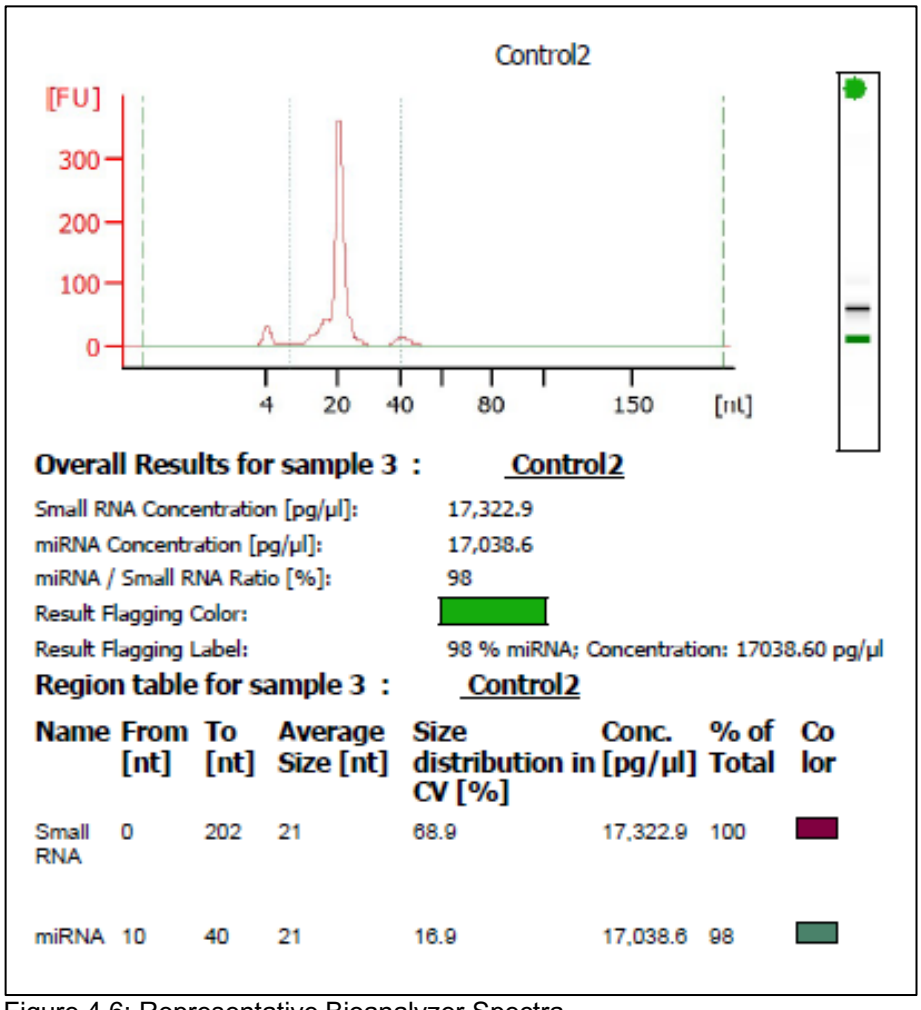

Figure 4.6: Representative Bioanalyzer Spectra

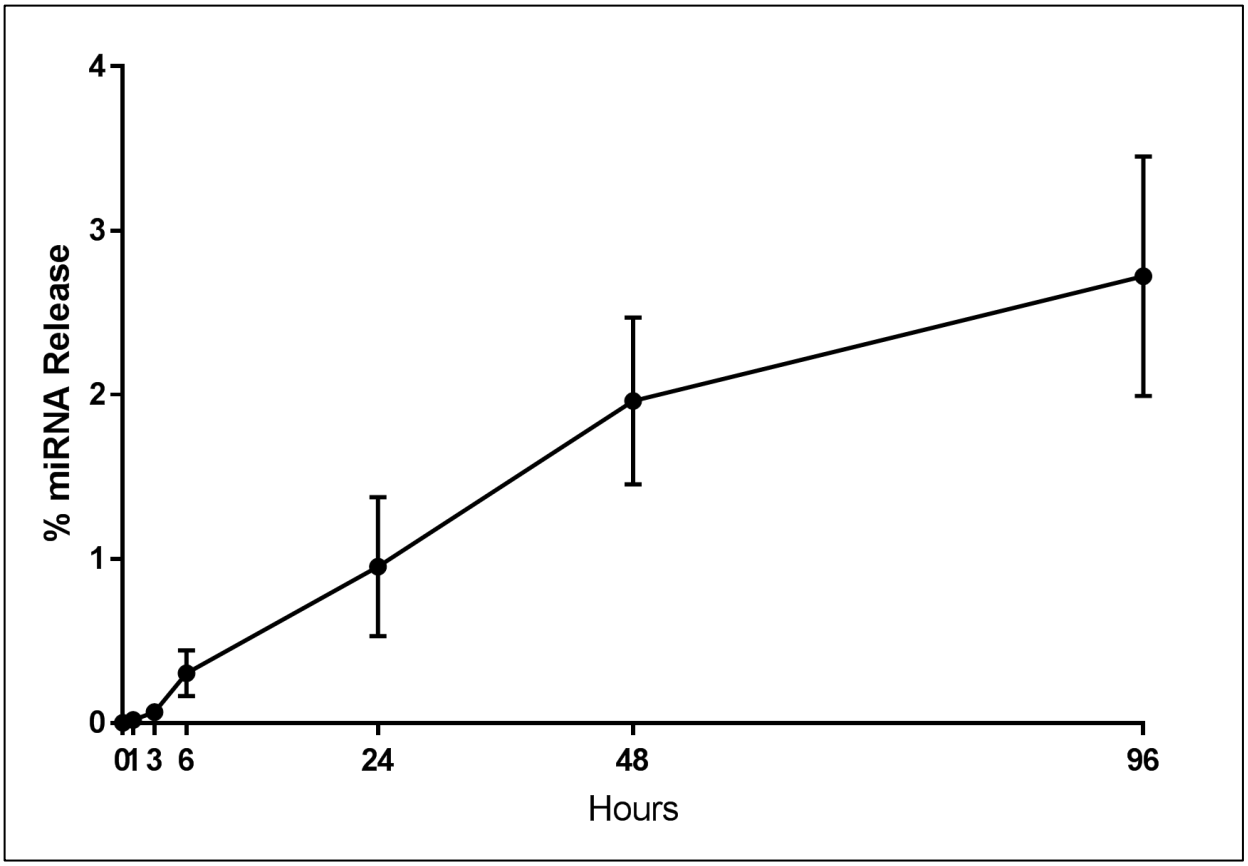

Figure 4.7: Nanoparticle Release Profile of a miRNA product. Error bars are depicted as SEM.

4.3.2 Particle Localization

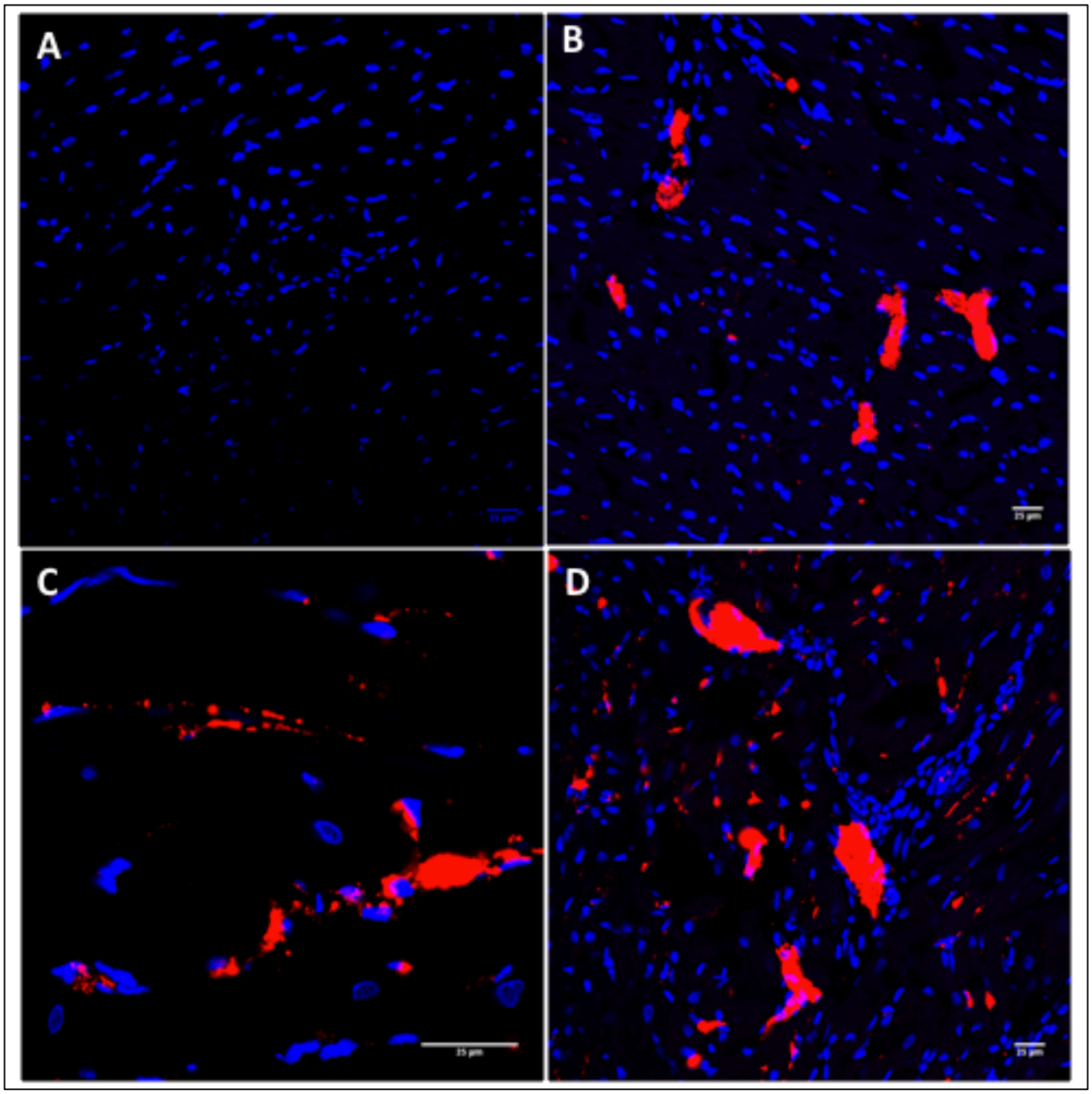

Figure 4.8: Particle Localization in 6-hour recirculating Models. Blue=stained nuclei, Red=nanoparticles A: Control, 20X magnification. B: Low Concentration, 20X magnification. C: High Concentration 63X magnification. D: High Concentration.

Cell nuclei were stained using Hoechst dye (blue) and nanoparticles were loaded with rhodamine 6G. Six-hour perfusion groups are shown in Figure 4.8. Panel A in Figure 4.8 shows no particle uptake in the control group while B, C, and D show particles located in the tissue, surrounding and in nuclei. Low concentration (2mg nanoparticles) in Panel B showed slightly lower particle uptake and was only investigated in preliminary studies and not for cardiac functionality due to lower uptake. High concentration (40mg) (Panel D) shows a more diffuse particle uptake profile. Panel C shows high concentration results at a higher magnification where passive particle uptake by the nuclei is shown.

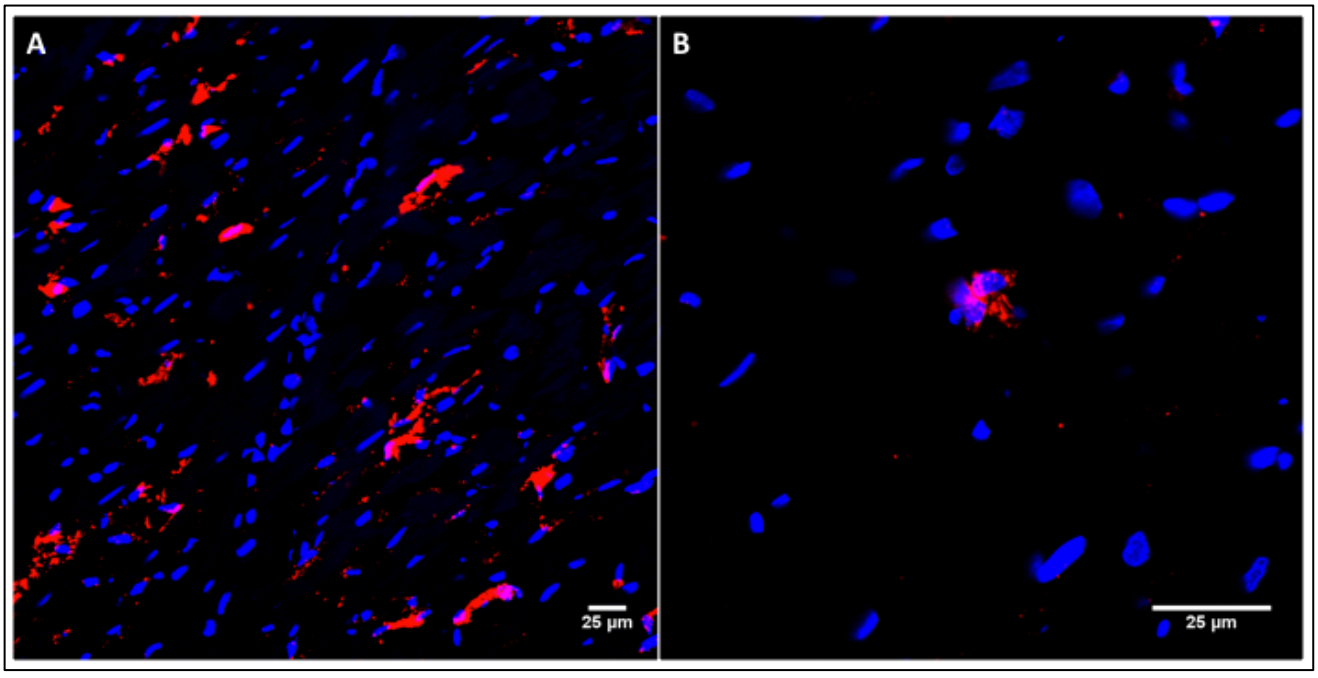

Figure 4.9: Burst Release followed by 3hrs of Perfusion. A: 20X b: 63X

Figure 4.9 shows particles uptake in the non-recirculating three-hour perfusion model. Nanoparticles (40mg) were introduced in a burst release manner. Images show that complete particle washout did not occur, and uptake occurred despite fluid not recirculating.

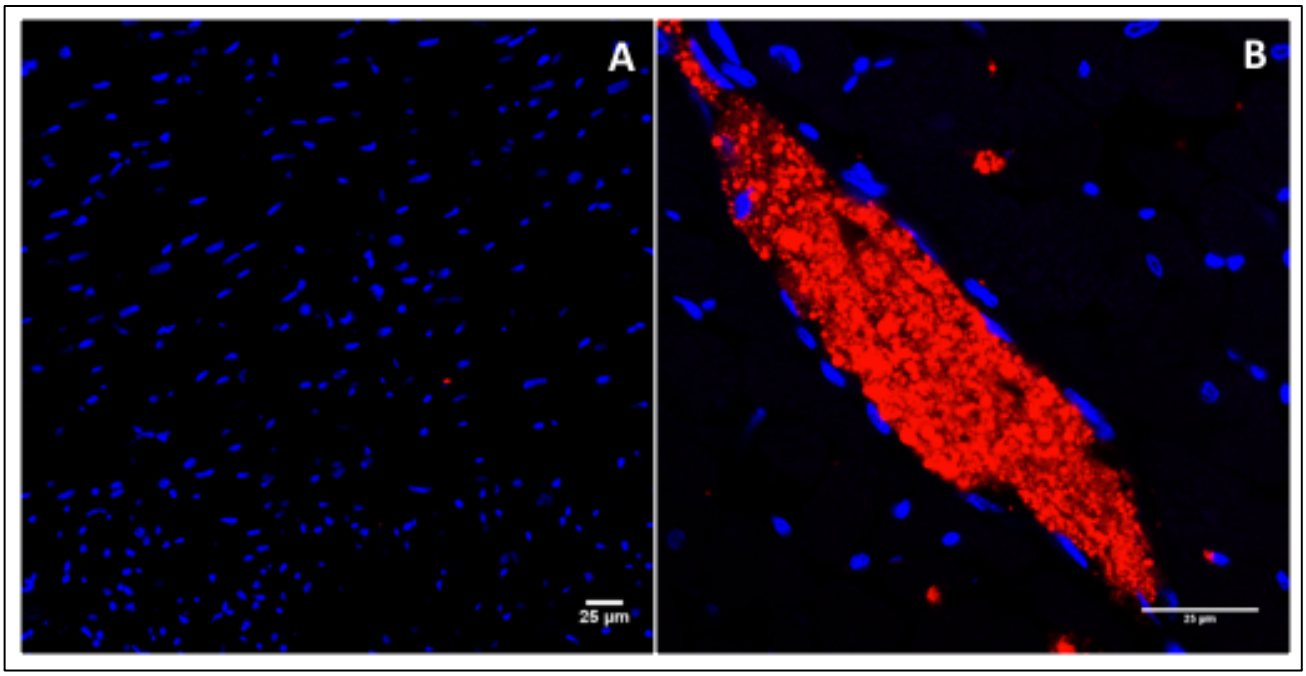

Figure 4.10: A. Normokalemic Krebs perfusion. B. 37°C Perfusion

Preliminary experiments to elucidate solution and temperature dependence were shown in Figures 10. Using a KHB solution with high nanoparticle concentration showed minimal to no particle uptake (Figure 4.10A). Perfusion at higher temperature (37°C) with UWMPS showed diffuse particle uptake in the tissue but frequent aggregation in blood vessels (Figure 4.10B).

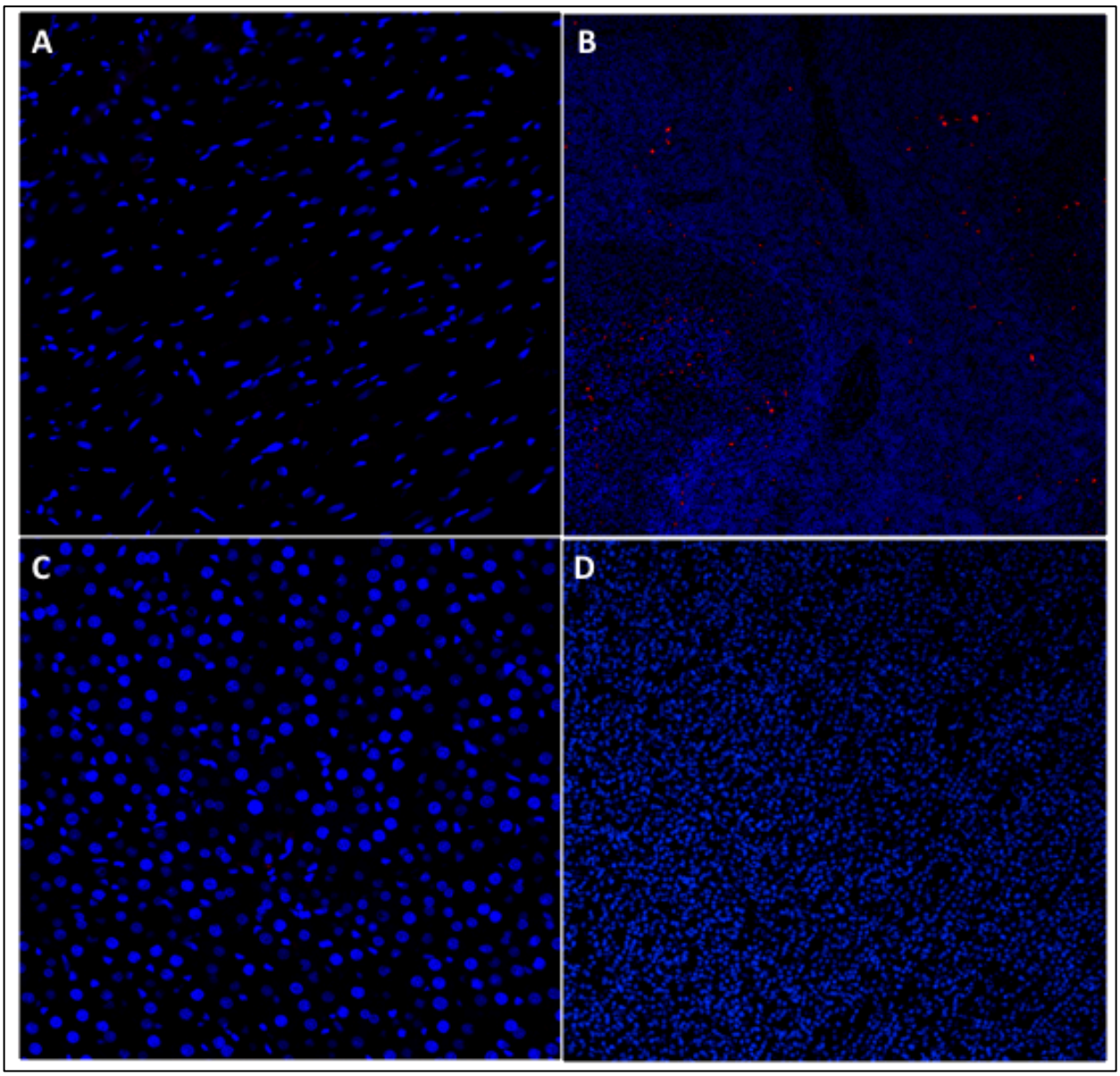

Figure 4.11. 24 hours after tail vein injection of high concentration nanoparticles. A: Heart B: Spleen C: Liver D: Lungs

In vivo experiments were performed by tail vein injections with a high nanoparticle concentration in rats and circulation for 24 hrs. Particle uptake by the heart was virtually nonexistent (Figure 4.11A) while the spleen showed the highest amount of particle

uptake (Figure 4.11B). Both the liver and the kidneys showed no significant particle uptake (Figure 4.11C and Figure 4.11D, respectively).

4.3.3 Coronary Flow and Water Retention

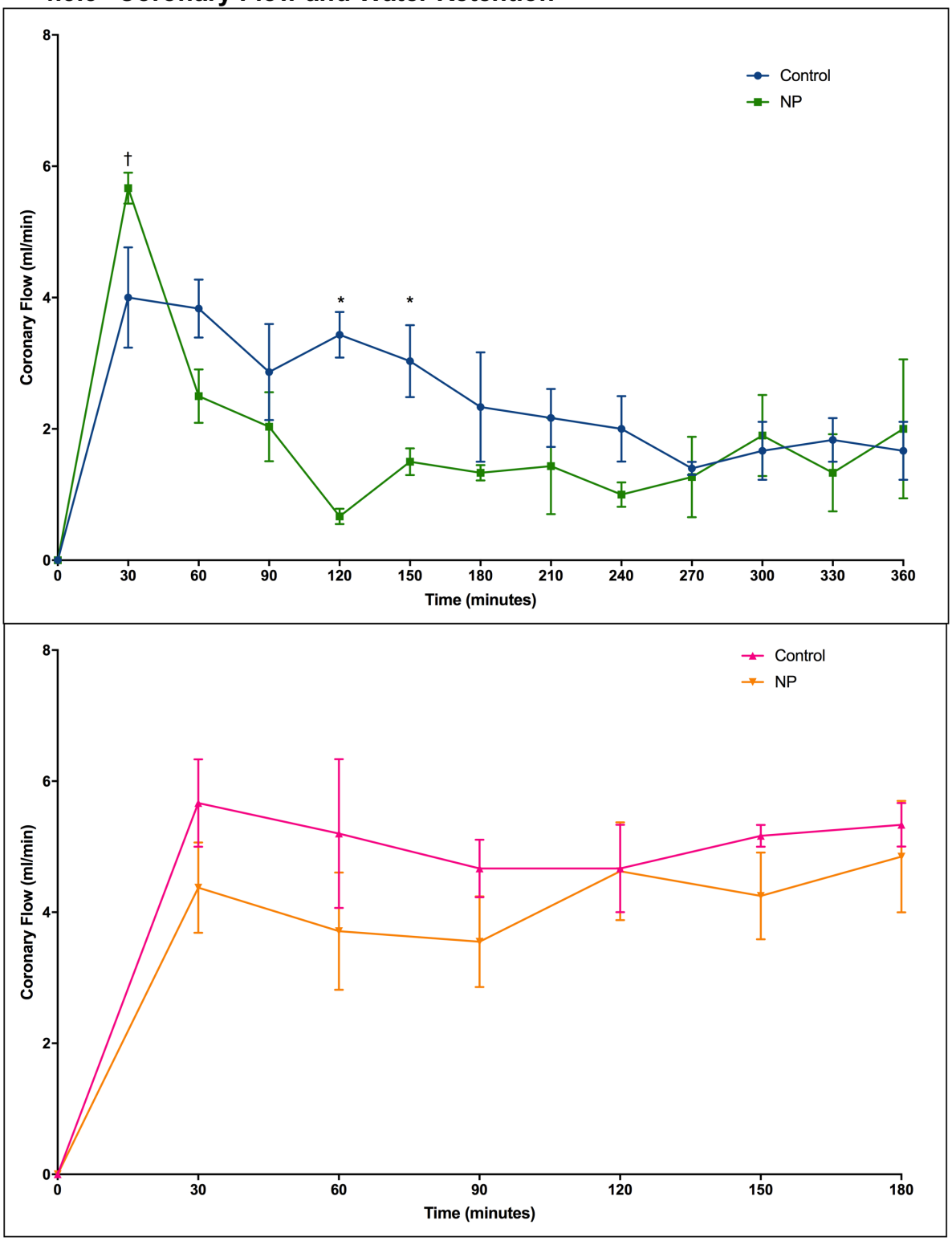

Figure 4.12: Coronary flow (ml/min) NP=nanoparticles. Values reported as Percentages ± SEM. *-p<0.05 vs other group at same time point. †-p<0.05 vs all other time points within the same group. Top Panel: 6 hours Recirculating. Bottom Panel: 3 hours Non-Recirculating.

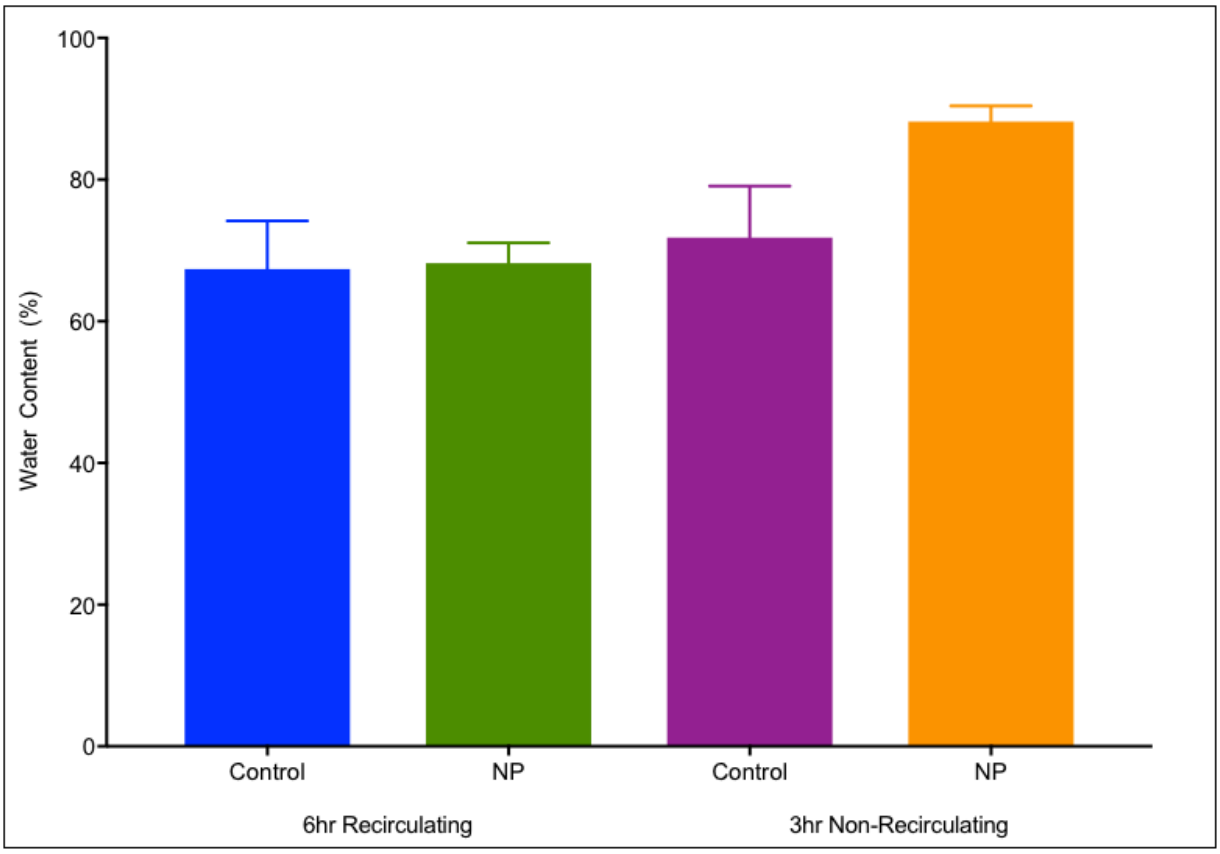

Figure 4.13: Water Content. Values reported as Value ± SEM.

Coronary flow over time is depicted in Figure 4.12. Both six-hour groups demonstrated a decline in coronary flow over the six-hour interval and never returned the coronary flow value depicted at 30 minutes. The three-hour group maintained coronary flow after stabilization and throughout the 3-hour interval and no statistical significance between stabilization (30 minutes) and any other time points was found. Water Content (Figure 4.13) was slightly higher in the 3hr NP group but was overall unchanged across groups.

4.3.4 Oxygen Consumption

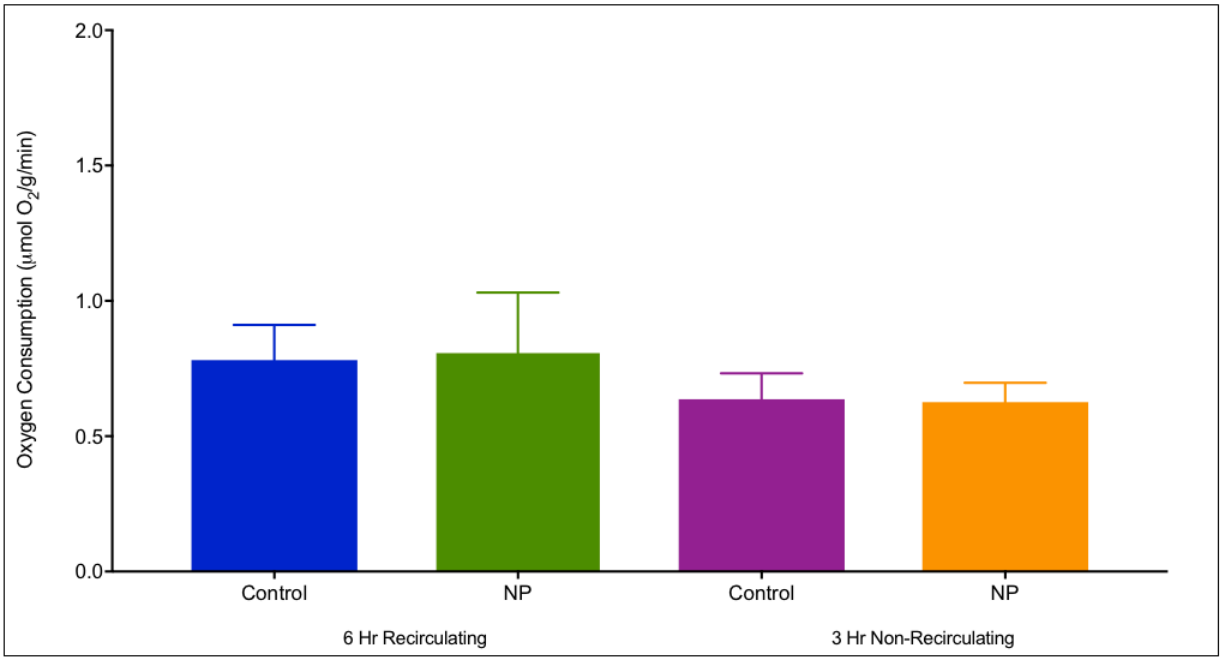

Figure 4.14: Oxygen Consumption. Values reported as mean ± SEM. NP=nanoparticle.

Average Oxygen Consumption is depicted in Figure 4.14. The 3 hours groups demonstrated slightly lower oxygen consumption in general, but these differences did not reach statistical significance. Differences across all groups were minimal, indicating parameters did not significantly affect oxygen consumption.

4.3.5 Lactate Accumulation

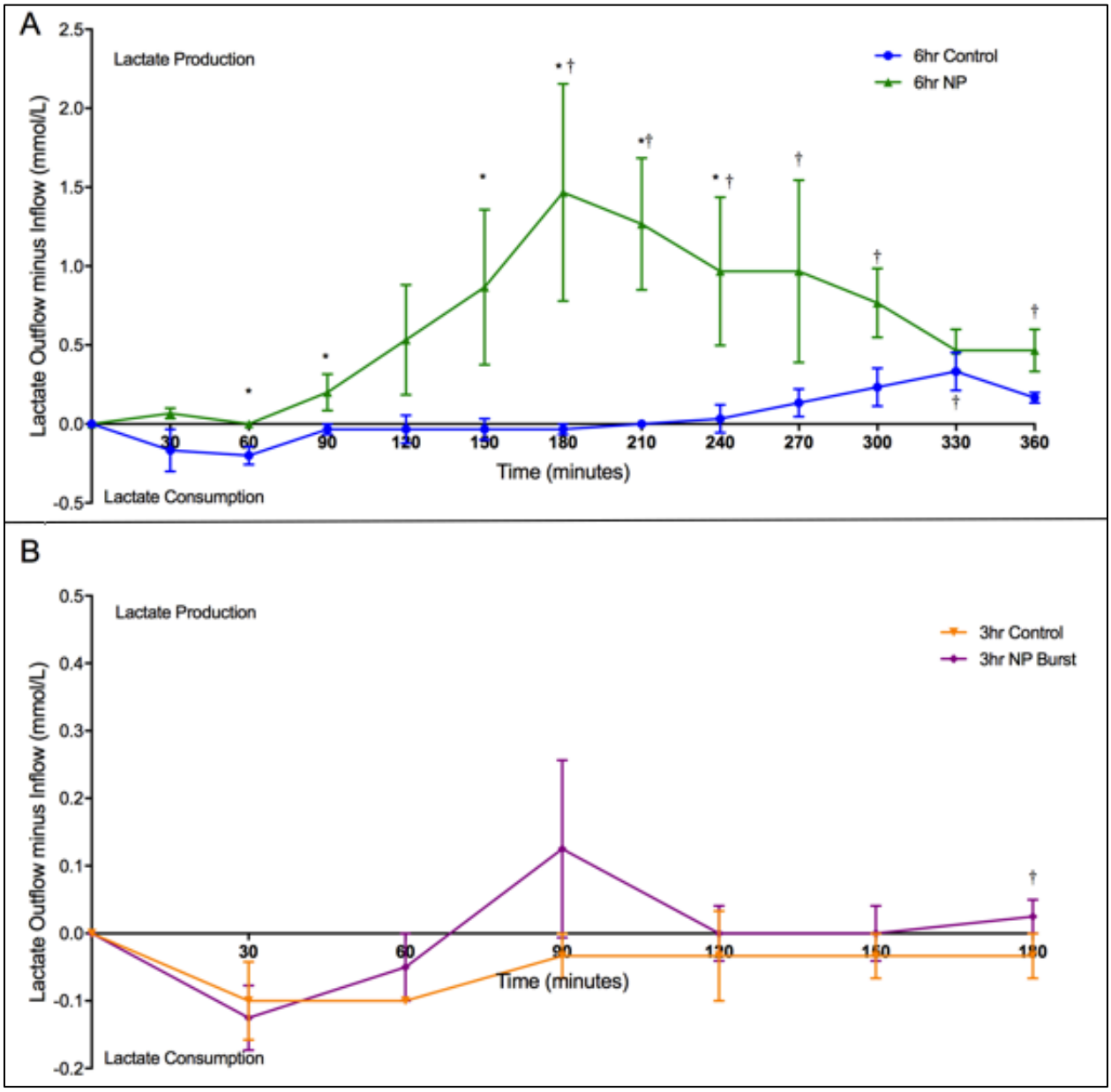

Figure 4.15: Lactate Behavior over time. Reported as values ± SEM. Values above 0 represent lactate Production while values below 0 represent lactate consumption.*-p<0.05 vs control group at same time point. †-p<0.05 vs t=30min within same group. A: 6-hour Recirculating Groups. B: 3 Hour Non-Recirculating Groups.

Lactate change over time is shown in Figure 4.15. Lactate production or consumption values were derived from subtracting lactate inflow from lactate outflow. In both the 3-hour groups and the 6-hour Control group, lactate production was low, and the hearts were net lactate consumers. However, the 6-hour NP group demonstrate net-lactate release over most of the perfusion period – significantly higher for most time points compared to the 6-hour Control group.

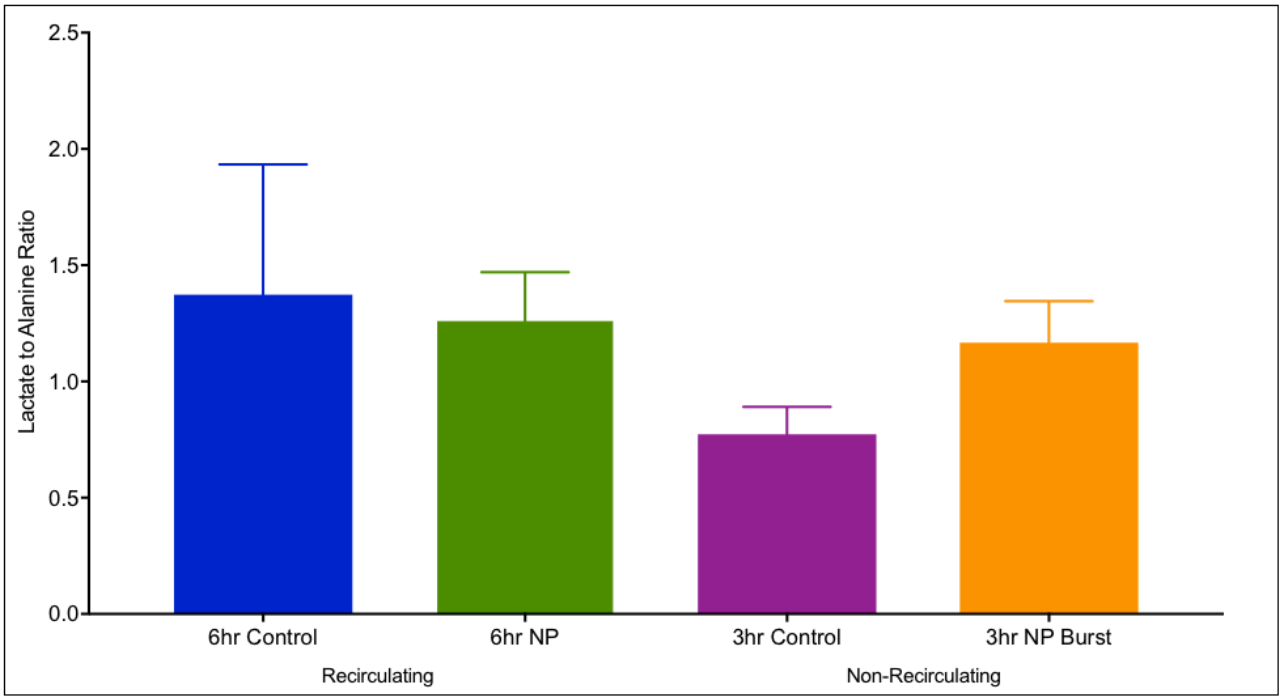

Figure 4.16: Lactate to Alanine ratio. Reported as ± SEM.

The lactate to alanine ratio was lowest in the 3-hour control group in comparison to all other groups, but none of the differences reached statistical significance. Generally, these values are consistent with hypothermic machine perfusion metabolic profiles.

4.3.6 Energetic Phosphates

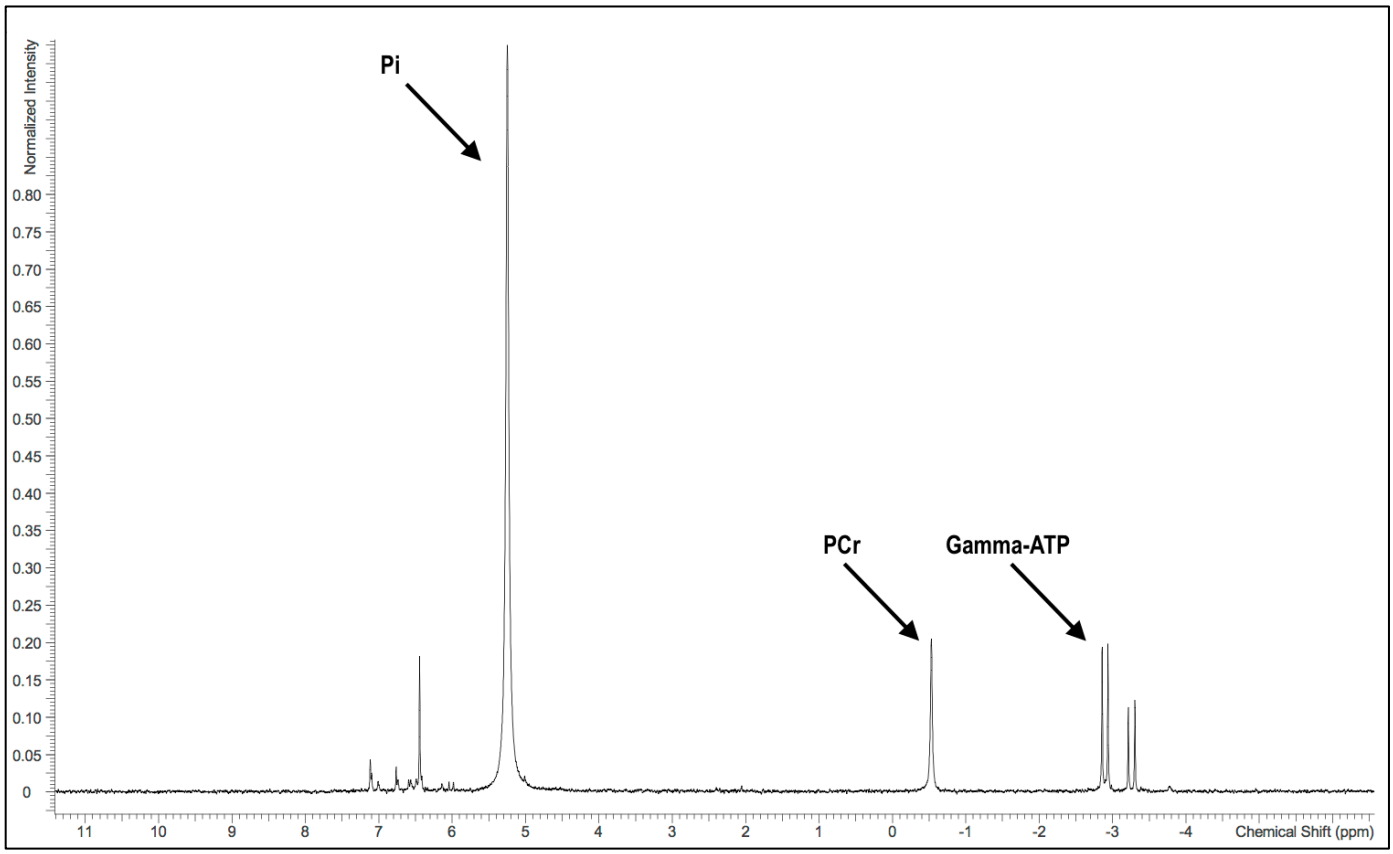

Figure 4.17: Phosphorus-31 MRS Spectra of Perfused Heart. Peaks of interest indicated by arrows.

Energy phosphate values were generated using Phosphorus NMR. Spectra were analyzed between the chemical shift range of -11 to 11ppm for detection of peaks of interest. Figure 4.17 shows the inorganic phosphate (Pi) peak resolved at about 5ppm, the phosphocreatine (PCr) peak between -1 and 0 ppm, and the γ-ATP peak at about -3ppm. The γ-ATP was experiences peak splitting. Peaks in all groups were resolved at the same chemical shift values shown in the figure, though their abundance varied.

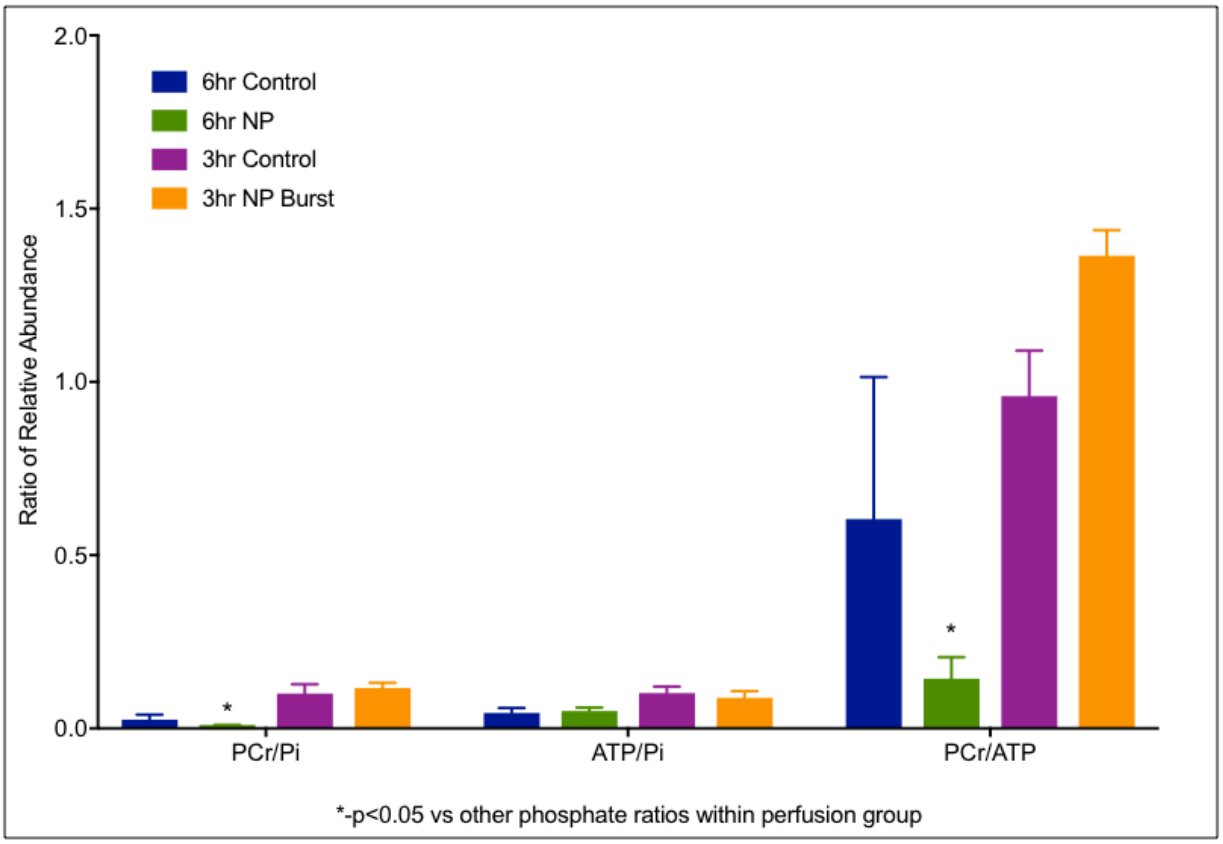

Figure 4.18: Energetic Phosphates in Nanoparticle Perfusion Models. NP=nanoparticle. *-p<0.05 vs all other perfusion groups within ratio group.

The 6-hour nanoparticle perfusion group demonstrated lower ratios across all energetic phosphate ratio groups. This difference reached statistical significance for the PCr/Pi and PCr/ATP variables by one-way analysis of variance. Both 3-hour groups were higher than the 6-hour groups in PCr/ATP. PCr (Phosphocreatine) was the dominant energetic substance in the 3-hour nanoparticle group.

4.4 Discussion

The purpose of this study is to optimize perfusion solutions by creating a loaded nanoparticle for delivery to the heart during the preservation interval. PLGA nanoparticles are ideal due to their biocompatibility and the ability to tune their properties. They possess the ability to be taken up by cells and deliver products while largely evading multiple clearance and filtration pathways. Because of these properties, they are optimal candidates for delivery of therapeutics and miRNA to the heart during perfusion. For heart uptake applications, coronary vasculature size defines the upper limit for nanoparticle diameter. The diameter of the human aorta ranges from two to three centimeters, but the capillaries represent the smallest pathway through which a particle would need to travel. Human capillaries have a diameter ranging from 4 to 5 microns, so nanoparticles should ideally be much smaller in order to travel successfully through the vasculature and not aggregate and occlude capillary flow. Particles were formed in this study using an established double emulsion solvent evaporation method where sonication bursts allow for the creation of small particle. Furthermore, filtration of the particles removes any particles large than 450 nanometers. I used miRNA as our test encapsulated material as it will be further investigated in future studies, however the focus of this study was to demonstrate the ability for the isolated, cold-perfused organ to take up nanoparticles. This establishes nanoparticles as viable additives for delivering miRNA to the heart in this hypothermic model. Complexing miRNA with a cation prior to encapsulation has been proven to mitigate issues with encapsulating a large, negative particle (Moore et al. 2016; Woodrow et al. 2009). I demonstrated that it results in a high

encapsulation efficiency rate. The release profile of the particle suggests a release amount in the picomole range which is comparable to miRNA release in cellular medium(Devulapally et al. 2015). The release profile in the single digits is in accordance with expected miRNA release in this setting and might be enough to have a downstream effect. This could also suggest the need to incorporate a large amount of miRNA in the fabrication process in order to ensure a high percentage is released at the onset. Cardiac perfusion intervals in our lab range from two to fourteen hours and particles can be further tuned to the specific perfusion interval. This study shows that miRNA release or product release does occur over a six-hour interval and would be viable to continue studying in isolated perfusion models.

Successful particle fabrication was demonstrated, but delivery in a machine perfusion model had not yet been fully characterized. Investigating nanoparticle delivery in a six-hour model represented our first approach. Six hours of recirculating nanoparticle perfusion was performed to maximize particle uptake as any perfusate that flows through the heart and exits as waste is then eventually recycled back to the heart. However, during the interval, assessment of the hearts indicated reduced coronary flow despite images showing tissue and cellular particle uptake. Lower particle concentrations and non-recirculation were tried with no difference in profiles. Overall, in six-hour groups we showed a reduced ability of the heart to maintain high energy phosphate stores and an increase in the lactate to alanine ratio suggesting higher anaerobic activity occurring. Six hours of perfusion could be causing particles to get trapped in current eddies which causes vasculature blockages and would account for the reduced coronary flow. This reduced flow would explain the reduced energy profile

and increased lactate production as the nutrient rich perfusate is not fully reaching the heart. Perfusate solution, temperature, and particle concentration were eliminated as issues by performing the experiment with different solutions, at 37 degrees, and with 2mg of particles. Cardiac functionality was unchanged.

Though the functional profile of the 6-hour heart was marginal, uptake of particles still occurred. However, a shorter time frame (3 hours) was investigated to try to mitigate functional issues. In these groups, the lactate to alanine ratio was reduced and high energy phosphate stores were better maintained. All 3-hour groups maintained coronary flow and oxygen consumption. A better profile could be seen due to a shorter time frame and elimination of recycled products entering the heart. Overall, three hours of nanoparticle perfusion represents a superior avenue to pursue nanoparticle delivery.

These studies had a few limitations. Six hours of non-recirculating nanoparticle perfusion was not tested due to eventual clinical limitations. To look down the line at the clinical application of this would require a large volume of perfusate solution and over 100 nanomoles of miRNA per each experiment. While this could be investigated, I chose to investigate other potential perfusion models first. Future studies should investigate miRNA-499 effect in the three-hour perfusion model. Particle uptake was seen, but qualitative effect must be determined. MiRNA effect in a three-hour recirculating and three-hour non-recirculating model will be determined by investigating downstream miRNA-499 targets and miRNA expression. This study represents a step forward in using nanoparticles for gene delivery in a hypothermic machine perfusion model.

Chapter Five

Summary

5.1 Conclusions

Findings in Aim 1 demonstrated that exogenous delivery of substrates to the heart during machine perfusion appears to be necessary to maximize oxidative metabolism of the cold perfused heart. Octanoate and acetate were both preferentially oxidized when added to the perfusate. Endogenous substrates were favored when β-hydroxybutyrate was the only substrate present in the preservation solution. All exogenous substrates increased TCA cycle intermediate concentrations. At least over a 6-hour perfusion interval, an anaplerotic substrate is not necessary to maintain oxidative metabolism as evidenced by no further enrichment in isotopomer contributions or TCA cycle intermediates when propionate was added to the perfusate. These results have important implications for designing perfusion solutions for the machine perfused heart.

Metformin, an insulin-sensitizing agent, has shown a cardioprotective effect in surgical outcomes. The addition of metformin and insulin to a perfusion solution were investigated in Aim 2 for their ability to alter substrate oxidation while maintain cardiac function in a normokalemic, hyperkalemic, and bypass model. While neither additive affected myocardial efficiency after reperfusion, important effects on substrate selection were noted. During normokalemic perfusion, insulin reduced ketone oxidation and increased utilization of lactate and pyruvate. Metformin's primary effect on substrate selection was exerted during cardioplegia leading to reduced ketone and fatty acid oxidation under conditions that might be encountered during hypothermic machine

perfusion. These findings suggest that metformin may be a preferred additive to alter substrate oxidation profiles in the cold perfused heart.

Nanoparticles are a unique method to deliver otherwise unstable or degradable therapeutics to a target organ during hypothermic machine perfusion. Fabricated particles must encapsulate and release the product without significantly altering cardiac performance when added to the perfusion solution. Loaded nanoparticles were successfully constructed in an appropriate size range for the cardiac vasculature and with the ability to encapsulate product. Successful release and tissue targeting of nanoparticles was demonstrated over a six-hour time interval. Investigation of different delivery strategies suggested improved metabolic and energetic profiles when a nanoparticle burst release technique was utilized compared to a continuous recirculating model.

An optimal perfusion solution for HMP has not been identified and myocardial metabolism under these conditions is not well understood. My experiments identified substrates that are preferentially oxidized by the heart during HMP, as well as additives that may alter cardiac metabolism towards oxidation of favored substrates to improve preservation of the donor heart. The ability to target the perfused myocardium with drugs, gene products or miRNA by encapsulation into nanoparticles not only serves to improve preservation of the organ but also provides an opportunity to repair the damaged heart while undergoing HMP.

5.2 Future Studies

The current experiments demonstrated that certain myocardial substrates and additives have important effects on metabolism of the heart. It will be important the confirm these findings in human hearts to determine preferred additives for clinical application of this technique. While substrate selection of the human heart may be different, principles developed in the current study will still apply. We previously successfully utilized human hearts rejected for transplantation to validate findings from animal studies and plan on evaluating human heart metabolic preferences in this model. Additionally, while nanoparticle experiments suggested delivery of product to myocytes, ultimately a successful target effect must be demonstrated. Future studies will investigate the ability of nanoparticle encapsulated miRNA-499 to suppress calcineurin activity and thus modify ischemic injury and apoptosis in hearts undergoing HMP.

Chapter Six

Appendix

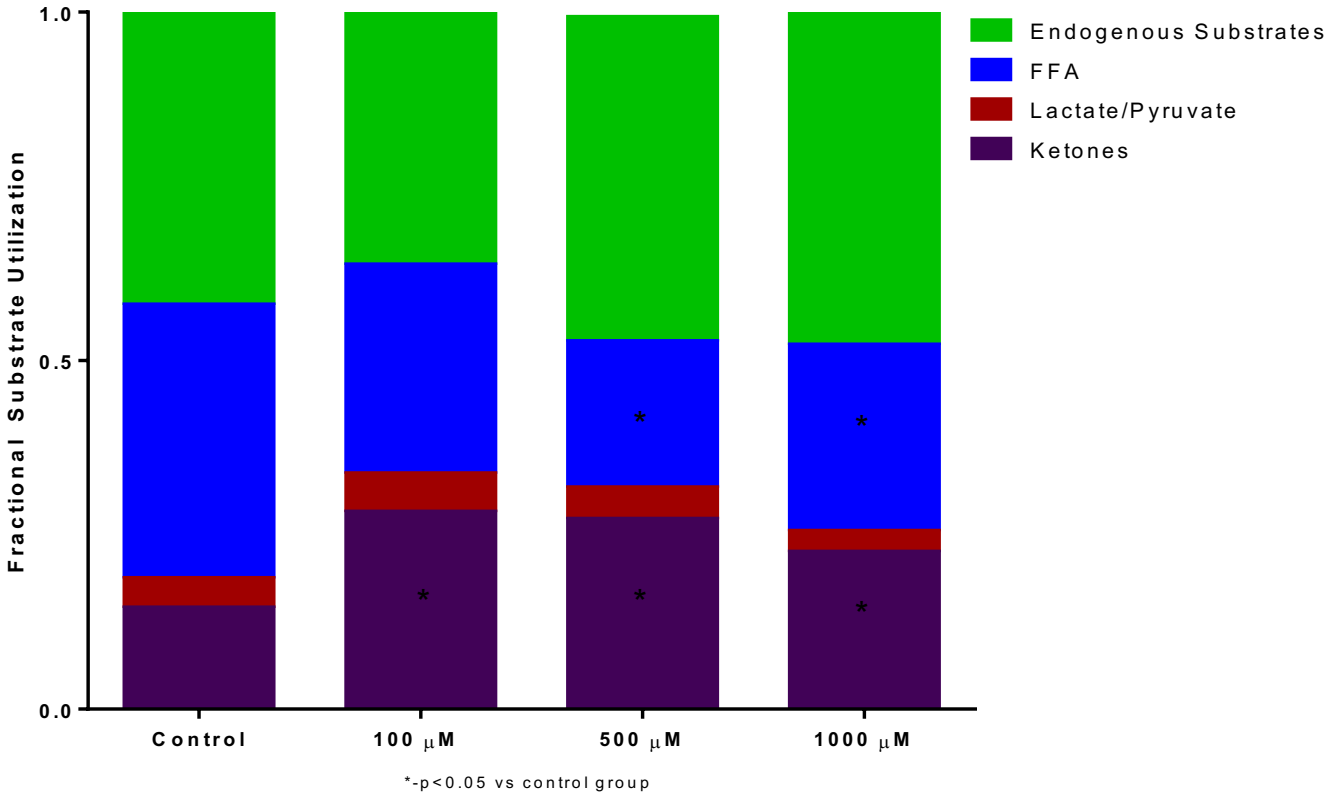

Figure 6.1: Metformin Dosage Experiment to determine the ideal concentration to deliver via perfusate. Fractional Substrate utilization in response to dosage. *-p<0.05 vs all other groups within that substrate

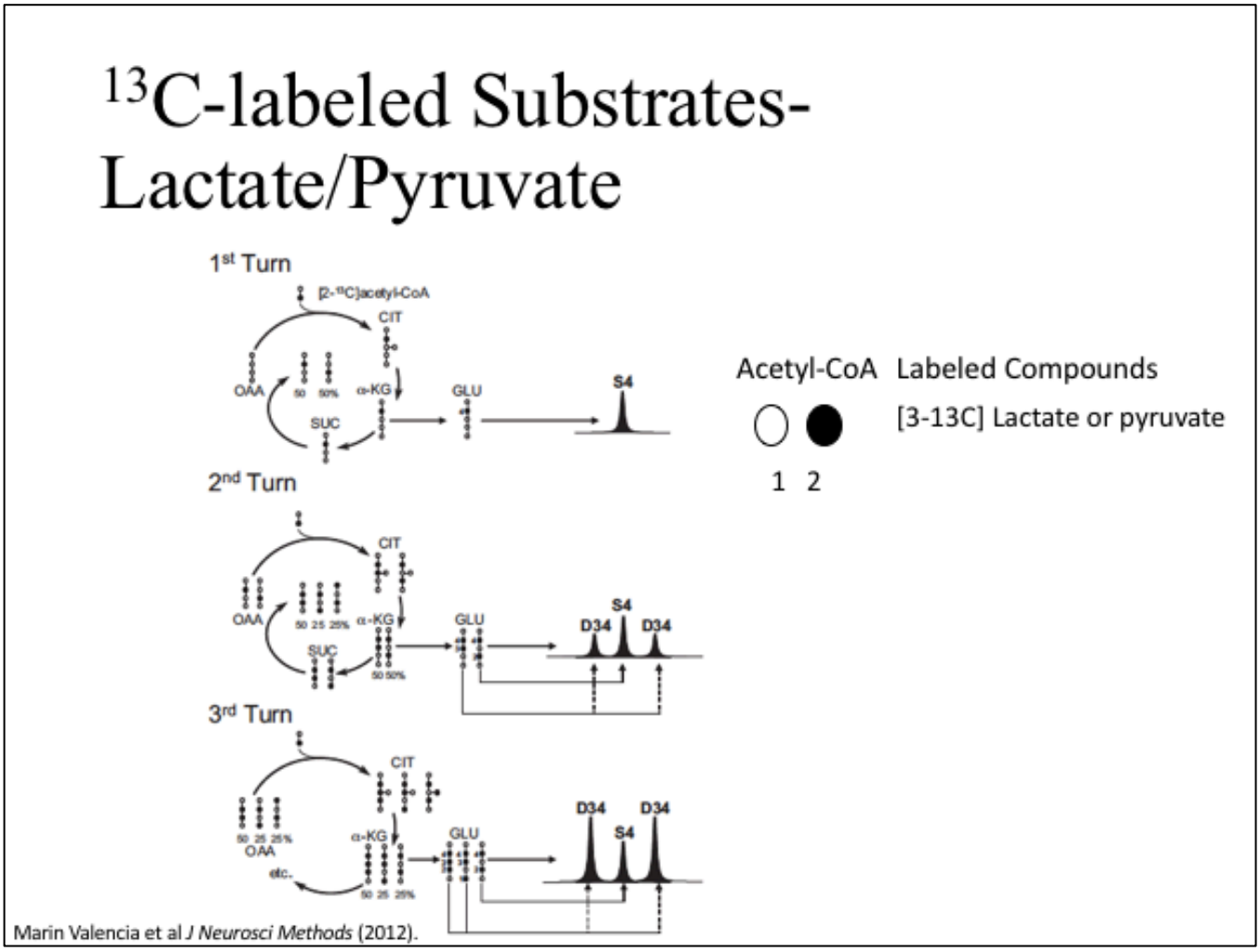

Figure 6.2: Glutamate Peaks resulting from 3-13C labelled lactate or pyruvate and its turns through the TCA cycle. Glutamate peaks are generated from NMR and used for subsequent fractional contribution to oxidative metabolism measurements.

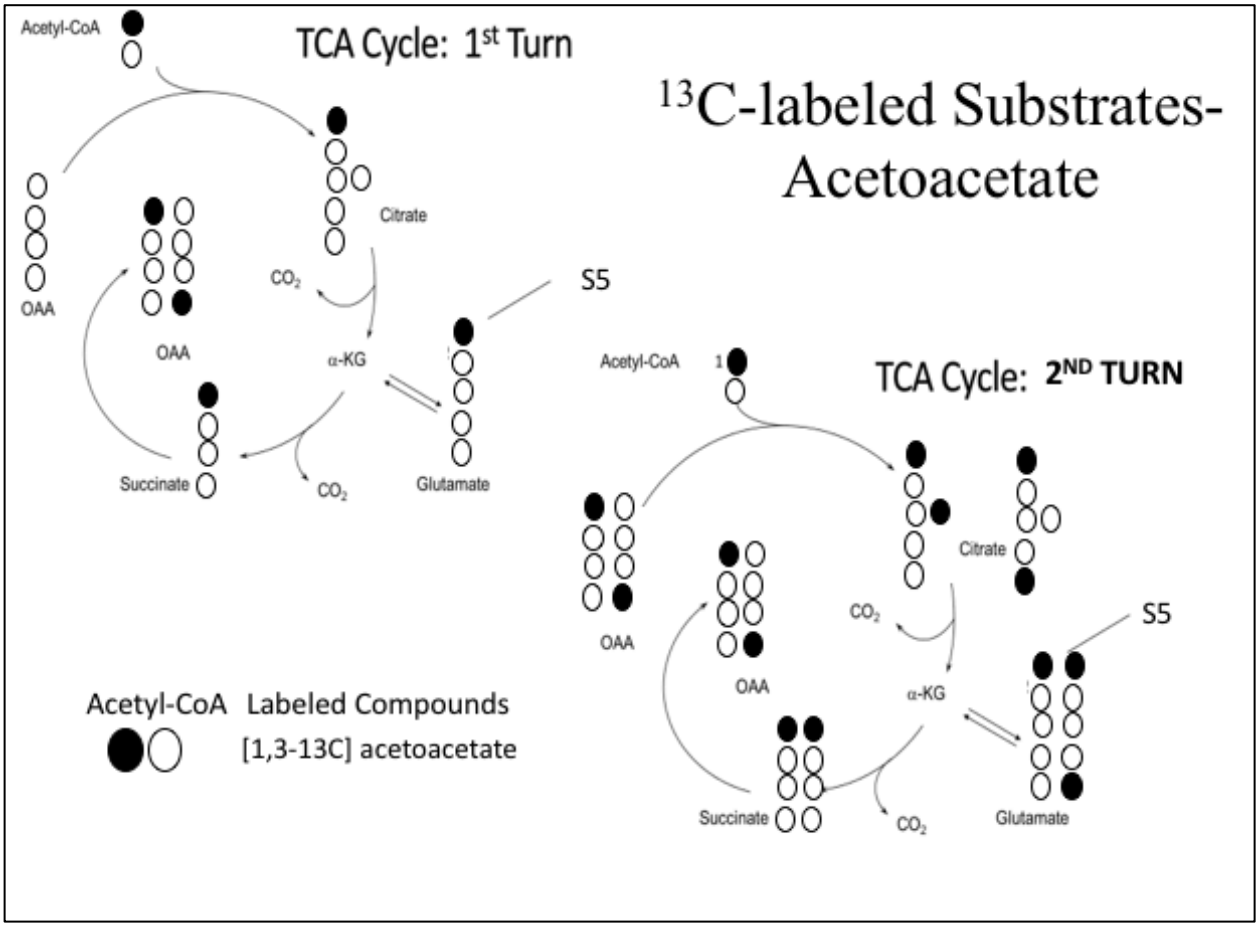

Figure 6.3: Glutamate Peaks resulting from 1,3-13C labelled acetoacetate and its turns through the TCA cycle. Glutamate peaks are generated from NMR and used for subsequent fractional contribution to oxidative metabolism measurements.

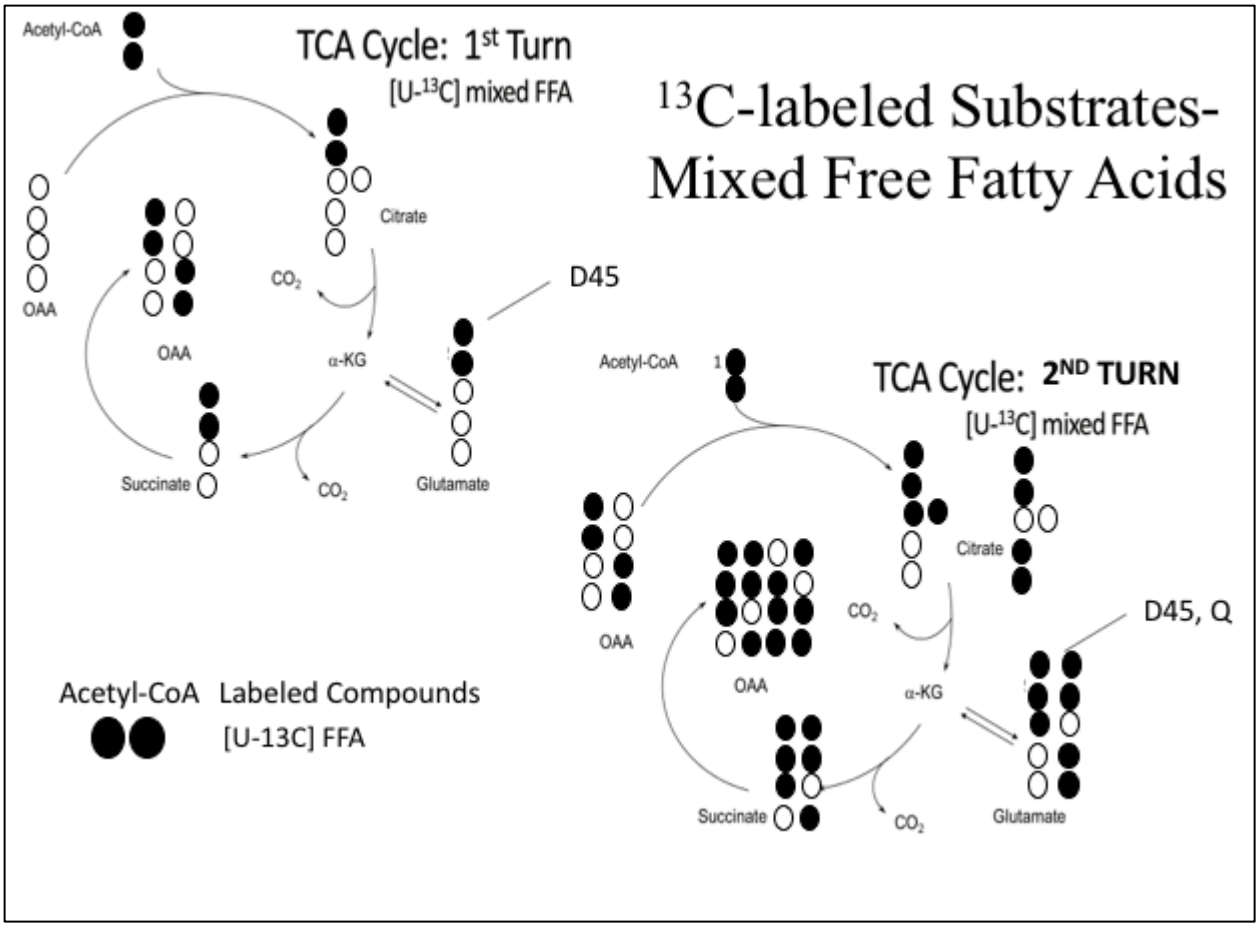

Figure 6.4: Glutamate Peaks resulting from uniformly labeled fatty acids and its turns through the TCA cycle. Glutamate peaks are generated from NMR and used for subsequent fractional contribution to oxidative metabolism measurements.

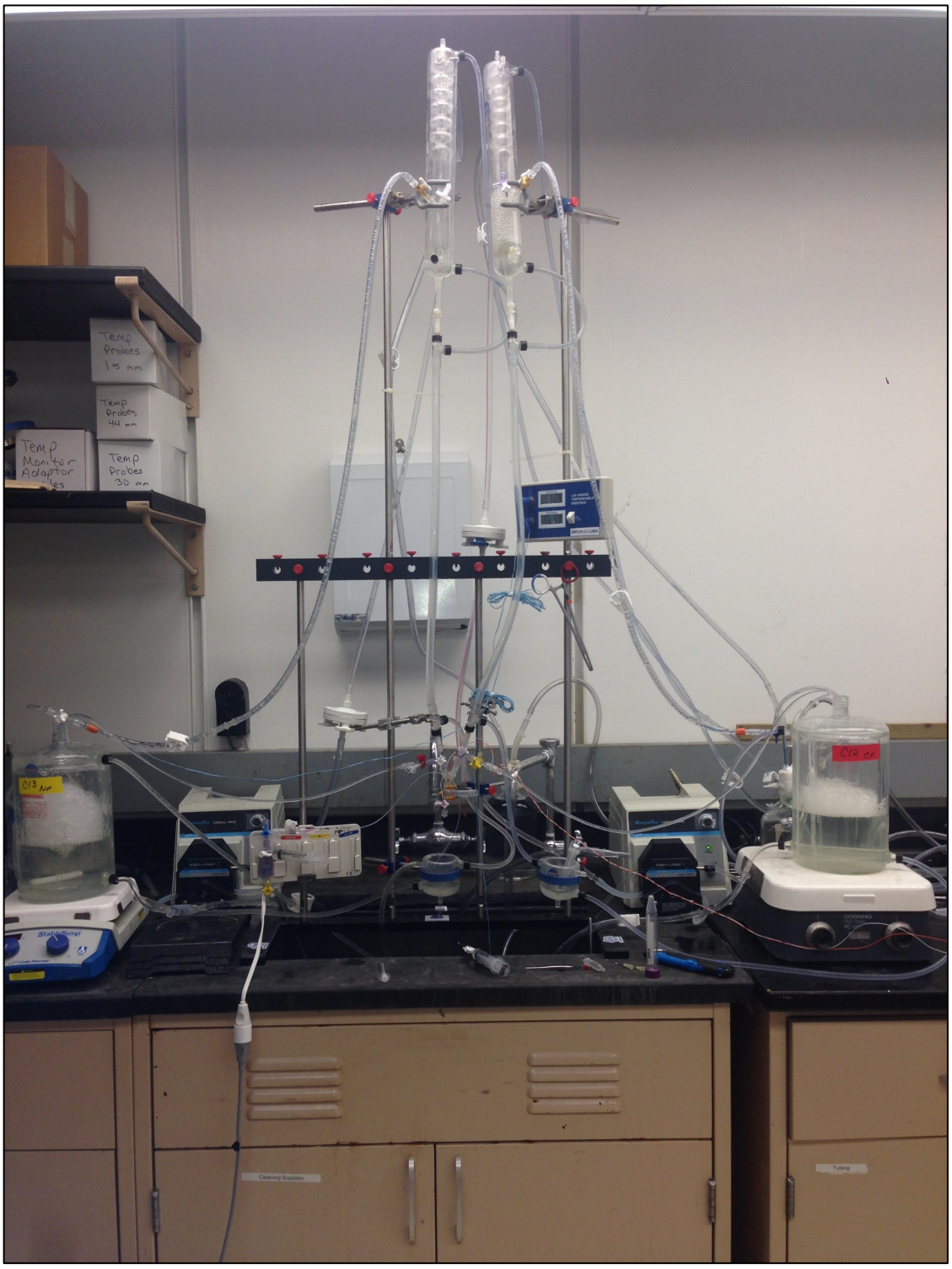

Figure 6.5: Langendorff Perfusion Apparatus in the lab.

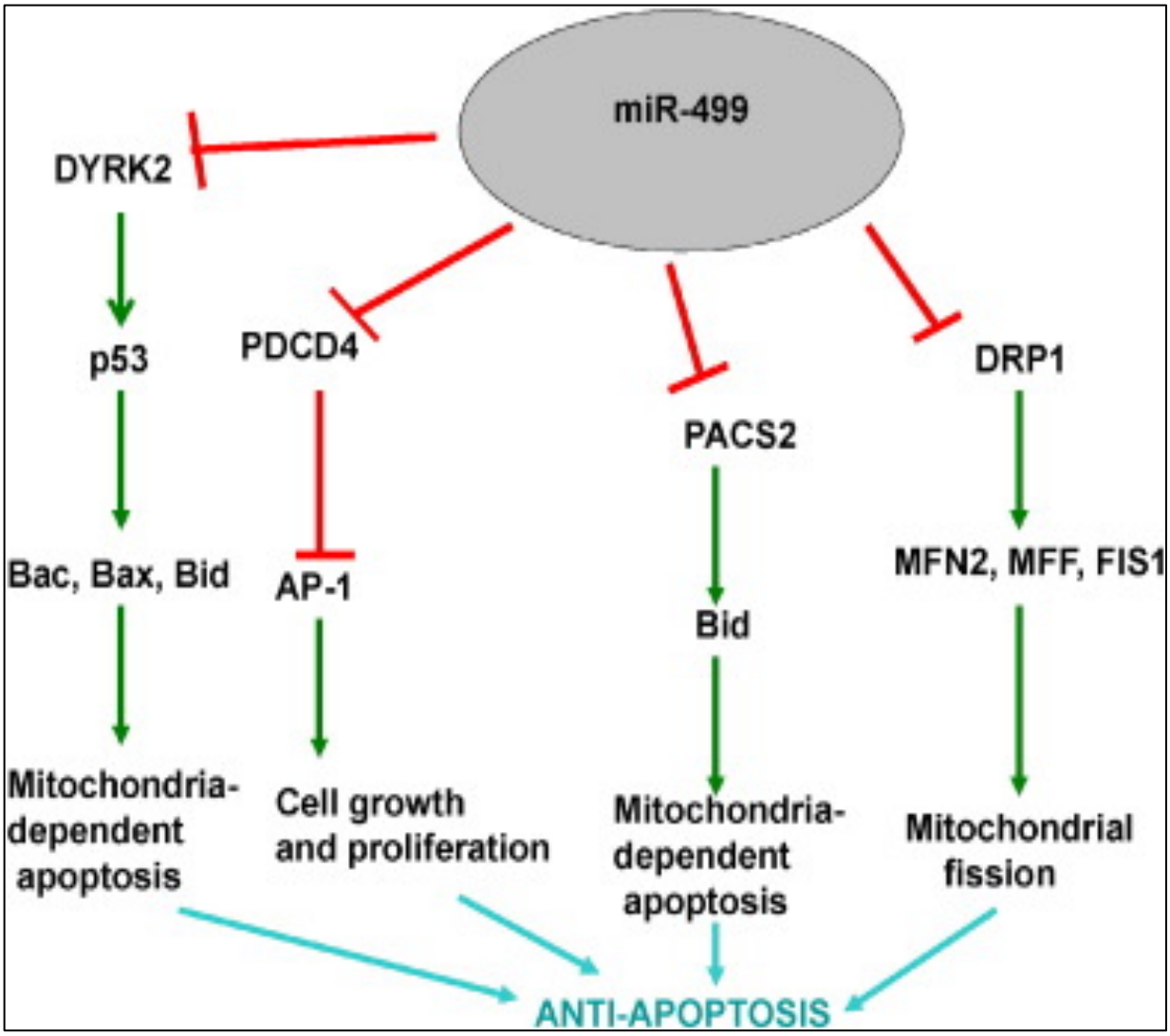

Figure 6.6: miR-499 pathway inhibition (Wang et al. 2011)

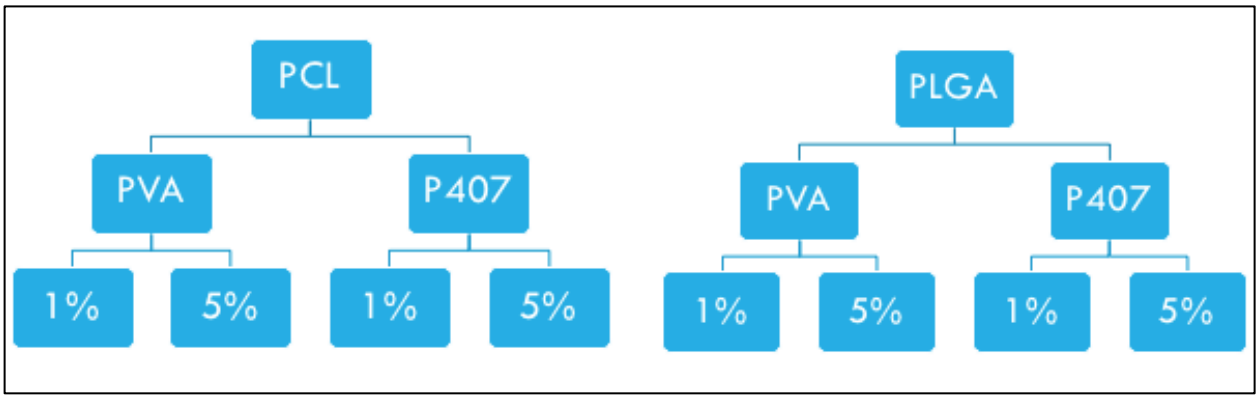

Figure 6.7: PLGA, PCL, PVA, and P407 combinations for preliminary investigation in determining ideal nanoparticle fabrication method. PCL= Poly(caprolactone). PLGA=poly (lactic-co-glycolic) acid. PVA= poly (vinyl alcohol). P407=polaxomer 407 surfactant

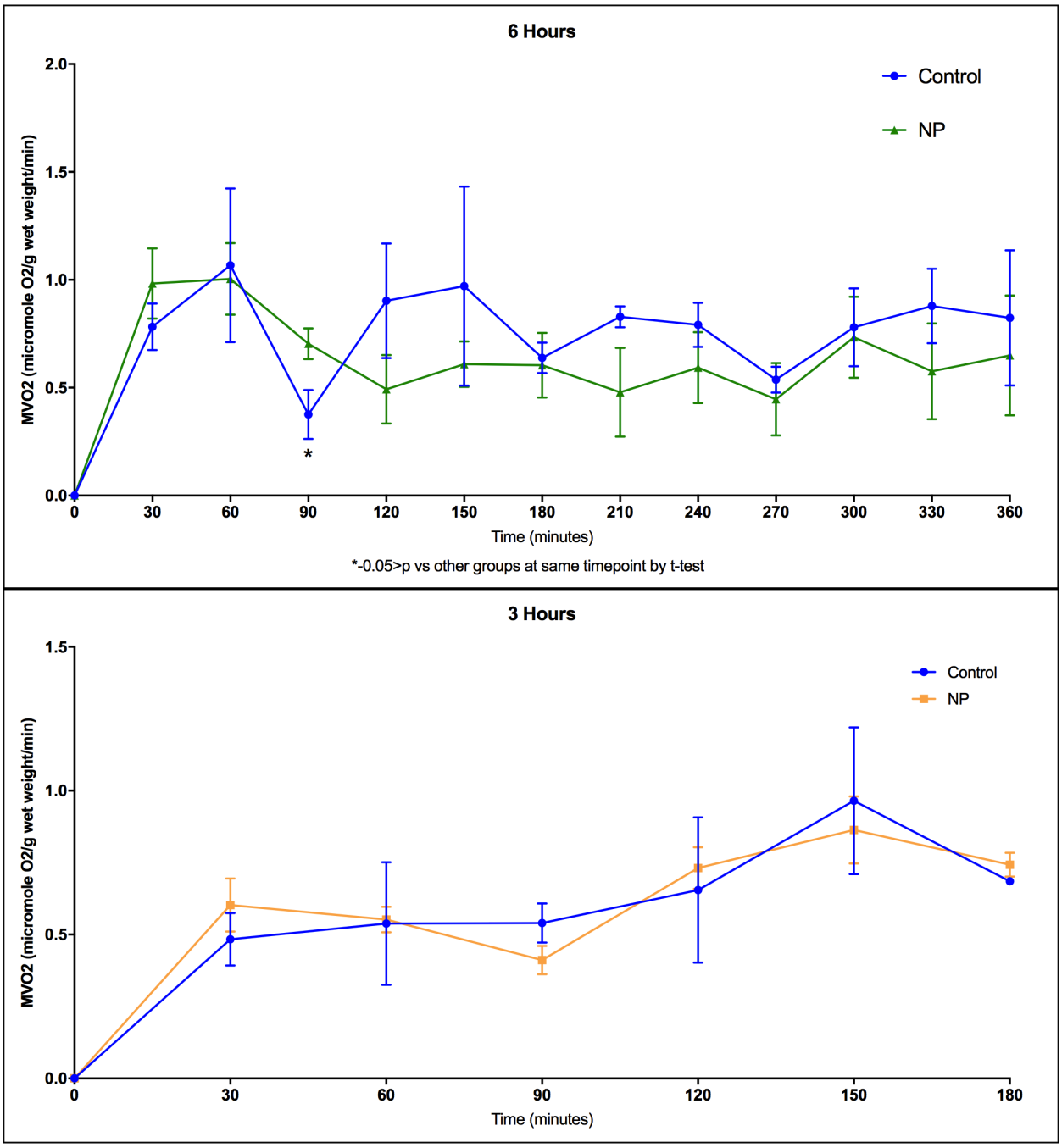

Figure 6.8: Myocardial oxygen consumption over time. Mean ± SEM. Top Panel: 6 hours Recirculating. Bottom Panel: 3 Hour Non-recirculating. 8=p<0.05 vs other group at same time point.

Bibliography

Agrawal, R. S., S. Muangman, M. D. Layne, L. Melo, M. A. Perrella, R. T. Lee, L. Zhang, M. Lopez-Ilasaca, and V. J. Dzau. 2004. 'Pre-emptive gene therapy using recombinant adeno-associated virus delivery of extracellular superoxide dismutase protects heart against ischemic reperfusion injury, improves ventricular function and prolongs survival', *Gene Therapy*, 11: 962.

Alexis, Frank, Eric Pridgen, Linda K. Molnar, and Omid C. Farokhzad. 2008. 'Factors Affecting the Clearance and Biodistribution of Polymeric Nanoparticles', *Molecular Pharmaceutics*, 5: 505-15.

Allard, Michael F., Sarah L. Henning, Richard B. Wambolt, Shaun R. Granleese, Dean R. English, and Gary D. Lopaschuk. 1997. 'Glycogen Metabolism in the Aerobic Hypertrophied Rat Heart', *Circulation*, 96: 676.

Amberger, A., Gerald Schneeberger S Fau - Hernegger, Gerald Hernegger G Fau - Brandacher, Peter Brandacher G Fau - Obrist, Peter Obrist P Fau - Lackner, Raimund Lackner P Fau - Margreiter, Walter Margreiter R Fau - Mark, and W. Mark. 2002. 'Gene expression profiling of prolonged cold ischemia and reperfusion in murine heart transplants', *Transplantation*, 74: 1441-49.

Ardehali, Abbas, Fardad Esmailian, Mario Deng, Edward Soltesz, Eileen Hsich, Yoshifumi Naka, Donna Mancini, Margarita Camacho, Mark Zucker, Pascal Leprince, Robert Padera, and Jon Kobashigawa. 2015. 'Ex-vivo perfusion of donor hearts for human heart transplantation (PROCEED II): a prospective, open-label, multicentre, randomised non-inferiority trial', *The Lancet*, 385: 2577-84.

Barnard, C. N. 1967. 'The operation. A human cardiac transplant: an interim report of a successful operation performed at Groote Schuur Hospital, Cape Town', *S. Afr Med J.*, 41: 1271-74.

Barnard Cn Fau - Barnard, M. S., D. K. Barnard Ms Fau - Cooper, C. A. Cooper Dk Fau - Curchio, J. Curchio Ca Fau - Hassoulas, D. Hassoulas J Fau - Novitsky, A. Novitsky D Fau - Wolpowitz, and A. Wolpowitz. 1981. 'The present status of heterotopic cardiac transplantation', *The Journal of Thoracic and Cardiovascular Surgery*, 81: 433-39.

Barringhaus, Kurt G., and Phillip D. Zamore. 2009. 'microRNAs: Regulating A Change of Heart', *Circulation*, 119: 2217-24.

Batchuluun, Battsetseg, Noriyuki Sonoda, Ryoichi Takayanagi, and Toyoshi Inoguchi. 2014. *The Cardiovascular Effects of Metformin: Conventional and New Insights*.

Beatrice Mc Fau - Stiers, D. L., D. R. Stiers Dl Fau - Pfeiffer, and D. R. Pfeiffer. 1984. 'The role of glutathione in the retention of Ca2+ by liver mitochondria', *J Biol Chem*, 259: 1279-87.

Bell, Robert M., Mihaela M. Mocanu, and Derek M. Yellon. 2011. 'Retrograde heart perfusion: The Langendorff technique of isolated heart perfusion', *Journal of Molecular and Cellular Cardiology*, 50: 940-50.

Birks, E. J., Nicholas R. Yacoub Mh Fau - Banner, Asghar Banner Nr Fau - Khaghani, and A. Khaghani. 2004. 'The role of bridge to transplantation: should LVAD patients be transplanted?', *Current Opinion in Cardiology*, 19: 148-53.

Bishop, Corey J., Kristen L. Kozielski, and Jordan J. Green. 2015. 'Exploring the role of polymer structure on intracellular nucleic acid delivery via polymeric nanoparticles', *J Control Release*, 219: 488-99.

Bostjancic, E., Dusan Zidar N Fau - Stajer, Damjan Stajer D Fau - Glavac, and D. Glavac. 2010. 'MicroRNAs miR-1, miR-133a, miR-133b and miR-208 are dysregulated in human myocardial infarction', *Cardiology*, 115: 163-9.

Brant, S., C. Holmes, M. Cobert, L. Powell, J. Shelton, M. Jessen, and M. Peltz. 2016. 'Successful transplantation in canines after long-term coronary sinus machine perfusion preservation of donor hearts', *J Heart Lung Transplant*, 35: 1031-6.

Brant, S. M., M. L. Cobert, L. M. West, J. M. Shelton, M. E. Jessen, and M. Peltz. 2014. 'Characterizing cardiac donation after circulatory death: implications for perfusion preservation', *Ann Thorac Surg*, 98: 2107-13; discussion 13-4.

Brink, Johan G., and Joannis Hassoulas. 2009. 'The first human heart transplant and further advances in cardiac transplantation at Groote Schuur Hospital and the University of Cape Town', *Cardiovascular Journal of Africa*, 20: 31-35.

Brunengraber, H., and C. R. Roe. 2006. 'Anaplerotic molecules: current and future', *J Inherit Metab Dis*, 29: 327-31.

Brunmair, B., K. Staniek, F. Gras, N. Scharf, A. Althaym, R. Clara, M. Roden, E. Gnaiger, H. Nohl, W. Waldhausl, and C. Furnsinn. 2004. 'Thiazolidinediones, like metformin, inhibit respiratory complex I: a common mechanism contributing to their antidiabetic actions?', *Diabetes*, 53: 1052-9.

Burgess, S. C., R. A. Carvalho, M. E. Merritt, J. G. Jones, C. R. Malloy, and A. D. Sherry. 2001. '13C isotopomer analysis of glutamate by J-resolved heteronuclear single quantum coherence spectroscopy', *Anal Biochem*, 289: 187-95.

Callis, T. E., Hee Young Pandya K Fau - Seok, Ru-Hang Seok Hy Fau - Tang, Mariko Tang Rh Fau - Tatsuguchi, Zhan-Peng Tatsuguchi M Fau - Huang, Jian-Fu Huang Zp Fau - Chen, Zhongliang Chen Jf Fau - Deng, Bronwyn Deng Z Fau - Gunn, Janelle Gunn B Fau - Shumate, Monte S. Shumate J Fau - Willis, Craig H.

Willis Ms Fau - Selzman, Da-Zhi Selzman Ch Fau - Wang, and D. Z. Wang. 2009. 'MicroRNA-208a is a regulator of cardiac hypertrophy and conduction in mice', *J Clin Invest*, 119: 2772-86.

Calvert, John W., Susheel Gundewar, Saurabh Jha, James J.M. Greer, William H. Bestermann, Rong Tian, and David J. Lefer. 2008. 'Acute Metformin Therapy Confers Cardioprotection Against Myocardial Infarction Via AMPK-eNOS,ÄìMediated Signaling', *Diabetes*, 57: 696-705.

Chatham, JohnC, Bertrand Bouchard, and Christine Des Rosiers. 2003. 'A comparison between NMR and GCMS 13C-isotopomer analysis in cardiac metabolism', *Molecular and Cellular Biochemistry*, 249: 105-12.

Chen, L. L., Jun Yin H Fau - Huang, and J. Huang. 2007. 'Inhibition of TGF-beta1 signaling by eNOS gene transfer improves ventricular remodeling after myocardial infarction through angiogenesis and reduction of apoptosis', *Cardiovasc Pathol*, 16: 221-30.

Chen, L. L., Hang Zhu Tb Fau - Yin, Jun Yin H Fau - Huang, Lian Sheng Huang J Fau - Wang, Ke Jiang Wang Ls Fau - Cao, Zhi Jian Cao Kj Fau - Yang, and Z. J. Yang. 'Inhibition of MAPK signaling by eNOS gene transfer improves ventricular remodeling after myocardial infarction through reduction of inflammation'.

Chen-Scarabelli, Carol, Louis Saravolatz, Benjamin Hirsh, Pratik Agrawal, and Tiziano M. Scarabelli. 2015. 'Dilemmas in end-stage heart failure', *Journal of Geriatric Cardiology : JGC*, 12: 57-65.

Chiou, H. C., S. M. Tangco Mv Fau - Levine, D. Levine Sm Fau - Robertson, K. Robertson D Fau - Kormis, C. H. Kormis K Fau - Wu, G. Y. Wu Ch Fau - Wu, and G. Y. Wu. 1994. 'Enhanced resistance to nuclease degradation of nucleic acids complexed to asialoglycoprotein-polylysine carriers', *Nucleic Acids Res.*, 22: 5439-46.

Christe, M. E., and R. L. Rodgers. 1995. 'Cardiac glucose and fatty acid oxidation in the streptozotocin-induced diabetic spontaneously hypertensive rat', *Hypertension*, 25: 235-41.

Christensen, M. M., K. Hojlund, O. Hother-Nielsen, T. B. Stage, P. Damkier, H. Beck-Nielsen, and K. Brosen. 2015. 'Endogenous glucose production increases in response to metformin treatment in the glycogen-depleted state in humans: a randomised trial', *Diabetologia*, 58: 2494-502.

Cobert, M. L., L. M. Peltz M Fau - West, M. E. West Lm Fau - Jessen, and M. E. Jessen. 2010. 'Importance of organ preservation solution composition in reducing myocardial edema during machine perfusion for heart transplantation', *Transplant Proc*, 42: 1591-4.

Cobert, M. L., M. Peltz, L. M. West, M. E. Merritt, and M. E. Jessen. 2012. 'Glucose is an ineffective substrate for preservation of machine perfused donor hearts', *J Surg Res*, 173: 198-205.

Cobert, Michael L., Matthew E. Merritt, LaShondra M. West, Colby Ayers, Michael E. Jessen, and Matthias Peltz. 2014. 'Metabolic Characteristics of Human Hearts Preserved for 12 Hours by Static Storage, Antegrade Perfusion or Retrograde Coronary Sinus Perfusion', *The Journal of Thoracic and Cardiovascular Surgery*, 148: 2310-15.e1.

Collier, C. A., C. R. Bruce, A. C. Smith, G. Lopaschuk, and D. J. Dyck. 2006. 'Metformin counters the insulin-induced suppression of fatty acid oxidation and stimulation of triacylglycerol storage in rodent skeletal muscle', *Am J Physiol Endocrinol Metab*, 291: E182-9.

Devulapally, R., N. M. Sekar, T. V. Sekar, K. Foygel, T. F. Massoud, J. K. Willmann, and R. Paulmurugan. 2015. 'Polymer nanoparticles mediated codelivery of antimiR-10b and antimiR-21 for achieving triple negative breast cancer therapy', *ACS Nano*, 9: 2290-302.

Dong, S., Jian Cheng Y Fau - Yang, Jingyuan Yang J Fau - Li, Xiaojun Li J Fau - Liu, Xiaobin Liu X Fau - Wang, Dong Wang X Fau - Wang, Thomas J. Wang D Fau - Krall, Ellise S. Krall Tj Fau - Delphin, Chunxiang Delphin Es Fau - Zhang, and C. Zhang. 2009. 'MicroRNA expression signature and the role of microRNA-21 in the early phase of acute myocardial infarction', *J. Biol Chem*, 284: 29514-25.

Dvir, Tal, Michael Bauer, Avi Schroeder, Jonathan H. Tsui, Daniel G. Anderson, Robert Langer, Ronglih Liao, and Daniel S. Kohane. 2011. 'Nanoparticles Targeting the Infarcted Heart', *Nano Letters*, 11: 4411-14.

Elsässer, Albrecht, Keisuke Suzuki, and Jutta Schaper. 2000. 'Unresolved Issues Regarding the Role of Apoptosis in the Pathogenesis of Ischemic Injury and Heart Failure', *Journal of Molecular and Cellular Cardiology*, 32: 711-24.

Fan, G. C., Jiang Ren X Fau - Qian, Qunying Qian J Fau - Yuan, Persoulla Yuan Q Fau - Nicolaou, Yang Nicolaou P Fau - Wang, W. Keith Wang Y Fau - Jones, Guoxiang Jones Wk Fau - Chu, Evangelia G. Chu G Fau - Kranias, and E. G. Kranias. 'Novel cardioprotective role of a small heat-shock protein, Hsp20, against ischemia/reperfusion injury', *Circulation*, 111: 1792-9.

Friedrich, Erik B., and Michael Böhm. 2007. 'Management of end stage heart failure', *Heart*, 93: 626-31.

Gadde, S., and K. J. Rayner. 2016. 'Nanomedicine Meets microRNA: Current Advances in RNA-Based Nanotherapies for Atherosclerosis', *Arterioscler Thromb Vasc Biol*, 36: 73-9.

Garcia Saez, D., B. Zych, A. Sabashnikov, C. T. Bowles, F. De Robertis, P. N. Mohite, A. F. Popov, O. Maunz, N. P. Patil, A. Weymann, T. Pitt, L. McBrearty, B. Pates, R. Hards, M. Amrani, T. Bahrami, N. R. Banner, and A. R. Simon. 'Evaluation of the organ care system in heart transplantation with an adverse donor/recipient profile'. *Ann Thorac Surg*, 98: 2099-105.

Gibala, M. J., M. E. Young, and H. Taegtmeyer. 2000. 'Anaplerosis of the citric acid cycle: role in energy metabolism of heart and skeletal muscle', *Acta Physiologica Scandinavica*, 168: 657-65.

Gropler, R. J. 2009. 'Lost in Translation: Modulation of the Metabolic-Functional Relation in the Diabetic Human Heart', *Circulation*, 119: 2020-2.

Group, The BARI 2D Study. 2009. 'A Randomized Trial of Therapies for Type 2 Diabetes and Coronary Artery Disease', *New England Journal of Medicine*, 360: 2503-15.

Guibert, Edgardo E., Alexander Y. Petrenko, Cecilia L. Balaban, Alexander Y. Somov, Joaquín V. Rodriguez, and Barry J. Fuller. 2011. 'Organ Preservation: Current Concepts and New Strategies for the Next Decade', *Transfusion Medicine and Hemotherapy*, 38: 125-42.

Ha, T. T., Lyre Anni Huy Nt Fau - Murao, Nguyen Thi Phuong Murao La Fau - Lan, Tran Thi Lan Nt Fau - Thuy, Ha Manh Thuy Tt Fau - Tuan, Cao Thi Phi Tuan Hm Fau - Nga, Vo Van Nga Ct Fau - Tuong, Tran Van Tuong Vv Fau - Dat, Mihoko Dat Tv Fau - Kikuchi, Michio Kikuchi M Fau - Yasunami, Kouichi Yasunami M Fau - Morita, Vu Thi Que Morita K Fau - Huong, Kenji Huong Vt Fau - Hirayama, and K. Hirayama. 2011. 'Elevated levels of cell-free circulating DNA in patients with acute dengue virus infection', *PLOS ONE*, 6: 25969.

Halarnkar, Premjit P., and Gary J. Blomquist. 1989. 'Comparative aspects of propionate metabolism', *Comparative Biochemistry and Physiology Part B: Comparative Biochemistry*, 92: 227-31.

Haller Jd Fau - Cerruti, M. M., and M. M. Cerruti. 1968. 'Heart transplantion in man: compilation of cases. January 1, 1964 to October 23, 1968', *1968*, 22: 840-3.

Harris, T. A., Marcella Yamakuchi M Fau - Ferlito, Joshua T. Ferlito M Fau - Mendell, Charles J. Mendell Jt Fau - Lowenstein, and C. J. Lowenstein. 2014. 'MicroRNA-126 regulates endothelial expression of vascular cell adhesion molecule 1', *Life Sci*, 98: 18-23.

Hirsch, L. R., J. A. Stafford Rj Fau - Bankson, S. R. Bankson Ja Fau - Sershen, B. Sershen Sr Fau - Rivera, R. E. Rivera B Fau - Price, J. D. Price Re Fau - Hazle, N. J. Hazle Jd Fau - Halas, J. L. Halas Nj Fau - West, and J. L. West. 2003. 'Nanoshell-mediated near-infrared thermal therapy of tumors under magnetic resonance guidance', *Proc Natl Acad Sci USA*, 100: 13549-54.

Houten, S. M., and R. J. Wanders. 2010. 'A general introduction to the biochemistry of mitochondrial fatty acid beta-oxidation', *J Inherit Metab Dis*, 33: 469-77.

Huang, B., Melissa M. Wu P Fau - Bowker-Kinley, Robert A. Bowker-Kinley Mm Fau - Harris, and R. A. Harris. 2002. 'Regulation of pyruvate dehydrogenase kinase expression by peroxisome proliferator-activated receptor-alpha ligands, glucocorticoids, and insulin', *Diabetes*, 51: 276-83.

Ilium, Lisbeth, S. S. Davis, C. G. Wilson, N. W. Thomas, M. Frier, and J. G. Hardy. 1982. 'Blood clearance and organ deposition of intravenously administered colloidal particles. The effects of particle size, nature and shape', *International Journal of Pharmaceutics*, 12: 135-46.

Jacobs, S., Bart Rega F Fau - Meyns, and B. Meyns. 2010. 'Current preservation technology and future prospects of thoracic organs. Part 2: heart', *Curr Opin Organ Transplant*, 15: 156-9.

Jadhav, S., W. Ferrell, I. A. Greer, J. R. Petrie, S. M. Cobbe, and N. Sattar. 2006. 'Effects of metformin on microvascular function and exercise tolerance in women with angina and normal coronary arteries: a randomized, double-blind, placebo-controlled study', *J Am Coll Cardiol*, 48: 956-63.

Jeffrey, F. M., C. J. Storey, A. D. Sherry, and C. R. Malloy. 1996. '13C isotopomer model for estimation of anaplerotic substrate oxidation via acetyl-CoA', *Am J Physiol*, 271: E788-99.

Jeong, J. H., Tae Gwan Kim Sw Fau - Park, and T. G. Park. 2004. 'Biodegradable triblock copolymer of PLGA-PEG-PLGA enhances gene transfection efficiency', *Pharmacological Research*, 21: 51-4.

Jiralerspong, Sao, Shana L. Palla, Sharon H. Giordano, Funda Meric-Bernstam, Cornelia Liedtke, Chad M. Barnett, Limin Hsu, Mien-Chie Hung, Gabriel N. Hortobagyi, and Ana M. Gonzalez-Angulo. 2009. 'Metformin and Pathologic Complete Responses to Neoadjuvant Chemotherapy in Diabetic Patients With Breast Cancer', *Journal of Clinical Oncology*, 27: 3297-302.

Kafil, Vala, and Yadollah Omidi. 2011. 'Cytotoxic Impacts of Linear and Branched Polyethylenimine Nanostructures in A431 Cells', *BioImpacts : BI*, 1: 23-30.

Kajihara, N., Yoshihisa Morita S Fau - Tanoue, Noriko Tanoue Y Fau - Boku, Masataka Boku N Fau - Eto, Takahiro Eto M Fau - Nishida, Ryuji Nishida T Fau - Tominaga, and R. Tominaga. 2006. 'The UW solution has greater potential for longer preservation periods than the Celsior solution: comparative study for ventricular and coronary endothelial function after 24-h heart preservation', *Eur J Cardiothorac Surg*, 29.

Kalogeris, Theodore, Christopher P. Baines, Maike Krenz, and Ronald J. Korthuis. 2012. 'Cell Biology of Ischemia/Reperfusion Injury', *International review of cell and molecular biology*, 298: 229-317.

Kammermeier H Fau - Rudroff, W., and W. Rudroff. 1972. '[Function and energy metabolism of the isolated heart as influenced by variation in pH, P CO2 and HCO 3 . I. Contractile force and coronary flow]', *Pflugers Arch*, 334: 39-49.

Kanoh, M., J. Takemura G Fau - Misao, Y. Misao J Fau - Hayakawa, T. Hayakawa Y Fau - Aoyama, K. Aoyama T Fau - Nishigaki, T. Nishigaki K Fau - Noda, T. Noda T Fau - Fujiwara, K. Fujiwara T Fau - Fukuda, S. Fukuda K Fau - Minatoguchi, H. Minatoguchi S Fau - Fujiwara, and H. Fujiwara. 1999. 'Significance of myocytes with positive DNA in situ nick end-labeling (TUNEL) in hearts with dilated cardiomyopathy: not apoptosis but DNA repair', *Circulation*, 99: 2757-64.

Kantrowitz A Fau - Haller, J. D., H. Haller Jd Fau - Joos, M. M. Joos H Fau - Cerruti, H. E. Cerruti Mm Fau - Carstensen, and H. E. Carstensen. 1968. 'Transplantation of the heart in an infant and an adult', *The American Journal of Cardiology*, 22: 782-90.

Kantrowitz, A. 1998. 'America's first human heart transplantation: the concept, the planning, and the furor', *ASAIO J*, 44: 244-52.

Kates, A. M., Carmen Herrero P Fau - Dence, Pablo Dence C Fau - Soto, Muthayyah Soto P Fau - Srinivasan, Deborah G. Srinivasan M Fau - Delano, Ali Delano Dg Fau - Ehsani, Robert J. Ehsani A Fau - Gropler, and R. J. Gropler. 2003. 'Impact of aging on substrate metabolism by the human heart', *J Am Coll Cardiol*, 41: 293-9.

Kauffman, K. J., M. J. Webber, and D. G. Anderson. 2016. 'Materials for non-viral intracellular delivery of messenger RNA therapeutics', *J Control Release*, 240: 227-34.

Kim, H. J., H. Kwon, J. W. Lee, H. J. Kim, S. B. Lee, H. S. Park, G. Sohn, Y. Lee, B. S. Koh, J. H. Yu, B. H. Son, and S. H. Ahn. 2015. 'Metformin increases survival in hormone receptor-positive, HER2-positive breast cancer patients with diabetes', *Breast Cancer Res.*, 17: 64.

Kong, Fanming, Fangfang Gao, Honggen Liu, Liwei Chen, Rongxiu Zheng, Jianchun Yu, Xiaojiang Li, Geli Liu, and Yingjie Jia. 2015. 'Metformin use improves the survival of diabetic combined small-cell lung cancer patients', *Tumor Biology*, 36: 8101-06.

Kotipalli A Fau - Gutti, Ravikumar, Chanchal K. Gutti R Fau - Mitra, and C. K. Mitra. 2016. 'Dynamics of miRNA biogenesis and nuclear transport', *J Integr Bioinform*, 13: 22-34.

Kukreja, R. C., Fadi N. Yin C Fau - Salloum, and F. N. Salloum. 2013. 'MicroRNAs: new players in cardiac injury and protection', *Mol Biol Rep*, 40: 2663-70.

Land, W. 2002. 'Postischemic Reperfusion Injury to Allografts – A Case for 'Innate Immunity'?', *European Surgical Research*, 34: 160-69.

LaNoue, K. F., J. Bryla, and J. R. Williamson. 1972. 'Feedback interactions in the control of citric acid cycle activity in rat heart mitochondria', *J Biol Chem*, 247: 667-79.

LaNoue, K., W. J. Nicklas, and J. R. Williamson. 1970. 'Control of citric acid cycle activity in rat heart mitochondria', *J Biol Chem*, 245: 102-11.

Laughlin, Maren R., and Frederick W. Heineman. 1994. 'The Relationship between Phosphorylation Potential and Redox State in the Isolated Working Rabbit Heart', *Journal of Molecular and Cellular Cardiology*, 26: 1525-36.

Lei, B., Martin E. Lionetti V Fau - Young, Margaret P. Young Me Fau - Chandler, Chiara Chandler Mp Fau - d'Agostino, Elaine d'Agostino C Fau - Kang, Martin Kang E Fau - Altarejos, Ken Altarejos M Fau - Matsuo, Thomas H. Matsuo K Fau - Hintze, William C. Hintze Th Fau - Stanley, Fabio A. Stanley Wc Fau - Recchia, and F. A. Recchia. 2004. 'Paradoxical downregulation of the glucose oxidation pathway despite enhanced flux in severe heart failure', *J Mol Cell Cardiol*, 36: 567-76.

Leist, M., A. F. Single B Fau - Castoldi, S. Castoldi Af Fau - Kuhnle, P. Kuhnle S Fau - Nicotera, and P. Nicotera. 1997. 'Intracellular adenosine triphosphate (ATP) concentration: a switch in the decision between apoptosis and necrosis', *J Am Coll Cardiol*, 185: 1481-6.

Leverve, X. M., B. Guigas, D. Detaille, C. Batandier, E. A. Koceir, C. Chauvin, E. Fontaine, and N. F. Wiernsperger. 2003. 'Mitochondrial metabolism and type-2 diabetes: a specific target of metformin', *Diabetes Metab*, 29: 6s88-94.

Li, Q., Y. Bolli R Fau - Qiu, X. L. Qiu Y Fau - Tang, Y. Tang Xl Fau - Guo, B. A. Guo Y Fau - French, and B. A. French. 2001. 'Gene therapy with extracellular superoxide dismutase protects conscious rabbits against myocardial infarction', *Circulation*, 103: 1893-8.

Li, W., F. Bian, P. Chaudhuri, X. Mao, H. Brunengraber, and X. Yu. 2011. 'Delineation of substrate selection and anaplerosis in tricarboxylic acid cycle of the heart by 13C NMR spectroscopy and mass spectrometry', *NMR Biomed*, 24: 176-87.

Li, Y., S. Guo, G. Liu, Y. Yuan, W. Wang, Z. Zheng, S. Hu, and B. Ji. 2016. 'Three Preservation Solutions for Cold Storage of Heart Allografts: A Systematic Review and Meta-Analysis', *Artif Organs*, 40: 489-96.

Li, Y., Q. Zeng, G. Liu, J. Du, B. Gao, W. Wang, Z. Zheng, S. Hu, and B. Ji. 2017. 'Development and Evaluation of Heartbeat: A Machine Perfusion Heart Preservation System', *Artif Organs*, 41: E240-E50.

Liao, Jian-You, Li-Ming Ma, Yan-Hua Guo, Yu-Chan Zhang, Hui Zhou, Peng Shao, Yue-Qin Chen, and Liang-Hu Qu. 2010. 'Deep Sequencing of Human Nuclear and Cytoplasmic Small RNAs Reveals an Unexpectedly Complex Subcellular Distribution of miRNAs and tRNA 3′ Trailers', *PLOS ONE*, 5: e10563.

Lopaschuk, Gary D., John R. Ussher, Clifford D. L. Folmes, Jagdip S. Jaswal, and William C. Stanley. 2010. 'Myocardial Fatty Acid Metabolism in Health and Disease', *Physiol Rev*, 90: 207-58.

Lund, Lars H., Leah B. Edwards, Anne I. Dipchand, Samuel Goldfarb, Anna Y. Kucheryavaya, Bronwyn J. Levvey, Bruno Meiser, Joseph W. Rossano, Roger D. Yusen, and Josef Stehlik. 2016. 'The Registry of the International Society for Heart and Lung Transplantation: Thirty-third Adult Heart Transplantation Report—2016; Focus Theme: Primary Diagnostic Indications for Transplant', *The Journal of Heart and Lung Transplantation*, 35: 1158-69.

Macdonald, P. S., Mark Chew Hc Fau - Connellan, Kumud Connellan M Fau - Dhital, and K. Dhital. 2016. 'Extracorporeal heart perfusion before heart transplantation: the heart in a box', *Curr Opin Organ Transplant*, 21: 336-42.

Mack, C. A., E. A. Patel Sr Fau - Schwarz, P. Schwarz Ea Fau - Zanzonico, R. T. Zanzonico P Fau - Hahn, A. Hahn Rt Fau - Ilercil, R. B. Ilercil A Fau - Devereux, S. J. Devereux Rb Fau - Goldsmith, T. F. Goldsmith Sj Fau - Christian, T. A. Christian Tf Fau - Sanborn, I. Sanborn Ta Fau - Kovesdi, N. Kovesdi I Fau - Hackett, O. W. Hackett N Fau - Isom, R. G. Isom Ow Fau - Crystal, T. K. Crystal Rg Fau - Rosengart, and T. K. Rosengart. 1998. 'Biologic bypass with the use of adenovirus-mediated gene transfer of the complementary deoxyribonucleic acid for vascular endothelial growth factor 121 improves myocardial perfusion and function in the ischemic porcine heart', *J Thorac Cardiovasc Surg*, 115: 168-76.

Malloy, C. R., A. D. Sherry, and F. M. Jeffrey. 1990. 'Analysis of tricarboxylic acid cycle of the heart using 13C isotope isomers', *Am J Physiol*, 259: H987-95.

Malloy, Craig R., John G. Jones, F. Mark Jeffrey, Michael E. Jessen, and A. Dean Sherry. 1996. 'Contribution of various substrates to total citric acid cycle flux and]anaplerosis as determined by13C isotopomer analysis and O2 consumption in the heart', *Magnetic Resonance Materials in Physics, Biology and Medicine*, 4: 35-46.

Matoba, T., and K. Egashira. 2014. 'Nanoparticle-mediated drug delivery system for cardiovascular disease', *Int Heart J*, 55: 281-6.

Maulik, N., D. K. Yoshida T Fau - Das, and D. K. Das. 1998. 'Oxidative stress developed during the reperfusion of ischemic myocardium induces apoptosis', *Free Radic Biol Med*, 15: 869-75.

McAnulty, J. F., J. H. Southard, and F. O. Belzer. 1988. 'Comparison of the effects of adenine-ribose with adenosine for maintenance of ATP concentrations in 5-day hypothermically perfused dog kidneys', *Cryobiology*, 25: 409-16.

McAnulty Jf Fau - Southard, J. H., F. O. Southard Jh Fau - Belzer, and F. O. Belzer. 1987. 'Improved maintenance of adenosine triphosphate in five-day perfused kidneys with adenine and ribose', *Transplant Proc*, 19: 1376-9.

Messer, S., A. Ardehali, and S. Tsui. 2015. 'Normothermic donor heart perfusion: current clinical experience and the future', *Transpl Int*, 28: 634-42.

Michel, S. G., G. M. La Muraglia, 2nd, M. L. Madariaga, J. S. Titus, M. K. Selig, E. A. Farkash, J. S. Allan, L. M. Anderson, and J. C. Madsen. 2015. 'Twelve-Hour Hypothermic Machine Perfusion for Donor Heart Preservation Leads to Improved Ultrastructural Characteristics Compared to Conventional Cold Storage', *Ann Transplant*, 20: 461-8.

Minasian, S. M., M. M. Galagudza, Y. V. Dmitriev, A. A. Karpov, and T. D. Vlasov. 2015. 'Preservation of the donor heart: from basic science to clinical studies', *Interact Cardiovasc Thorac Surg*, 20: 510-9.

Minasian, S. M., Yuri V. Galagudza Mm Fau - Dmitriev, Dmitry I. Dmitriev Yv Fau - Kurapeev, Timur D. Kurapeev Di Fau - Vlasov, and T. D. Vlasov. 2010. 'Myocardial protection against global ischemia with Krebs-Henseleit buffer-based cardioplegic solution', *Ross Fiziol Zh Im I M Sechenova*, 96: 353-61.

Mohammad, A. K., and J. J. Reineke. 2013. 'Quantitative detection of PLGA nanoparticle degradation in tissues following intravenous administration', *Mol Pharm*, 10: 183-9.

Mohara, J., T. Morishita Y Fau - Takahashi, K. Takahashi T Fau - Oshima, T. Oshima K Fau - Yamagishi, I. Yamagishi T Fau - Takeyoshi, K. Takeyoshi I Fau - Matsumoto, and K. Matsumoto. 1999. 'A comparative study of Celsior and University of Wisconsin solutions based on 12-hr preservation followed by transplantation in canine models', *J Heart Lung Transplant*, 18: 1202-10.

Molavi, B., N. Rassouli, S. Bagwe, and N. Rasouli. 2007. 'A review of thiazolidinediones and metformin in the treatment of type 2 diabetes with focus on cardiovascular complications', *Vasc Health Risk Manag*, 3: 967-73.

Moore, L. B., A. J. Sawyer, J. Saucier-Sawyer, W. M. Saltzman, and T. R. Kyriakides. 2016. 'Nanoparticle delivery of miR-223 to attenuate macrophage fusion', *Biomaterials*, 89: 127-35.

Mozaffarian, Dariush, Emelia J. Benjamin, Alan S. Go, Donna K. Arnett, Michael J. Blaha, Mary Cushman, Sandeep R. Das, Sarah de Ferranti, Jean-Pierre Després, Heather J. Fullerton, Virginia J. Howard, Mark D. Huffman, Carmen R. Isasi, Monik C. Jiménez, Suzanne E. Judd, Brett M. Kissela, Judith H. Lichtman, Lynda D. Lisabeth, Simin Liu, Rachel H. Mackey, David J. Magid, Darren K. McGuire, Emile R. Mohler, Claudia S. Moy, Paul Muntner, Michael E. Mussolino, Khurram Nasir, Robert W. Neumar, Graham Nichol, Latha Palaniappan, Dilip K. Pandey, Mathew J. Reeves, Carlos J. Rodriguez, Wayne Rosamond, Paul D. Sorlie, Joel Stein, Amytis Towfighi, Tanya N. Turan, Salim S. Virani, Daniel Woo, Robert W. Yeh, and Melanie B. Turner. 2015. 'Heart Disease and Stroke Statistics—2016 Update', *Circulation*.

Mues, C., J. Zhou, K. N. Manolopoulos, P. Korsten, D. Schmoll, L. O. Klotz, S. R. Bornstein, H. H. Klein, and A. Barthel. 2009. 'Regulation of glucose-6-phosphatase gene expression by insulin and metformin', *Horm Metab Res*, 41: 730-5.

Musi, N., M. F. Hirshman, J. Nygren, M. Svanfeldt, P. Bavenholm, O. Rooyackers, G. Zhou, J. M. Williamson, O. Ljunqvist, S. Efendic, D. E. Moller, A. Thorell, and L. J. Goodyear. 2002. 'Metformin increases AMP-activated protein kinase activity in skeletal muscle of subjects with type 2 diabetes', *Diabetes*, 51: 2074-81.

Nagoshi, Tomohisa, Michihiro Yoshimura, Giuseppe M. C. Rosano, Gary D. Lopaschuk, and Seibu Mochizuki. 2011. 'Optimization of Cardiac Metabolism in Heart Failure', *Current Pharmaceutical Design*, 17: 3846-53.

Nakano, Y., T. Matoba, M. Tokutome, D. Funamoto, S. Katsuki, G. Ikeda, K. Nagaoka, A. Ishikita, K. Nakano, J. Koga, K. Sunagawa, and K. Egashira. 2016. 'Nanoparticle-Mediated Delivery of Irbesartan Induces Cardioprotection from Myocardial Ischemia-Reperfusion Injury by Antagonizing Monocyte-Mediated Inflammation', *Sci Rep*.

Ofenstein, J. P., L. J. Dominguez, J. R. Sowers, and A. P. Sarnaik. 1999. 'Effects of insulin and metformin on glucose metabolism in rat vascular smooth muscle', *Metabolism*, 48: 1357-60.

Owen, O. E., Richard W. Kalhan Sc Fau - Hanson, and R. W. Hanson. 2002. 'The key role of anaplerosis and cataplerosis for citric acid cycle function', *J Biol Chem*, 277: 30409-12.

Palama, Ilaria E., Barbara Cortese, Stefania D'Amone, and Giuseppe Gigli. 2015. 'mRNA delivery using non-viral PCL nanoparticles', *Biomaterials Science*, 3: 144-51.

Panunti, B., B. Kunhiraman, and V. Fonseca. 2005. 'The impact of antidiabetic therapies on cardiovascular disease', *Curr Atheroscler Rep*, 7: 50-7.

Park, T. G., Sung Wan Jeong Jh Fau - Kim, and S. W. Kim. 2006. 'Current status of polymeric gene delivery systems', *Adv Drug Deliv Rev*, 58: 467-86.

Peled, Yael, Jacob Lavee, Eugenia Raichlin, Moshe Katz, Michael Arad, Yigal Kassif, Amir Peled, Elad Asher, Dan Elian, Yedael Har-Zahav, Nir Shlomo, Dov Freimark, Ilan Goldenberg, and Robert Klempfner. 2017. 'Metformin therapy reduces the risk of malignancy after heart transplantation', *The Journal of Heart and Lung Transplantation*, 36: 1350-57.

Peltz, M., M. L. Cobert, D. H. Rosenbaum, L. M. West, and M. E. Jessen. 2008. 'Myocardial perfusion characteristics during machine perfusion for heart transplantation', *Surgery*, 144: 225-32.

Peltz, M., T. T. He, G. A. th Adams, R. Y. Chao, and M. E. Jessen. 2004. 'Myocardial oxygen demand and redox state affect fatty acid oxidation in the potassium-arrested heart', *Surgery*, 136: 150-9.

Petros, R. A., and J. M. DeSimone. 2010. 'Strategies in the design of nanoparticles for therapeutic applications', *Nat Rev Drug Discov*, 9: 615-27.

Poston, Robert S., Junyan Gu, Deyanira Prastein, Fred Gage, John W. Hoffman, Michael Kwon, Agnes Azimzadeh, Richard N. Pierson, III, and Bartley P. Griffith. 2004. 'Optimizing Donor Heart Outcome After Prolonged Storage With Endothelial Function Analysis and Continuous Perfusion', *Ann Thorac Surg*, 78: 1362-70.

Preusse Cj Fau - Winter, J., H. D. Winter J Fau - Schulte, W. Schulte Hd Fau - Bircks, and W. Bircks. 1985. 'Energy demand of cardioplegically perfused human hearts', *J Cardiovasc Surg*, 26: 558-63.

Qian, Li, Linda W. Van Laake, Yu Huang, Siyuan Liu, Michael F. Wendland, and Deepak Srivastava. 2011. 'miR-24 inhibits apoptosis and represses Bim in mouse cardiomyocytes', *The Journal of Experimental Medicine*, 208: 549.

Reed, Mark K., Chen Barak, Craig R. Malloy, Stephen P. Maniscalco, and Michael E. Jessen. 1996. 'Effects of glutamate and aspartate on myocardial substrate oxidation during potassium arrest', *The Journal of Thoracic and Cardiovascular Surgery*, 112: 1651-60.

Ren, X. P., J. Wu, X. Wang, M. A. Sartor, K. Jones, J. Qian, P. Nicolaou, T. J. Pritchard, and G. C. Fan. 2009. 'MicroRNA-320 is involved in the regulation of cardiac ischemia/reperfusion injury by targeting heat-shock protein 20', *Circulation*, 119.

Rivard, Andrew L., Robert Gallegos, Irene M. Ogden, and Richard W. Bianco. 2009. 'Perfusion Preservation of the Donor Heart: Basic Science to Pre-Clinical', *The Journal of Extra-corporeal Technology*, 41: 140-48.

Rosenbaum, D. H., M. Peltz, J. M. DiMaio, D. M. Meyer, M. A. Wait, M. E. Merritt, W. S. Ring, and M. E. Jessen. 2008. 'Perfusion preservation versus static preservation for cardiac transplantation: effects on myocardial function and metabolism', *J Heart Lung Transplant*, 27: 93-9.

Rosenbaum, David H., Matthias Peltz, Matthew E. Merritt, Jeffrey E. Thatcher, Hideki Sasaki, and Michael E. Jessen. 2007. 'Benefits of Perfusion Preservation in Canine Hearts Stored for Short Intervals', *Journal of Surgical Research*, 140: 243-49.

Rudd, D. M., and G. P. Dobson. 2011. 'Eight hours of cold static storage with adenosine and lidocaine (Adenocaine) heart preservation solutions: toward therapeutic suspended animation', *J Thorac Cardiovasc Surg*, 142: 1552-61.

Russell, R. R., and H. Taegtmeyer. 1991. 'Changes in citric acid cycle flux and anaplerosis antedate the functional decline in isolated rat hearts utilizing acetoacetate', *Journal of Clinical Investigation*, 87: 384-90.

Sack, M. N., S. Rader Ta Fau - Park, J. Park S Fau - Bastin, S. A. Bastin J Fau - McCune, D. P. McCune Sa Fau - Kelly, and D. P. Kelly. 1996. 'Fatty acid oxidation enzyme gene expression is downregulated in the failing heart', *Circulation*, 94: 2837-42.

Saeedi, R., H. L. Parsons, R. B. Wambolt, K. Paulson, V. Sharma, J. R. Dyck, R. W. Brownsey, and M. F. Allard. 2008. 'Metabolic actions of metformin in the heart can occur by AMPK-independent mechanisms', *Am J Physiol Heart Circ Physiol*, 294: H2497-506.

Schonfeld P Fau - Bohnensack, R., G. Bohnensack R Fau - Bohme, W. Bohme G Fau - Kunz, and W. Kunz. 1983. 'Influence of the beta-hydroxybutyrate/acetoacetate ratio on the redox states of mitochondrial NAD(P) and cytochrome c systems, extramitochondrial ATP/ADP ratio and the respiration of isolated liver mitochondria in the resting state', *Biomed Biochim Acts*, 42: 3-13.

Schowen, Richard L. 1993. 'Principles of biochemistry 2nd ed. (Lehninger, Albert L.; Nelson, David L.; Cox, Michael M.)', *Journal of Chemical Education*, 70: A223.

Shoghi, K. I., B. N. Finck, K. B. Schechtman, T. Sharp, P. Herrero, R. J. Gropler, and M. J. Welch. 2009. 'In vivo metabolic phenotyping of myocardial substrate metabolism in rodents: differential efficacy of metformin and rosiglitazone monotherapy', *Circ Cardiovasc Imaging*, 2: 373-81.

Siliprandi, Noris, FabioDi Lisa, and Roberta Menabò. 1991. 'Propionyl-L-carnitine: Biochemical significance and possible role in cardiac metabolism', *Cardiovascular Drugs and Therapy*, 5: 11-15.

Smith, R. S., Jr., Chun-Fang Agata J Fau - Xia, Lee Xia Cf Fau - Chao, Julie Chao L Fau - Chao, and J. Chao. 2005. 'Human endothelial nitric oxide synthase gene

delivery protects against cardiac remodeling and reduces oxidative stress after myocardial infarction', *Life Sci*, 76: 2457-71.

Soo Choi, Hak, Wenhao Liu, Preeti Misra, Eiichi Tanaka, John P. Zimmer, Binil Itty Ipe, Moungi G. Bawendi, and John V. Frangioni. 2007. 'Renal clearance of quantum dots', *Nature Biotechnology*, 25: 1165.

Southworth, R., S. C. Blackburn, K. A. B. Davey, G. K. Sharland, and P. B. Garlick. 2005. 'The low oxygen-carrying capacity of Krebs buffer causes a doubling in ventricular wall thickness in the isolated heart', *Canadian Journal of Physiology and Pharmacology*, 83: 174-82.

Stamp, Nikki L., Amit Shah, Viji Vincent, Brian Wright, Clare Wood, Warren Pavey, Chris Cokis, Sharon Chih, Lawrence Dembo, and Rob Larbalestier. 2015. 'Successful Heart Transplant after Ten Hours Out-of-body Time using the TransMedics Organ Care System', *Heart, Lung and Circulation*, 24: 611-13.

Stanley, W. C., F. A. Recchia, and G. D. Lopaschuk. 2005a. 'Myocardial substrate metabolism in the normal and failing heart', *Physiol Rev*, 85: 1093-129.

Stanley, William C., Fabio A. Recchia, and Gary D. Lopaschuk. 2005b. 'Myocardial Substrate Metabolism in the Normal and Failing Heart', *Physiol Rev*, 85: 1093-129.

Sundqvist, K. E., K. J. Peuhkurinen, J. K. Hiltunen, and I. E. Hassinen. 1984. 'Effect of acetate and octanoate on tricarboxylic acid cycle metabolite disposal during propionate oxidation in the perfused rat heart', *Biochimica et biophysica acta*, 801: 429-36.

Sutherland, Fiona J., and David J. Hearse. 2000. 'THE ISOLATED BLOOD AND PERFUSION FLUID PERFUSED HEART', *Pharmacological Research*, 41: 613-27.

Takada, M., W. W. Nadeau Kc Fau - Hancock, H. S. Hancock Ww Fau - Mackenzie, G. D. Mackenzie Hs Fau - Shaw, A. M. Shaw Gd Fau - Waaga, A. Waaga Am Fau - Chandraker, M. H. Chandraker A Fau - Sayegh, N. L. Sayegh Mh Fau - Tilney, and N. L. Tilney. 1998. 'Effects of explosive brain death on cytokine activation of peripheral organs in the rat', *Transplantation*, 65: 1533-42.

Tanaka, M., S. Ito H Fau - Adachi, H. Adachi S Fau - Akimoto, T. Akimoto H Fau - Nishikawa, T. Nishikawa T Fau - Kasajima, F. Kasajima T Fau - Marumo, M. Marumo F Fau - Hiroe, and M. Hiroe. 1994. 'Hypoxia induces apoptosis with enhanced expression of Fas antigen messenger RNA in cultured neonatal rat cardiomyocytes', *Circ Res*, 75: 426-33.

Thomson, J. G. 1969. 'Production of severe atheroma in a transplanted human heart', *Lancet*, 294: 1088-92.

Tolboom, Herman, Asya Makhro, Barbara A. Rosser, Markus J. Wilhelm, Anna Bogdanova, and Volkmar Falk. 2015. 'Recovery of donor hearts after circulatory death with normothermic extracorporeal machine perfusion†', *European Journal of Cardio-Thoracic Surgery*, 47: 173-79.

Van Caenegem, Olivier, Christophe Beauloye, Luc Bertrand, Sandrine Horman, Sophie Lepropre, Grégory Sparavier, Jonathan Vercruysse, Noëlla Bethuyne, Alain J. Poncelet, Pierre Gianello, Peter Demuylder, Eric Legrand, Gwen Beaurin, Françoise Bontemps, Luc M. Jacquet, and Jean-Louis Vanoverschelde. 2016. 'Hypothermic continuous machine perfusion enables preservation of energy charge and functional recovery of heart grafts in an ex vivo model of donation following circulatory death', *European Journal of Cardio-Thoracic Surgery*, 49: 1348-53.

van der Hoeven, J. A. B., R. J. Ploeg, F. Postema, G. Molema, P. de Vos, A. R. J. Girbes, P. T. R. van Suylichem, and G. J. Ter Horst. 1999. 'Induction of organ dysfunction and activation of inflammatory markers in donor liver and kidney during hypotensive brain death', *Transplant Proc*, 31: 1006-07.

van der Meer, R. W., L. J. Rijzewijk, H. W. de Jong, H. J. Lamb, M. Lubberink, J. A. Romijn, J. J. Bax, A. de Roos, O. Kamp, W. J. Paulus, R. J. Heine, A. A. Lammertsma, J. W. Smit, and M. Diamant. 2009. 'Pioglitazone improves cardiac function and alters myocardial substrate metabolism without affecting cardiac triglyceride accumulation and high-energy phosphate metabolism in patients with well-controlled type 2 diabetes mellitus', *Circulation*, 119: 2069-77.

Vaughan, E. E., J. V. DeGiulio, and D. A. Dean. 2006. 'Intracellular trafficking of plasmids for gene therapy: mechanisms of cytoplasmic movement and nuclear import', *Curr Gene Ther*, 6: 671-81.

Wahlberg Ja Fau - Love, R., L. Love R Fau - Landegaard, J. H. Landegaard L Fau - Southard, F. O. Southard Jh Fau - Belzer, and F. O. Belzer. 1987. '72-hour preservation of the canine pancreas', *Transplantation*, 43: 5-8.

Wang, J. X., J. Q. Jiao, Q. Li, B. Long, K. Wang, J. P. Liu, Y. R. Li, and P. F. Li. 2011. 'miR-499 regulates mitochondrial dynamics by targeting calcineurin and dynamin-related protein-1', *Nat Med*, 17: 71-8.

Wang, S., Brett A. Aurora Ab Fau - Johnson, Xiaoxia Johnson Ba Fau - Qi, John Qi X Fau - McAnally, Joseph A. McAnally J Fau - Hill, James A. Hill Ja Fau - Richardson, Rhonda Richardson Ja Fau - Bassel-Duby, Eric N. Bassel-Duby R Fau - Olson, and E. N. Olson. 2008. 'The endothelial-specific microRNA miR-126 governs vascular integrity and angiogenesis', *Dev Cell*, 15: 261-71.

Warnecke, G., Axel Schulze B Fau - Haverich, Uwe Haverich A Fau - Klima, and U. Klima. 2002. 'Celsior solution provides superior post-ischemic right ventricular function as compared with UW solution in a porcine heart transplantation model', *J Heart Lung Transplant*, 21: 586-9.

Weiss, R. G., and M. Maslov. 2004. *Normal myocardial metabolism: Fueling cardiac contraction*.

Wisneski, J. A., E. W. Gertz, R. A. Neese, L. D. Gruenke, D. L. Morris, and J. C. Craig. 1985. 'Metabolic fate of extracted glucose in normal human myocardium', *Journal of Clinical Investigation*, 76: 1819-27.

Wittwer, T., J. F. Wahlers T Fau - Cornelius, S. Cornelius Jf Fau - Elki, A. Elki S Fau - Haverich, and A. Haverich. 1999. 'Celsior solution for improvement of currently used clinical standards of lung preservation in an ex vivo rat model', *Eur J Cardiothorac Surg*, 15: 667-71.

Woodrow, K. A., Carmen J. Cu Y Fau - Booth, Jennifer K. Booth Cj Fau - Saucier-Sawyer, Monica J. Saucier-Sawyer Jk Fau - Wood, W. Mark Wood Mj Fau - Saltzman, and W. M. Saltzman. 2009. 'Intravaginal gene silencing using biodegradable polymer nanoparticles densely loaded with small-interfering RNA', *Nat Mater*, 8: 526-33.

Wu, P., R. A. Peters Jm Fau - Harris, and R. A. Harris. 2001. 'Adaptive increase in pyruvate dehydrogenase kinase 4 during starvation is mediated by peroxisome proliferator-activated receptor alpha', *Biochem Biophys Res Commun*, 287: 391-6.

Yang, J., Chenguang Marden Jj Fau - Fan, Salih Fan C Fau - Sanlioglu, Robert M. Sanlioglu S Fau - Weiss, Teresa C. Weiss Rm Fau - Ritchie, Robin L. Ritchie Tc Fau - Davisson, John F. Davisson Rl Fau - Engelhardt, and J. F. Engelhardt. 2003. 'Genetic redox preconditioning differentially modulates AP-1 and NF kappa B responses following cardiac ischemia/reperfusion injury and protects against necrosis and apoptosis', *Mol Ther*, 7: 341-53.

Yu, S., and G. Li. 2010. 'MicroRNA expression and function in cardiac ischemic injury', *Cardiovasc Transl Res*, 3: 241-5.

Zhang, L., X. Chen, T. Su, H. Li, Q. Huang, D. Wu, C. Yang, and Z. Han. 'Circulating miR-499 are novel and sensitive biomarker of acute myocardial infarction'.

Zhang, Yanfei, Meiping Guan, Zongji Zheng, Qian Zhang, Fang Gao, and Yaoming Xue. 2013. 'Effects of Metformin on CD133+ Colorectal Cancer Cells in Diabetic Patients', *PLOS ONE*, 8: e81264.